MICROCOPY RESOLUTION TEST CHART

NATIONAL BUREAU OF STANDARDS-1963-A

JOAP-TSC REPORT 84-01

EVALUATION OF USED CRANKCASE OILS
USING COMPUTERIZED INFRARED SPECTROMETRY

B.B. McCAA, LTC AND JOHN P. COATES

JUNE 84

JOINT OIL ANALYSIS PROGRAM

TECHNICAL SUPPORT CENTER

PENSACOLA, FL

DTIC
ELECTE
APR 2 9 1985
E
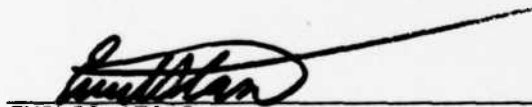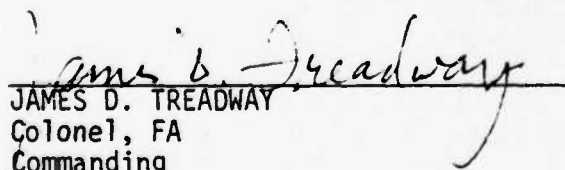
85 04 04 067

The views, opinions, and/or findings contained in the report are those of the authors and should not be construed as an official Department of Defense position, policy, or decision, unless so designated by other documentation. The citation in this report of trade names of commercially available products does not constitute official endorsement or approval of the use of such products. When government drawings, specifications, or other data are used for any purpose other than in connection with a definitely related government procurement operation, the United States Government thereby incurs no responsibility nor any obligation whatsoever; and the fact that the government may have formulated, furnished, or in any way supplied the said drawings, specifications, or other data, is not to be regarded by implication or otherwise as in any manner licensing the holder or any other person or corporation, or conveying any rights or permission to manufacture, use, or sell any patented invention that may in any way be related thereto.

This technical report has been reviewed and is approved for distribution.

CYRIL M. BROWN
Chief, Army Oil Analysis Program
Member, Joint Oil Analysis Program Coordinating Group

EMILIO STASI
Chief, Maintenance Division

JAMES D. TREADWAY
Colonel, FA
Commanding

SECURITY CLASSIFICATION OF THIS PAGE (When Data Entered)

REPORT DOCUMENTATION PAGE		READ INSTRUCTIONS BEFORE COMPLETING FORM
1. REPORT NUMBER JOAP-TSC 84-01	2. GOVT ACCESSION NO.	3. RECIPIENT'S CATALOG NUMBER
4. TITLE (and Subtitle) EVALUATION OF USED CRANKCASE OILS USING COMPUTERIZED INFRARED SPECTROMETRY		5. TYPE OF REPORT & PERIOD COVERED FINAL JAN 82 - JUN 84
		6. PERFORMING ORG. REPORT NUMBER
7. AUTHOR(s) Burwell B. McCaa, LTC, USA John P. Coates, Perkin-Elmer Corp.		8. CONTRACT OR GRANT NUMBER(s) Joint cooperative effort
9. PERFORMING ORGANIZATION NAME AND ADDRESS JOAP-TSC, Pensacola, FL jointly with Perkin-Elmer Corporation, IR Product Dept. 901 Ethan Allen Hwy., Ridgefield, CT 06877		10. PROGRAM ELEMENT, PROJECT, TASK AREA & WORK UNIT NUMBERS
11. CONTROLLING OFFICE NAME AND ADDRESS Commander, USAMC Materiel Readiness Support Activity Lexington, KY 40511-5101		12. REPORT DATE June 1984
		13. NUMBER OF PAGES ~~560~~
14. MONITORING AGENCY NAME & ADDRESS(if different from Controlling Office) JOAP-Technical Support Center Bldg. 780, NAS Pensacola, FL 32508-5300		15. SECURITY CLASS. (of this report) Unclassified
		15a. DECLASSIFICATION/DOWNGRADING SCHEDULE

16. DISTRIBUTION STATEMENT (of this Report)

Approved for public release; distribution unlimited

17. DISTRIBUTION STATEMENT (of the abstract entered in Block 20, if different from Report)

18. SUPPLEMENTARY NOTES

19. KEY WORDS (Continue on reverse side if necessary and identify by block number)

Infrared Spectroscopy	hydroxyl	fuel dilution
transmittance	oxidation	total acid number
absorbance	carboxylates	total solids
integrated area	nitration	viscosity
peak heights	sulfation	carbon loading, graphs

20. ABSTRACT (Continue on reverse side if necessary and identify by block number)

This is the final report of a study to determine whether computerized infrared spectroscopy is a feasible technique for oil condition monitoring. The study addresses the major factors that influence the performance of a lubricant in service and demonstrates that these factors may be monitored with infrared spectroscopy. The study identifies specific regions and peaks within the infrared spectra to be monitored in a routine oil condition monitoring program and proposes abnormal threshold for quantitative measures of these

DD FORM 1473 1 JAN 73 EDITION OF 1 NOV 65 IS OBSOLETE
S/N 0102-LF-014-6601

SECURITY CLASSIFICATION OF THIS PAGE (When Data Entered)

20. (cont) regions and peaks. Evaluation criteria for five Army combat and tactical vehicle engines and one Air Force administrative engine are developed. Further the study recommends a field test of the infrared methodology at a single Army installation.

PREFACE

We, the authors, wish to acknowledge the considerable assistance we have received in the conduct of this study and the preparation of this report. This study was a joint effort between the Joint Oil Analysis Program Technical Support Center (JOAP-TSC) and the Perkin-Elmer Infrared Product Department. Both the Joint Oil Analysis Program Coordinating Group and Perkin-Elmer Corporation have generously supported the frequent trips between Norwalk and Pensacola and the two and one half years of effort necessary for completion of the study. Further, our respective staffs have participated fully in the numerous laboratory and data analyses and re-analyses conducted during the study. Of special note are Mr. Griffin Jones of the JOAP-TSC, who conducted the most of the laboratory analyses of oil samples and prepared the initial draft of this report, and Ms. Lynn Setti of Perkin-Elmer Corporation, who performed supporting analyses on specially prepared samples. Further, we wish to acknowledge Ms. Jane Addy of the JOAP-TSC who performed the tedious jobs of entering all of the laboratory data into computer files and typing the final report, Mr. Alan Miller of the JOAP-TSC, who assisted in the statistical analyses and performed the final editing and collating of the report, and Mr. Art Haney of the University of West Florida, who graciously assisted our use of the University's computer facility.

Accession For

NTIS GRA&I	☒
DTIC TAB	☐
Unannounced	☐
Justification	

By
Distribution/
Availability Codes

| Dist | Avail and/or Special |
| A-1 | |

DTIC COPY INSPECTED 3

TABLE OF CONTENTS

TABLES

* IR refers to normal infrared spectra
* DIR refers to differential infrared spectra

SECTION I

BACKGROUND

This is the final report of a study by the Joint Oil Analysis Program Technical Support Center (JOAP-TSC) to determine whether computerized infrared (IR) spectroscopy is a feasible technique for oil condition monitoring in the Joint Oil Analysis Program. The study was initiated in January 1982, an in-process review (IPR) was held in May 1982, and data collection was terminated in June 1983. The test instrument, a Perkin-Elmer, Model 1330, infrared spectrophotometer, with a data station, was provided to the TSC by Perkin-Elmer Corporation for purposes of this study. Additionally, necessary instrument programming support and infrared spectroscopy consultation were provided by Perkin-Elmer Corporation in a cooperative study effort. Two papers based on the study were presented at the Joint Oil Analysis Program International Symposium in May 1983. They are included in the list of references at Appendix A.

Infrared spectroscopy is a fundamental tool for organic material analysis, and it may provide necessary information to assess the condition of used crankcase oils. Yet application to oil condition monitoring has been limited by an inability to quantitatively assess the total information content of the infrared spectrum and the lack of acceptable evaluation criteria for oil condition. This study addresses both of these limitations and the basic hypothesis that the infrared spectra contain information that will characterize degradation of in-service crankcase oils. The objectives of this study were to -

Objective 1. Evaluate the effectiveness of the Perkin-Elmer Model 1330, Computerized Infrared Spectrophotometer, as a used oil condition monitoring device.

Objective 2. Develop an improved oil condition monitoring methodology based on computerized infrared spectrophotometry.

Originator-supplied keywords included: → p 1473

1

SECTION II
DISCUSSION OF INFRARED SPECTROSCOPIC ANALYSIS
OF USED LUBRICATING OILS

A. Introduction.

This section is intended to provide a detailed account of the application of infrared spectroscopy (IR) to the analysis of used hydrocarbon based crankcase lubricants. The term, crankcase, is used as a generic term and most of the data provided are applicable to any type of equipment powered by an internal combustion engine. An analytical study of a lubricant in service can provide information that can be used to diagnose one or more of the following situations:

1. Contamination of the lubrication system
2. Changes in engine performance
3. Potential mechanical component failure
4. Lubricant failure

If a diagnosis is made in adequate time, it is possible to reduce downtime on equipment and reduce operating costs. All of the situations mentioned either cause or are the result of changes in the physical or chemical composition of the lubricant. Specific physical/chemical tests, such as viscosity, total acid/base numbers (TAN/TBN), total insolubles, etc., may be used to screen an oil in service. However, these tests all have significant drawbacks; some are time-consuming, some are inaccurate, and others are misleading.

The infrared spectrum of a molecular species is essentially a fingerprint. It is usually sensitive to minor changes in the chemical makeup or environment of a material. In the case of a lubricant in service, the spectrum may be used to detect contaminants and to indicate changes in operating conditions or potential component or lubricant failure.

B. The Chemistry of a Lubricant in Service.

Even under normal operating conditions, the environment in an internal combustion engine is potentially hostile to the lubricant. Most engines operate at moderately high temperatures with the bulk

2

oil temperature ranging from 90 to 140 degrees Celsius (194 to 284 degrees Fahrenheit), and as high as 175°C (347°F) for turbocharged engines. Normally these temperatures tend to be at the lower end of the range but are dependent on the operating conditions and environment of an individual engine. There are, however, regions in the engine, especially around the combustion zone, where extremely high temperatures exist. The lubricant in these regions either evaporates, burns or thermally or oxidatively degrades.

In addition, the combustion process generates gaseous products that react with the lubricant both at the ring zone and in the crankcase. The major materials involved are nitrogen oxides (NOx), sulfur oxides (SO4) (if sulfur is present in the fuel), oxidized and unburnt fuel, plus other reactive species, such as free radicals. Additives in the lubricant are designed to react with many of these degradation products to reduce their potency. This does not mean, however, that the basic lubricant does not degrade. The oxidizing nature of the environment and the elevated operating temperatures lead to degradation of the bulk lubricant. The presence of additives control the degradation process and permits the lubricant to function correctly. Obviously, the additives have a finite lifetime and at some point they become exhausted. At this stage, catastrophic breakdown of the lubricant can occur and this in turn may lead to equipment failure.

The products of fuel combustion, a combination of oxidized fuel and nitrogen oxides, leads to the formation of polymeric organic compounds that appear in the system as sludges and varnishes. The sludges, which are generally polar materials, are insoluble in the hydrocarbon base oil. They are maintained in suspension by dispersant additives. Dispersant dropout can cause sludge deposition with a resultant blockage to key oilways. Another insoluble material from fuel origin is carbon or soot. This usually is only experienced with diesel fueled engines and is the result of incomplete combustion. Some of the soot is removed with the exhaust gases but a reasonable amount does enter the crankcase and becomes dispersed in the lubricant. The dispersants and, to some extent, the oil filter prevent any adverse effects of soot contamination.

3

Fuel itself is a further potential contaminant. In cases where an engine is running rich or is over-choked, it is possible for a relatively high level of unburnt fuel to remain after the main combustion. Some of this fuel can wash down the walls of the cylinders and pass by the piston rings. This is undersirable for two reasons:

1. The washing effect of the fuel on the cylinder walls can remove the lubricating film which can lead to scoring of the piston skirt or piston seizure.

2. Any fuel entering the crankcase will dissolve in the oil and produce the condition known as fuel dilution which causes a reduction in viscosity and a resultant loss of lubrication efficiency.

Other sources of contamination can produce severe lubricant degradation and ultimately cause component failure. Typical contaminants are:

1. Water/glycol from coolant

2. Water from external contact

3. Dust and other siliceous material from the air intake

4. Incompatible fluids from oil top-off with wrong fluids. With the exception of the use of an incorrect fluid, all the other contaminants enter the oil after failure of a component, such as a seal, a gasket, or an air filter. The presence of any one of these contaminants is potentially disastrous because they lead to a loss of lubricity, an increase in viscosity or corrosion or, in the case of siliceous matter, extreme wear of key moving components.

C. The Role of Infrared Spectroscopy.

It is obvious that the early detection of external contaminants is essential for effective preventative maintenance. Infrared spectroscopy is capable of detecting all of the contaminants discussed above. In the case of siliceous dust, however, it may be too late to prevent substantial wear to key components once it is detected. For this and other abrasive materials, wear metal analysis may be a more sensitive method of measurement. All the other contaminants can be detected early enough to prevent major failure so long as oil samples are taken at regular time intervals. In addition to contaminant monitoring, infrared analysis of frequent oil samples can provide useful data concerning combustion products and oil degradation products. Both of these products are good indicators of engine and lubricant performance. In

4

the remaining parts of this section the relationships between the infrared spectrum and lubricant condition will be discussed.

D. The Infrared Spectrum as an Oil Condition Monitor.

    1. General Considerations.

Figure 1 shows a comparison between a used and a fresh diesel oil. The spectrum of the used lubricant (B) has some obvious differences from fresh oil (A). The main difference is the overall change in spectral background of the used oil - a significantly lower transmission plus a slope upwards in the direction of lower wavenumber (longer wavelength). This effect is characteristic of the scatter-absorption phenomenon associated with dispersed soot particles. From the degree of lowering of the overall background it could be deduced that soot is present but at a relatively low level.

The used sample also has a broad spectral feature between 3600 cm^{-1} and 3100 cm^{-1} which is attributed to a hydroxyl group and is probably an early indication of water contamination. Two weak spectral features just above 1000 cm^{-1} are indications of the presence of ethylene glycol. These tend to reinforce the notion of water contamination from a coolant leak. These deductions are made from experience and a trained eye. The data as presented are inadequate for any further interpretation. Also, without the fresh oil it would have been impossible to make any definitive interpretation. These two spectra, however, serve to illustrate three salient points that are important for successful used oil analysis.

First it is important to have a sample of a fresh oil. Ideally, it should be the same oil used in the original oil serviced in the engine. Secondly, it is very difficult to draw meaningful conclusions about the condition of an oil without previous knowledge of the performance characteristics of the particular engine or item of equipment. The comment made about the relative level of carbon loading was based on general observations, but it may have been misleading for the equipment involved. This illustrates the need for good documentation, that is, good maintenance records; and wherever possible, regular samples to help develop trends of normal performance.

FIGURE 1

COMPARISON OF USED AND FRESH DIESEL LUBRICANTS

A : FRESH OIL
B : USED OIL

6
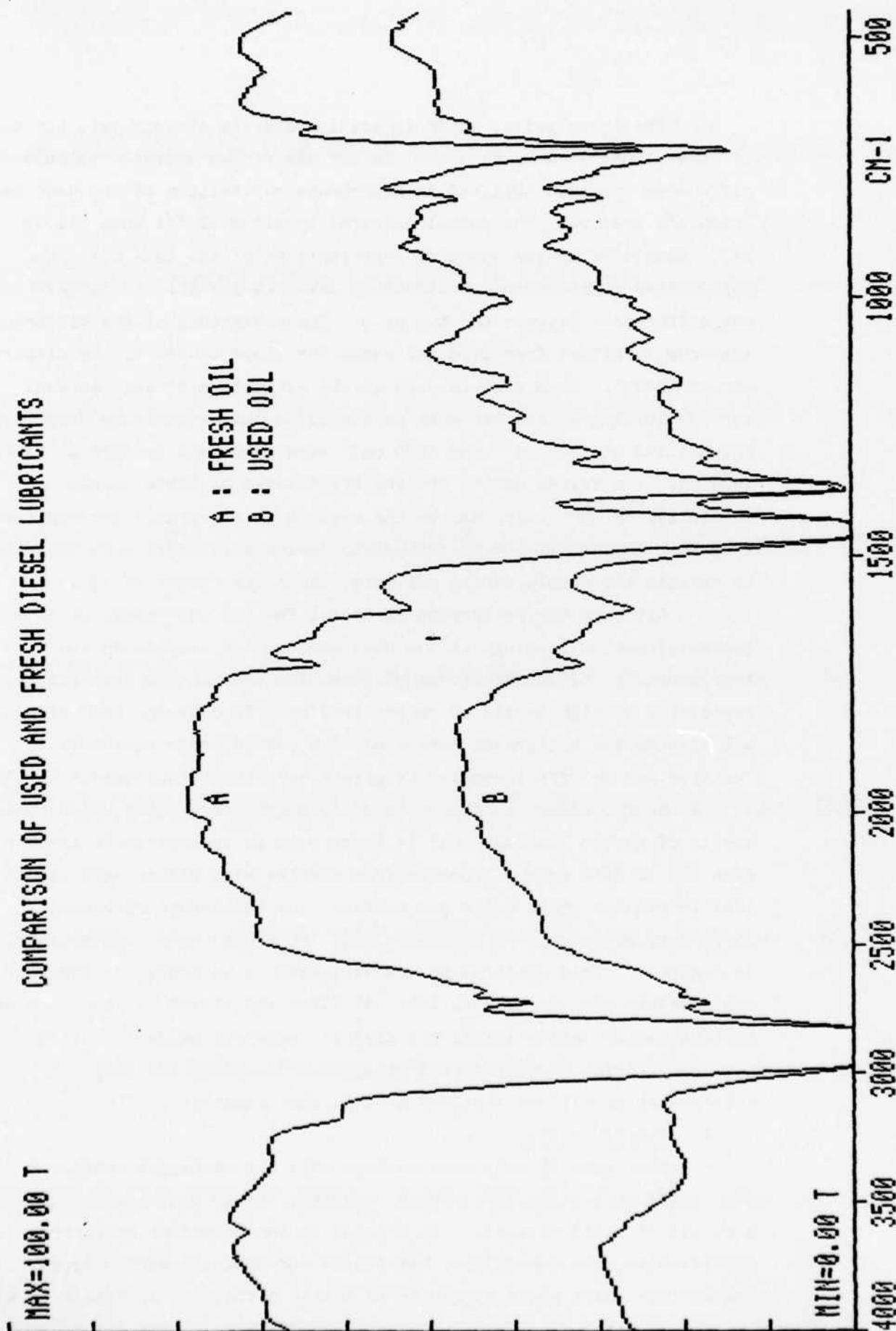
The third point, which is not immediately obvious yet, but which is well illustrated by Figure 2, is the use of the computer calculated difference spectrum obtained by absorbance subtraction of the used and fresh oil spectra. The normal infrared spectrum of the used oil is still dominated by the spectral contributions of the base oil. The application of absorbance subtraction makes it possible to observe the net differences between the two oils. The background of the difference spectrum is offset from zero and shows the slope caused by the dispersed carbon (soot). This fact is used in the evaluation of soot content (carbon loading). For the data presented in this report the background intensities at 3800 cm^{-1} and 1980 cm^{-1} were used as a measure of carbon loading. The values quoted are the absorbances at these points multiplied by 100X to normalize the results to absorbance per centimeter (abs/cm). Note that 0.1 mm pathlength sealed cells were used throughout to contain the sample during analysis, hence the factor of 100.

Although the background is useful for the determination of the degree of carbon loading, it can pose serious limitations on the assessment of the contributions of other features in the spectrum, especially at high levels of carbon loading. To overcome this effect, all spectra are background corrected by a second order (quadratic) function and an offset applied to give a zero absorbance baseline. The second order correction appears to be adequate for all but the highest levels of carbon loading, that is those with an absorbance/cm greater than 200 at 3800 cm^{-1}. Spectra from samples with higher soot levels ideally require third order correction. The background corrected difference spectrum for the used versus fresh oil shown earlier is given in Figure 3. This spectrum is now very easy to interpret in terms of contaminants and oil degradation. At first inspection it indicates some coolant contamination (water and glycol), moderate oxidation, very little nitration, and some fuel dilution. The basis for this interpretation will be provided with further examples.

2. Reference Oils.

Most mineral oils used as base oils for crankcase lubricant applications have similar infrared spectra. Minor differences occur as a result of small compositional changes in the component hydrocarbons, specifically, the paraffinic, naphthenic and aromatic carbon types. On the surface there would appear to be little difficulty in obtaining an

FIGURE 2

COMPARISON OF USED AND FRESH DIESEL LUBRICANTS

INITIAL DIFFERENCE SPECTRUM
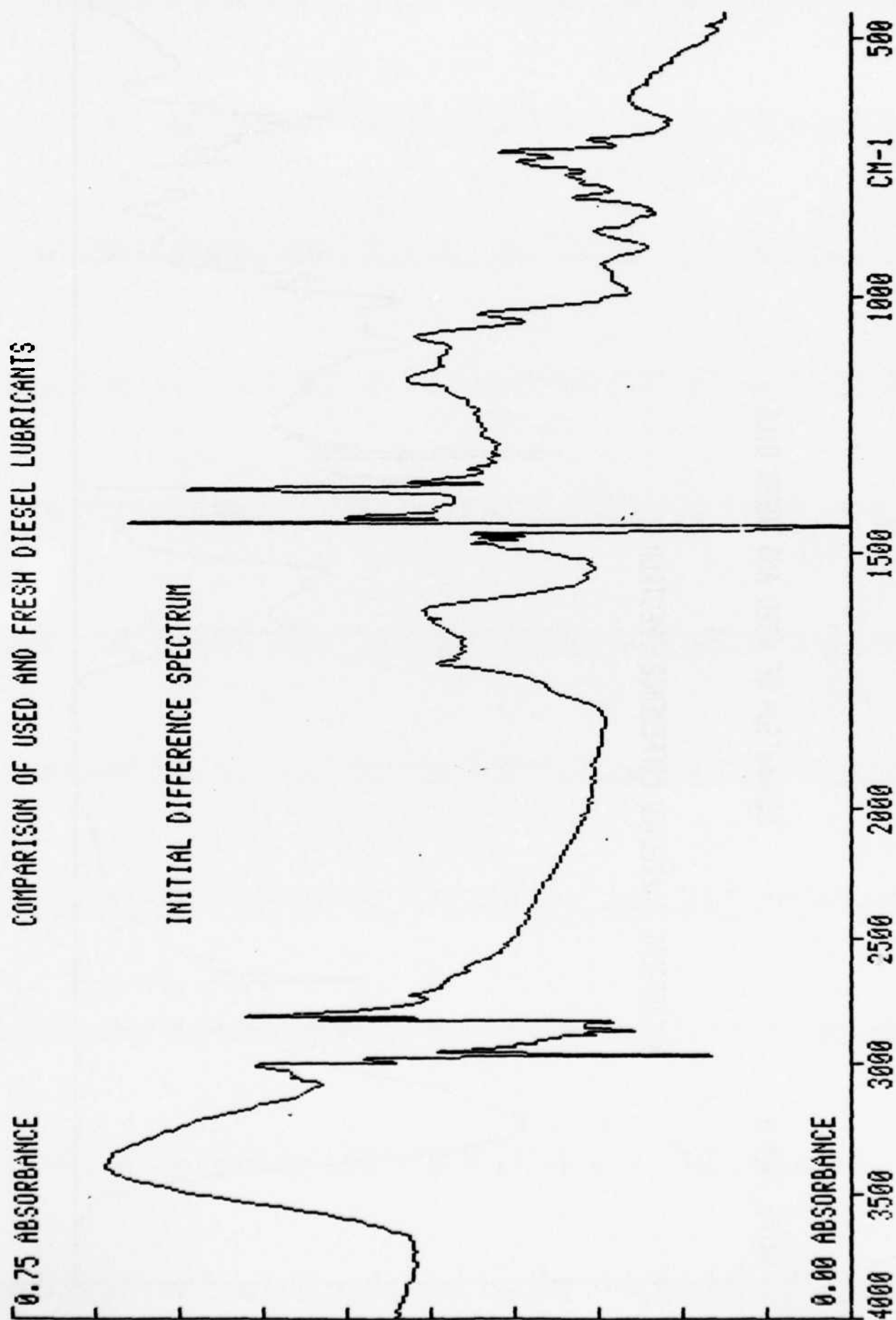
FIGURE 3

COMPARISON OF USED AND FRESH OILS

BACKGROUND CORRECTED DIFFERENCE SPECTRUM

MAX=0.3000 A

MIN=-0.0500 A

9
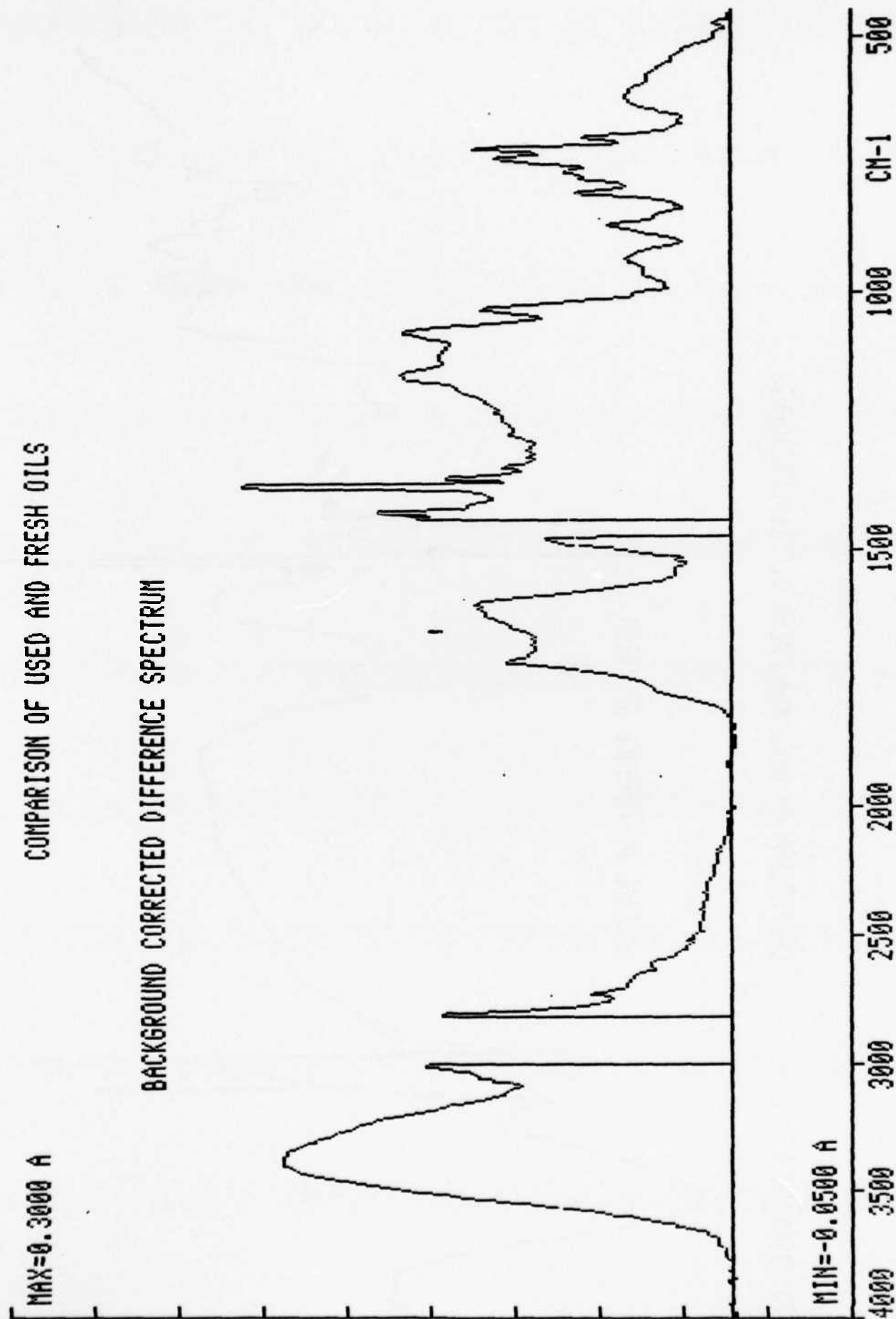
adequate reference oil. In the cases where only a rudimentary evaluation of a used oil is required, a reference spectrum from an oil of the same SAE grade is probably adequate. The results for carbon loading, coolant contamination, and possibly fuel diltuion and oxidation from an unmatched reference oil are usually quite useable as a guide to the condition of an oil. Additive variations usually have the greatest influence on the evaluation of oxidation. A typical example of reference oil variations is illustrated by Figure 4 where two adjacent oils in a series are compared. Both samples appear to be close to being fresh oils but with subtle variations in formulation. From a sampling point of view, these oils were either changed unnecessarily or the sampling interval was too long. Either way, this illustrates a need for an improved sampling schedule. The differences between the two oils, however, are not sufficient to invalidate results and generally meaningful data for oil condition can still be extracted with this degree of mismatch. It should be noted that most modern oil formulations do not use methacrylates as viscosity index (VI) improvers and, therefore, interferences from additives in the carbonyl oxidation region are not as severe as originally experienced. Methacrylates are still used as pour point depressants but at a much lower dosage than when used as viscosity modifiers. The only other common carbonyl containing additives are the dispersants.

The ideal situation for sampling would call for two samples to be taken at the time of an oil change or at the time of a top-off. One sample would be the latest fresh oil and the other the used oil just prior to the change or the top-off. This would provide a means for handling reference oils even if different suppliers were involved. Most of the oils encountered in this study were similar to A or B in Figure 4. A third type of reference oil that was occasionally used is shown in Figure 5. The main additive components are similar to those used in oil A, Figure 4. The main differences are in the higher aromatic content of the oil. This did cause an occasional problem with the evaluation of fuel dilution in cases where the change to this reference oil was not detected.

3. The Determination of Contaminants.

a. Total solids - carbon loading I/II (CL1/CL2). This particular example is intended to indicate the quantitative estimation

10

FIGURE 4

TWO ADJACENT OILS IN A SERIES - DIFFERENT FORMULATIONS INDICATED

A : CHA7H (2 HRS)
B : CHO8H (5 HRS)
- SPECTRUM OFFSET BY 15%T

MAX=100.00 T

MIN=0.00 T

11
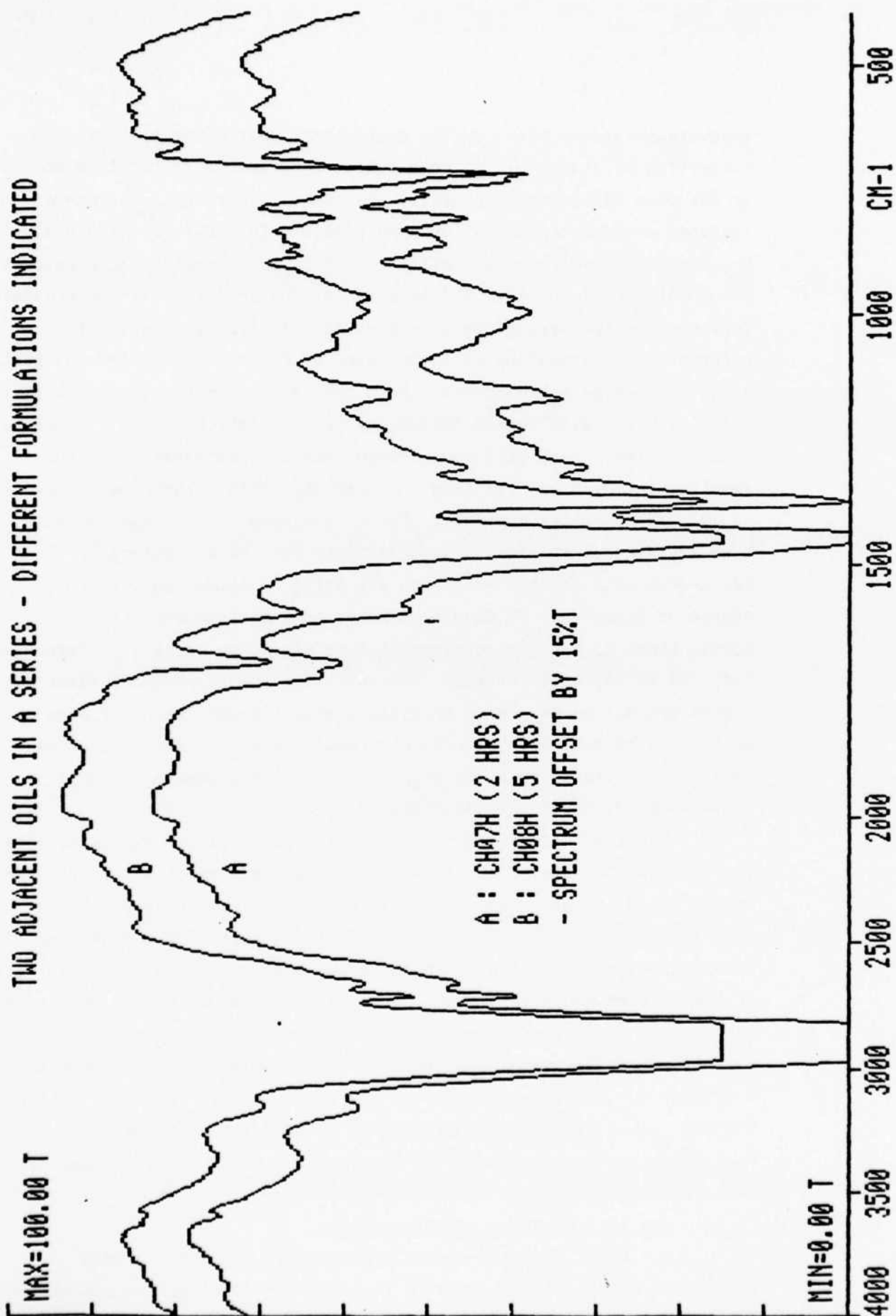
FIGURE 5

FRESH OIL REFERENCE NO.4 - (RG000 : DELTA 30)

12
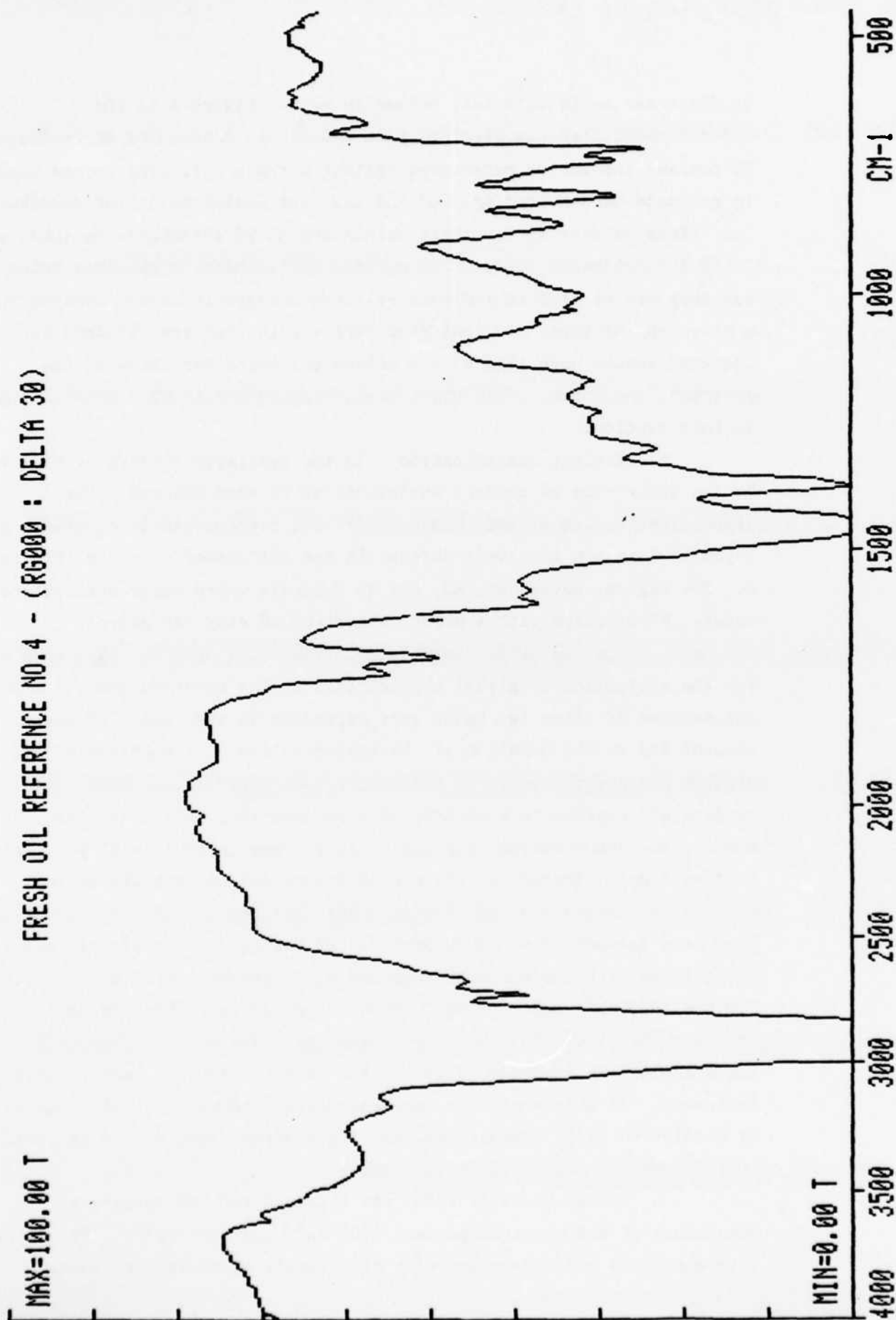
of dispersed solid material, primarily soot. Figure 6 is the uncorrected difference spectrum from a used oil containing approximately 5% pentane insolubles referenced against a fresh oil. The points used to estimate carbon loading, CL1 and CL2, are indicated on the spectrum. The values calculated for these points are 33.95 absorbance/cm (CL1) and 19.50 absorbance/cm (CL2). The numbers quoted have no absolute value but they can be used to indicate relative changes in carbon loading for a given engine type. As indicated earlier, the numbers obtained for an isolated sample have limited use unless the characteristics of the equipment are known. This point will be addressed in more detail later in this section.

b. Coolant contamination. In the overlayed spectra of Figure 7, the occurrence of coolant contamination is very obvious. The absorptions marked with an asterisk (*) are characteristic of ethylene glycol. They are also well defined in the difference spectrum, Figure 8. The regions marked W1, W2, and W3 indicate where water absorptions occur. W1 overlaps with a major absorption of ethylene glycol.

The two bands marked at 1087 cm^{-1} and 1043 cm^{-1} are chosen for the estimation of glycol concentration. The observed positions and intensities of these two bands vary depending on the amount of water present and on the duration of the contamination. If ethylene glycol is present and undetected in an engine for a long period, it does oxidatively degrade to a variety of compounds including aldehydes, ethers, and condensation compounds. In extreme cases it will polymerize to form a gel. Therefore, other absorptions can be anticipated in addition or in place of the normal bands assigned to ethylene glycol if long term contamination is suspected. In the particular example shown, intensities of 46.58 absorbance/cm and 41.77 absorbance/cm were obtained for the 1087 cm^{-1} and 1043 cm^{-1} bands respectively. These values indicate that the oil is heavily contaminated and must be changed immediately. Maintenance to locate and stop the coolant leak is also indicated. As a general rule, any measurable amount of ethylene glycol is considered to be undesirable, and its presence should be diagnostic of a current or potential coolant leak.

A high value of 23623 was obtained for the integrated absorbance of the spectrum between 3600 cm^{-1} and 3150 cm^{-1}. Values of this magnitude are consistent with high levels of coolant or water

FIGURE 6

DETECTION OF SOOT CONTAMINATION AND OTHER FINELY DISPERSED SOLIDS

MAX=0.5000 A

MIN=0.0000 A

CM-1

CL2
(1980 CM-1)

CL1
(3800 CM-1)

4000   3500   3000   2500   2000   1500   1000
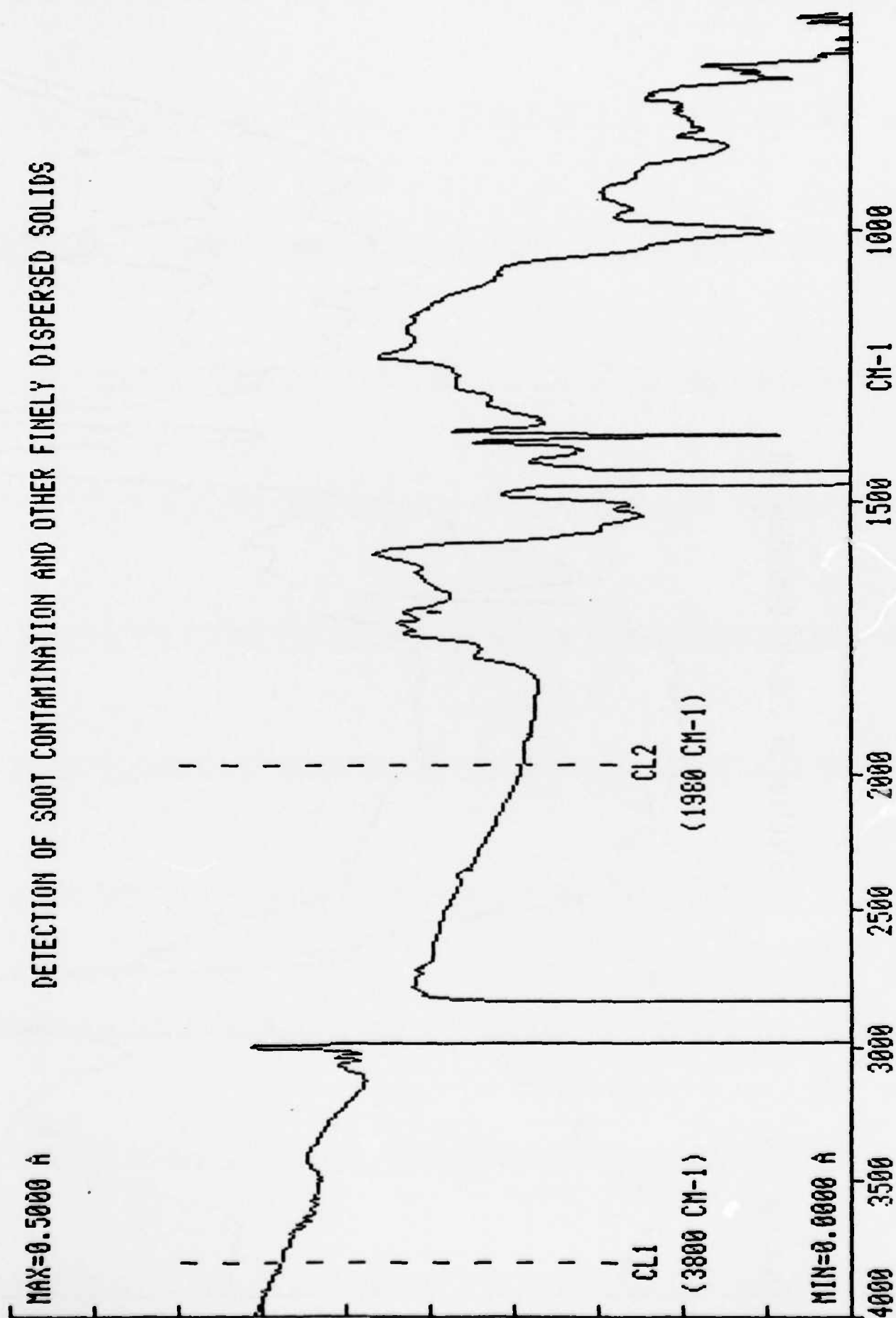
FIGURE 7

DETECTION OF COOLANT CONTAMINATION

MAX=100.00 T

MIN=0.00 T

CM-1

4000 3500 3000 2500 2000 1500 1000
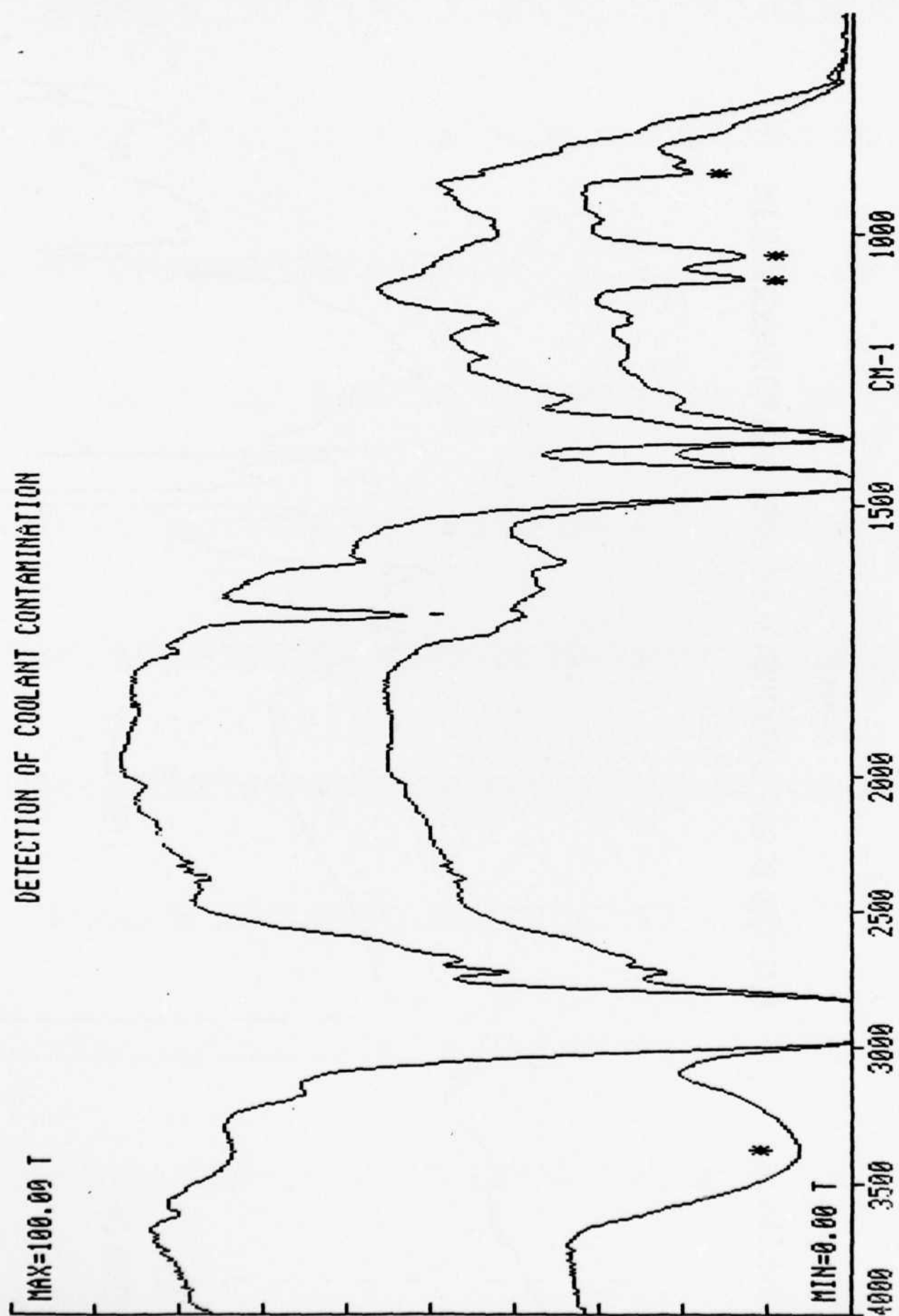
FIGURE 8

DETECTION OF COOLANT CONTAMINATION

MAX=0.9500 A

* KEY ABSORPTIONS FOR ETHYLENE GLYCOL
3370, 1087, 1043, 886 CM-1

MIN=-0.0500 A

16
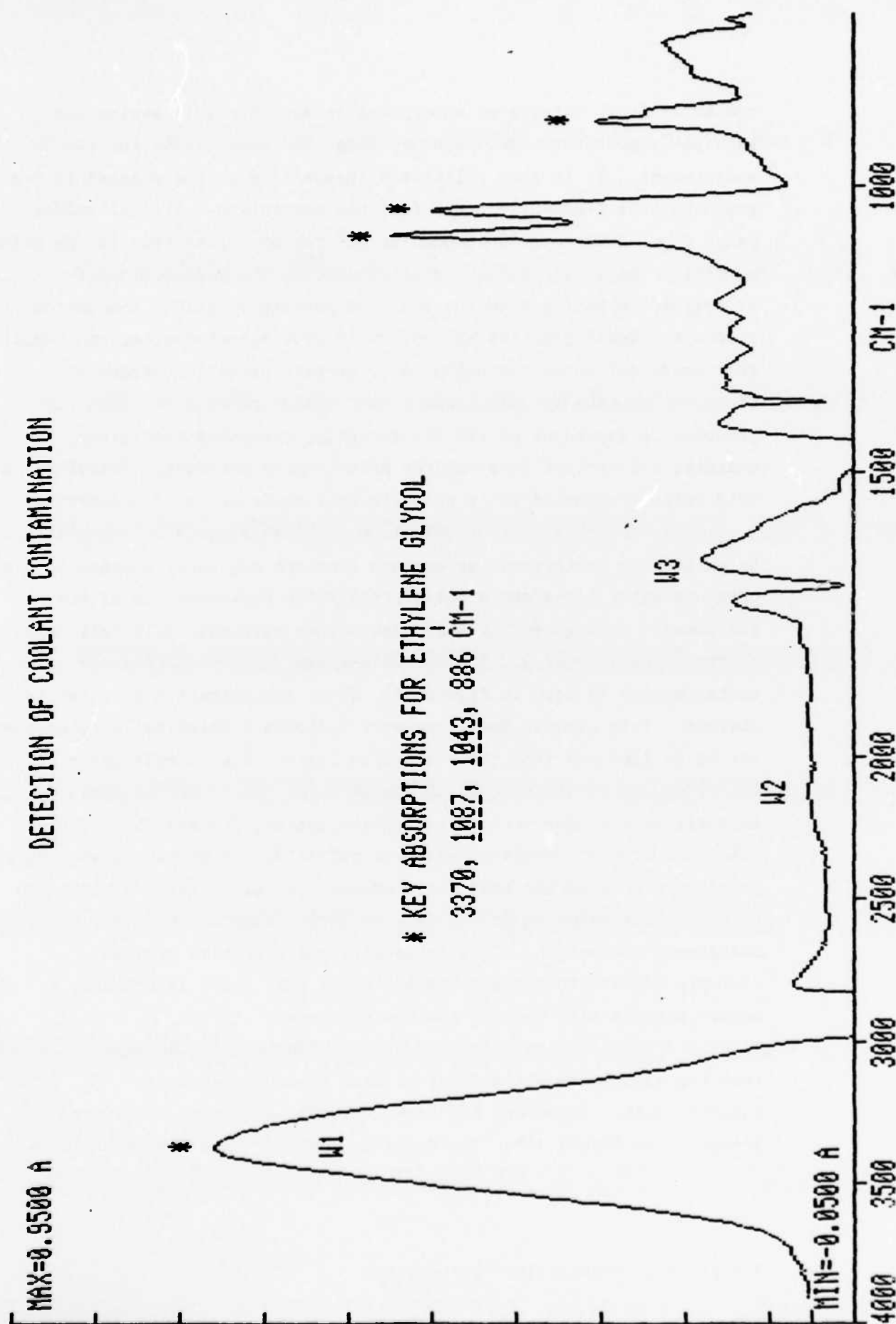
contamination. Integrated absorbance is used for this evaluation because it provides a good dynamic range and sensitivity for the measurement. It is also relatively insensitive to the changes in peak position that frequently occur for this absorption. Typical values range from -1000 to 3000 absorbance/cm^2 for an engine that is operating normally. Negative values are attributed to the consumption of hydroxide overbasing from the additive package by acidic combustion products. Small positive values, up to 3000 absorbance/cm, can result from condensation or the build-up of certain oxidation products. Condensation usually only appears as a transient component and its presence is dependent on vehicle garaging, operating conditions, humidity and ambient temperatures after engine shutdown. Therefore, if this value fluctuates it is probable that condensation is occurring.

c. Gross water contamination. The lubricants in equipment used in an aquatic environment or engines that are regularly cleaned by high pressure water hoses can exhibit gross water contamination of the lubricant. This generally only occurs when external seals fail or water enters through or around the oil filler cap. A typical example of gross contamination is seen in Figure 9*. Gross contamination by water is obvious. This example does, however, indicate a potential problem that has to be factored into the evaluation logic. The overall water absorption is so strong that it has an influence on the background intensities used for carbon loading evaluation, CL1 and CL2. The detection of high levels of water is sufficient to provide a warning for possible errors in the soot measurements. If high levels of soot and water contamination occur, it is also impossible to accurately apply the background correction. This is usually not a problem because contamination of this magnitude indicates that there is probably a severe problem with the oil and the equipment.

In samples with high water concentration, absorptions other than the main hydroxyl band may be used to determine water concentration. These are indicated with the difference spectrum presented in Figure 10*. The bands at 1640 cm^{-1} and 770 cm^{-1} can be

*Courtesy of Perkin-Elmer Corporation

17

FIGURE 9

GROSS WATER CONTAMINATION – NO GLYCOL
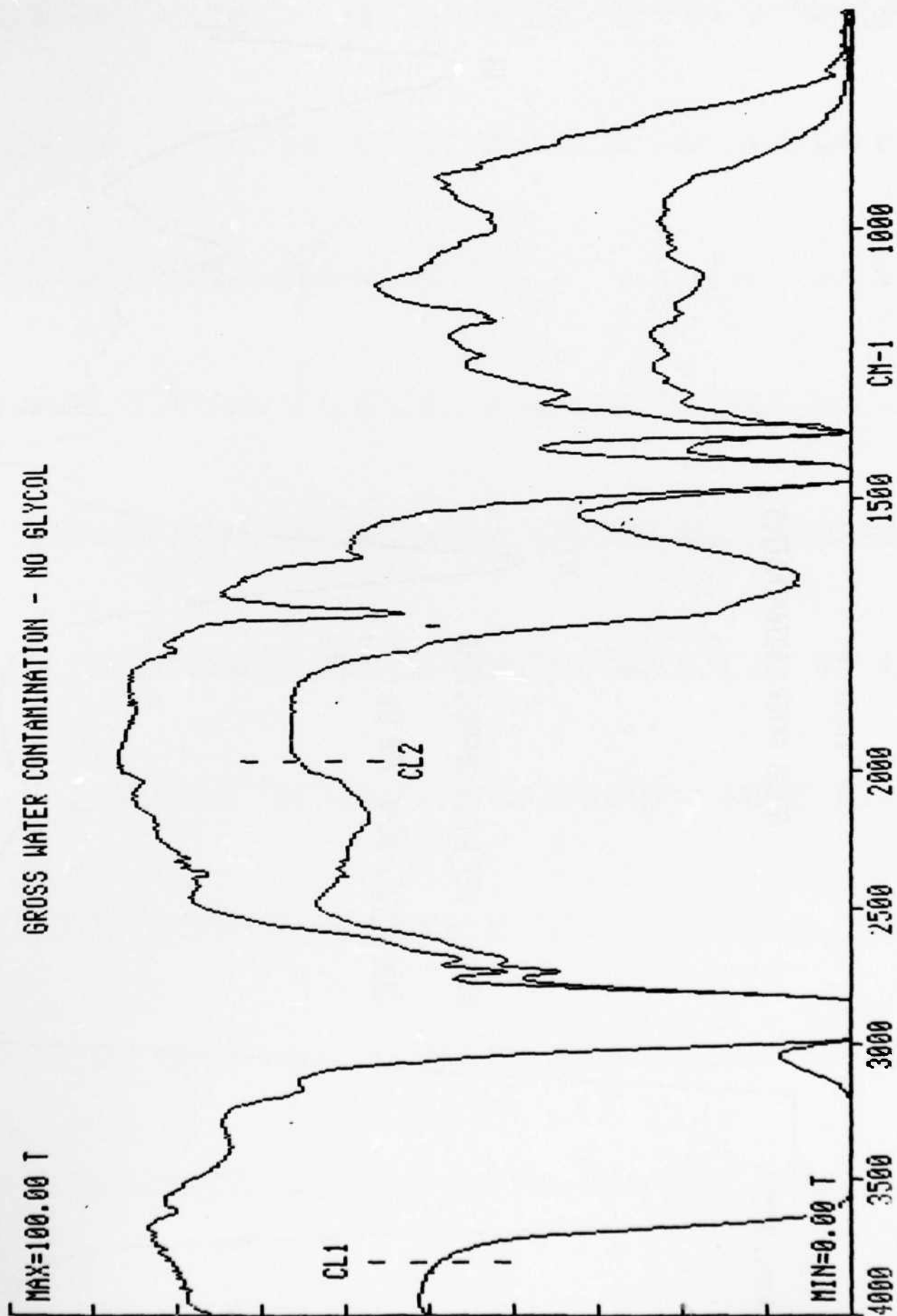
FIGURE 10

GROSS WATER CONTAMINATION

W1-W4 : KEY WATER ABSORPTIONS

3450, 2125, 1640, 770 CM-1

MAX=1.4000 A

MIN=-0.1000 A
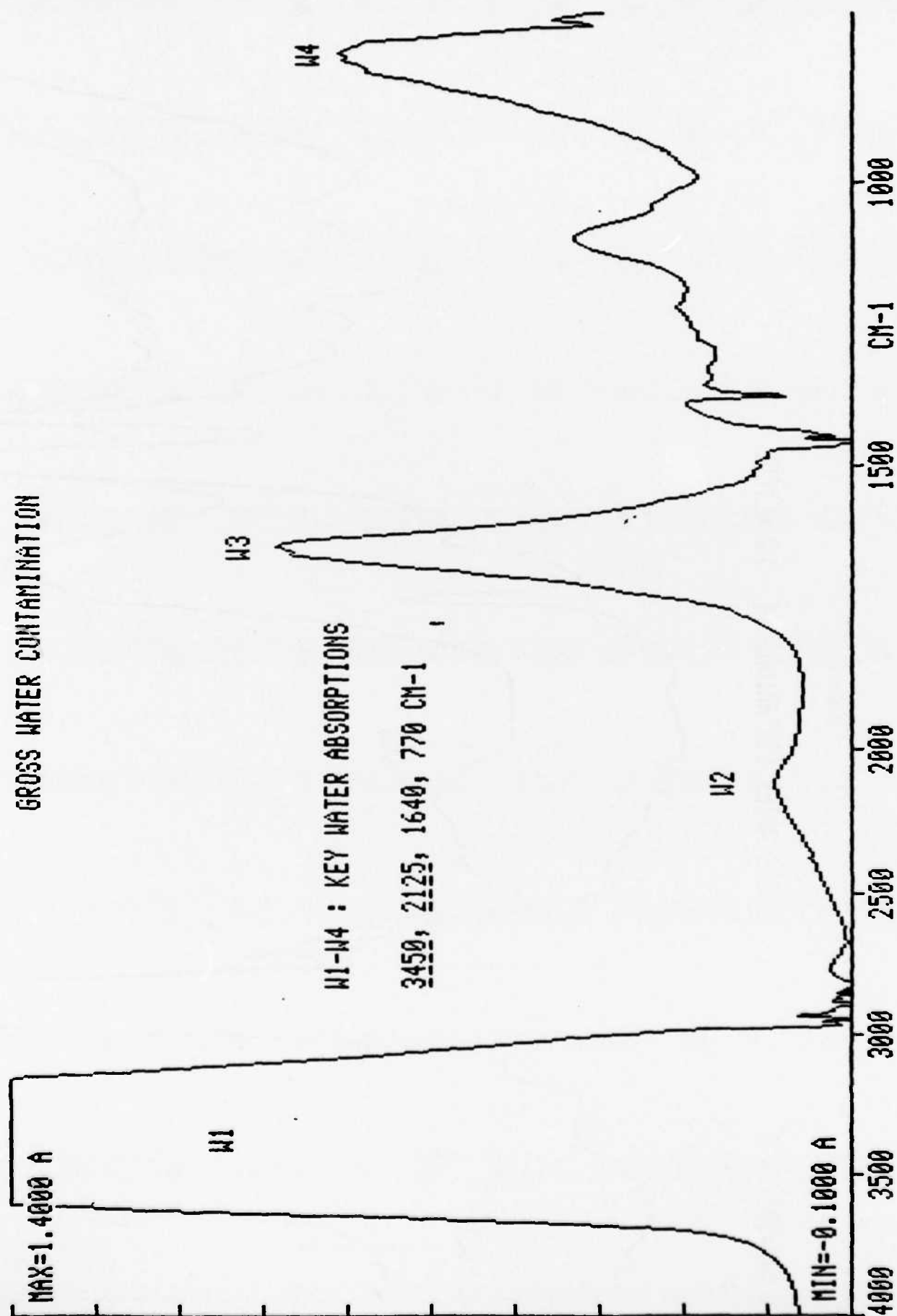
used if other contaminants are absent. Oxidation, nitration, and fuel dilution interfere at 1640 cm^{-1} and fuel dilution interferes at 770 cm^{-1}.

d. Fuel Contamination. The difference spectrum shown in Figure 11* was produced from an oil estimated to contain 5% unburnt fuel. Gasoline is relatively easy to detect in used oils either as raw, unburnt fuel or as non-volatile residues. This is due to the high aromatic content of gasoline. It is difficult, however, to give an accurate estimate of total fuel contamination. Standards prepared from fresh fuel only provide an approximate result because it is impossible to determine the total loss of fuel volatiles from the sample.

Diesel fuel dilution is more difficult to determine because it contains fewer aromatics and has a closer resemblance to the base oil than gasoline. This does not preclude the analysis, but it does reduce the sensitivity of the measurement. The measurement of diesel fuel is considered in more detail below.

4. Diesel Fuel Contamination.

The spectrum of diesel fuel closely resembles that of a hydrocarbon base oil but with a higher proportion of aromatic hydrocarbons. Figure 12 illustrates an example of high fuel dilution experienced with the LDS 465 engine in this study. The two spectra are from a fresh oil and a used sample containing approximately 20% fuel. This is clearly gross contamination and the presence of the fuel is shown by differences between the spectra. The contaminant is again more readily observed in the difference spectrum. If samples are taken frequently, then levels as low as 2-4% can be detected and the occurrence of fuel dilution can be confirmed by monitoring of the build-up. This point is demonstrated by Figure 13 where a series is studied from an early sample with only 3% fuel dilution (approximately 7.5% drop in viscosity) to a sample exhibiting 30% fuel dilution (63% drop in viscosity). A build-up in four main regions of the spectrum, FD1 (3050 cm^{-1}), FD2 (1610 cm^{-1}), FDI3 (905-685 cm^{-1}), and FD4 (473 cm^{-1}) is consistent for the samples in the series. These

*Courtesy of Perkin-Elmer Corporation

FIGURE 11

DETECTION OF FUEL CONTAMINATION (GASOLINE)

* KEY ABSORPTIONS ASSOCIATED WITH FUEL DILUTION

3052, 3024, 1605, 1034, 874, 811, 748 CM-1

MAX=0.3000 A

MIN=-0.0500 A

FIGURE 12

USED DIESEL LUBRICANT : LDS 465 ENGINE

A : FRESH OIL
B : USED OIL
(HIGH FUEL CONTAMINATION)
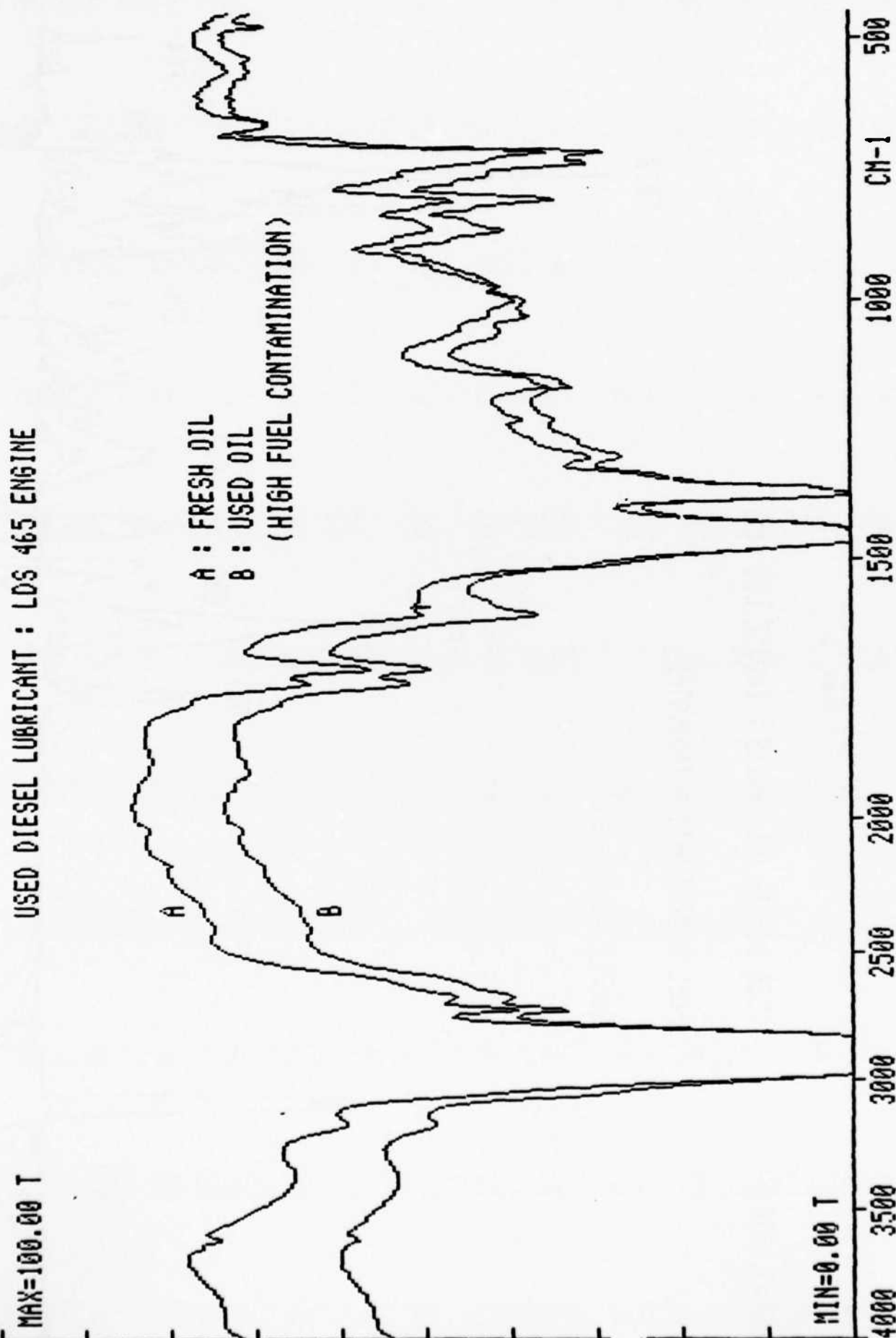
FIGURE 13

USED DIESEL OIL SERIES : ENGINE LDS 465

FUEL CONTAMINATION INDICATED

SAMPLES CD06P-CD11P

MAX=0.1750 A

MIN=-0.0250 A
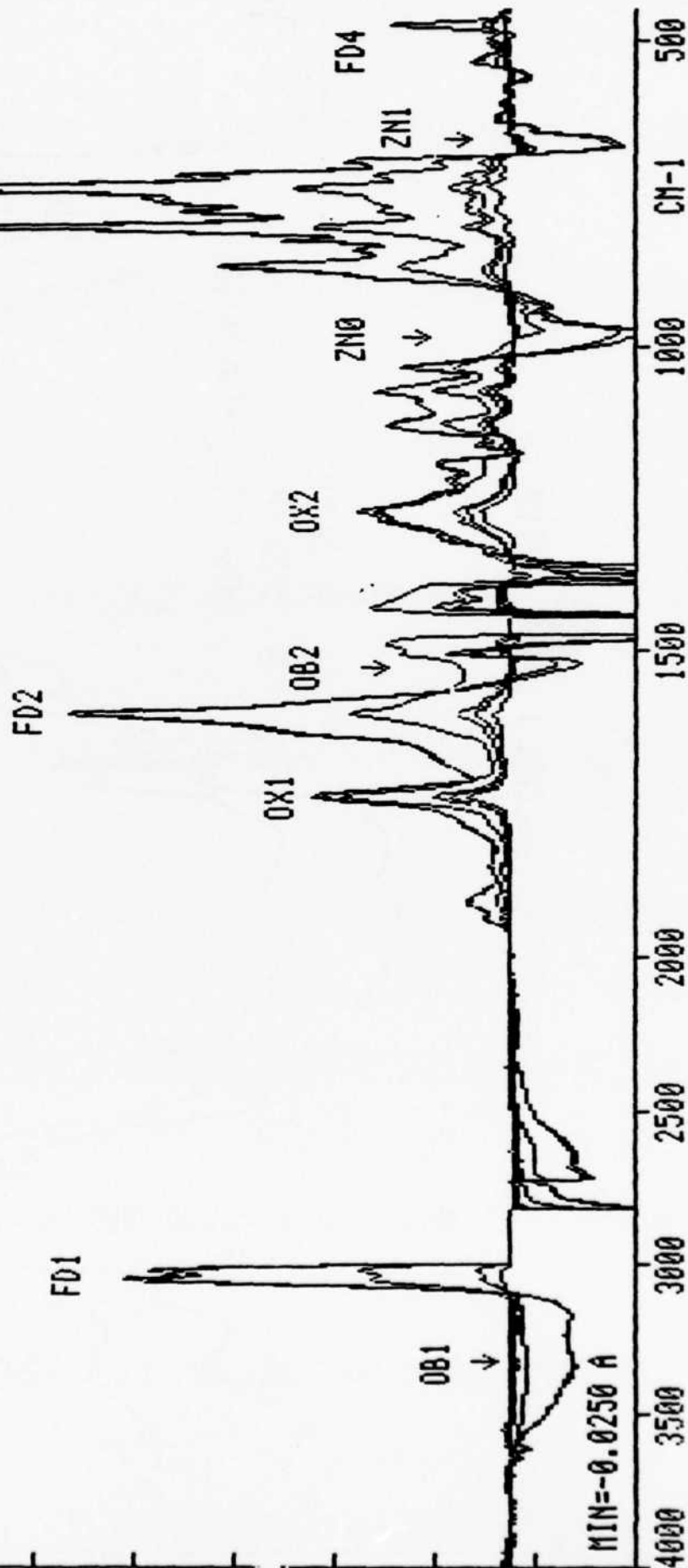
correspond to aromatic components. The small peak at FD4 is interesting because it is usually only observed to this degree in raw fuel. This fact is supported by the spectra shown in Figure 14* which were obtained from a fresh fuel and a fuel stripped of its volitile components. The presence of a peak at FD4 indicates that the contamination is from raw fuel introduced into the engine from the internal fuel lines rather than fuel introduced as unburnt fuel from the combustion chamber. Figures 15* and 16* are difference spectra generated by the subtraction of a clean lubricant from 5% fuel contaminated oil standards. The standards were produced from raw fuel (Figure 15) and evaporated fuel (Figure 16). Both spectra indicate that with a well matched reference oil it is easy to detect fuel at the 5% level. A further fact illustrated by these samples is that in the analytical measurement the contaminating fuel displaces a proportional amount of the lubricant. This results in negative regions of the spectrum. The displacement effect explains some incidences of negative values for the carbonyl region and the region between 1300 cm^{-1} and 10 cm^{-1}. Other contaminants when present at high concentrations, 5% or above, also analytically displace regions of the reference oil spectrum with the net effect of producing negative results. These negative values occur frequently in the data collected for this study.

5. Oxidative Degradation.

At elevated temperatures and in the presence of an oxidizing atmosphere and certain catalysts, an oil will undergo oxidative degradation. This is minimized in formulated lubricants by antioxidants. Once these are used, the oil will rapidly degenerate and lead to an uncontrolled oxidative breakdown. The effects of oxidation can be observed in many regions of the spectrum. The greatest effects are observed in many regions of the spectrum. The greatest effects are observed in the carbonyl region, 1900-1500 cm^{-1}. Figure 17* shows a typical profile obtained in the carbonyl region for an oil that is experiencing uncontrolled (uninhibited) oxidation. It is important to try to obtain information about the onset of this uncontrolled oxidative

*Courtesy of Perkin-Elmer Corporation

FIGURE 14

DIESEL FUEL : VOLATILES VS NON-VOLATILES

A : DISTILLATION RESIDUE
(NON-VOLATILES)
B : DISTILLED FRACTION
(VOLATILES)

25

FIGURE 15

SIMULATION OF FUEL CONTAMINATION : 5% EVAPORATED FUEL
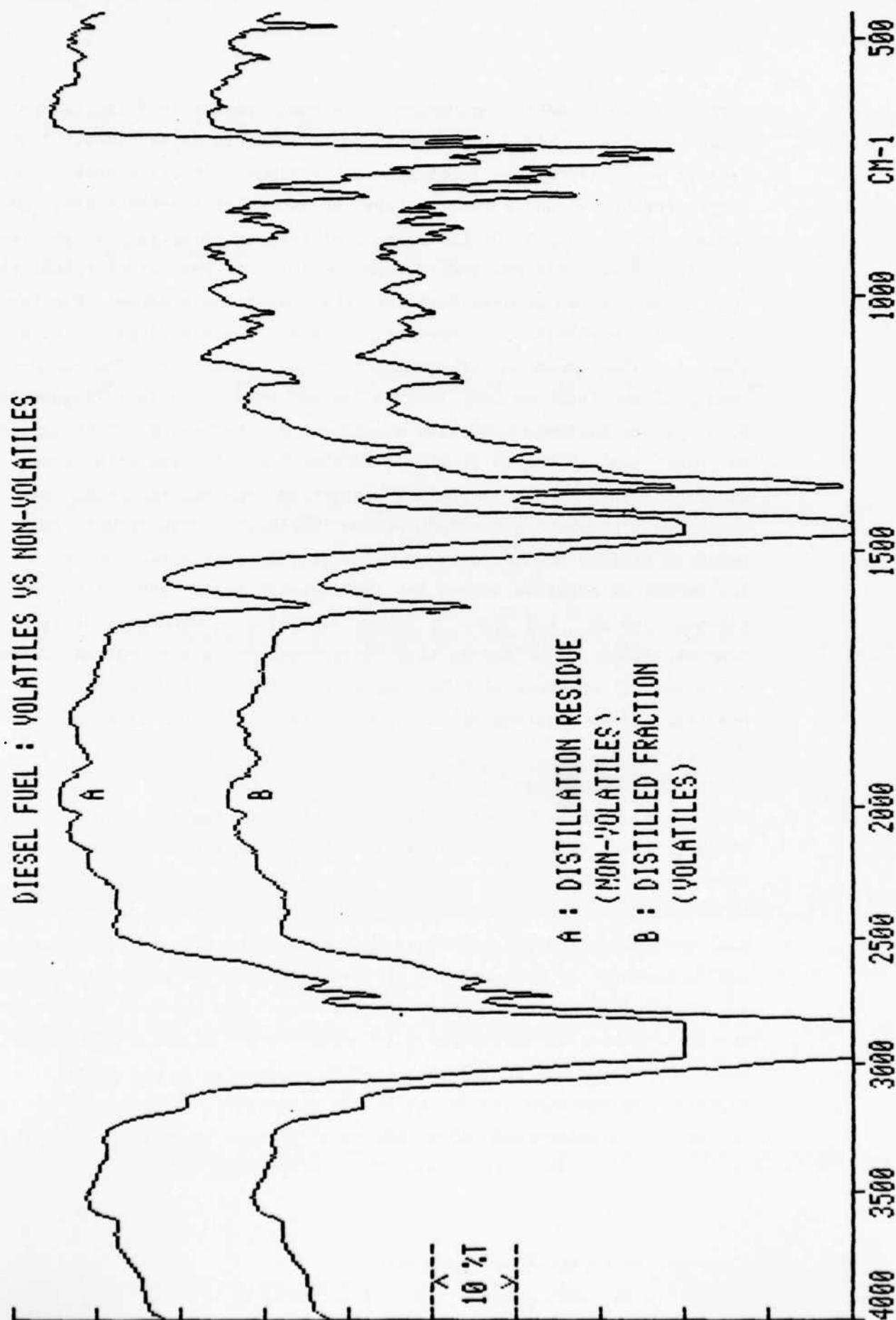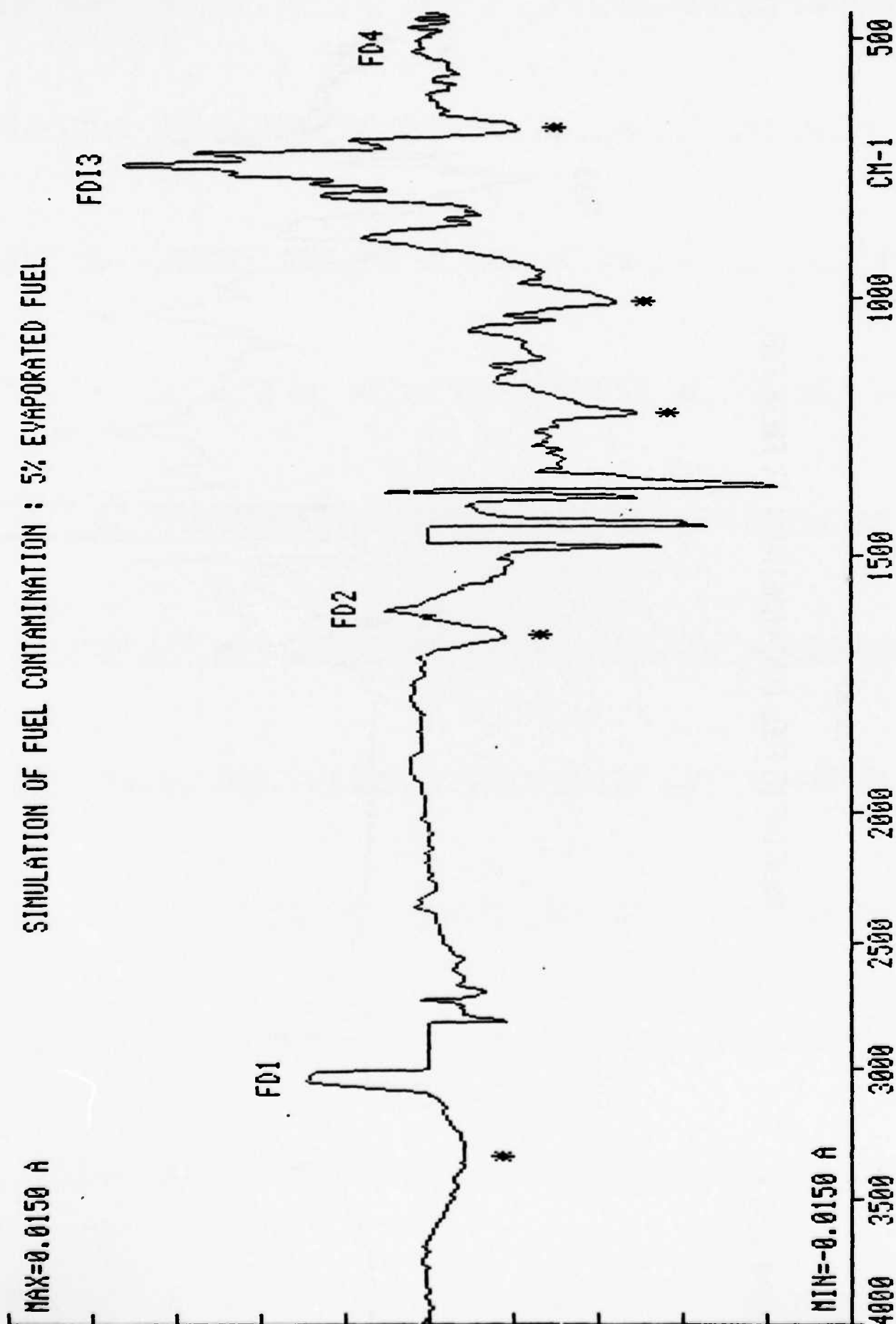
FIGURE 16

SIMULATION OF FUEL CONTAMINATION : 5% FRESH FUEL

MAX=0.0150 A

MIN=-0.0150 A
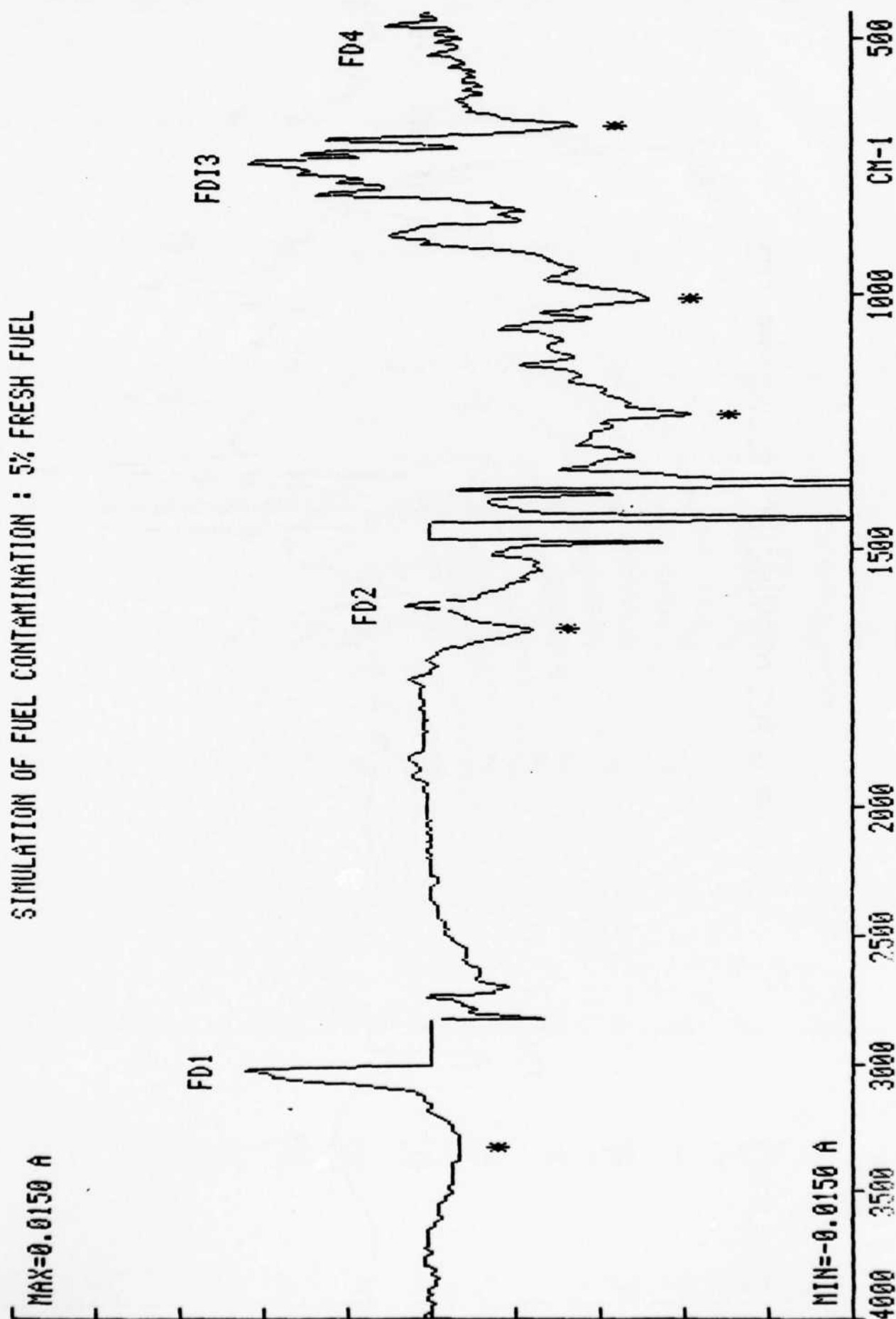
FIGURE 17

BASE OIL : SOLVENT NAPHTHENIC NEUTRAL

LAB. OXIDATION (FE/CU CATALYST)

MAX=1.1500 A

MIN=-0.0500 A

1900   1850   1800   1750   1700   1650   1600   1550 CM-1 1500

28
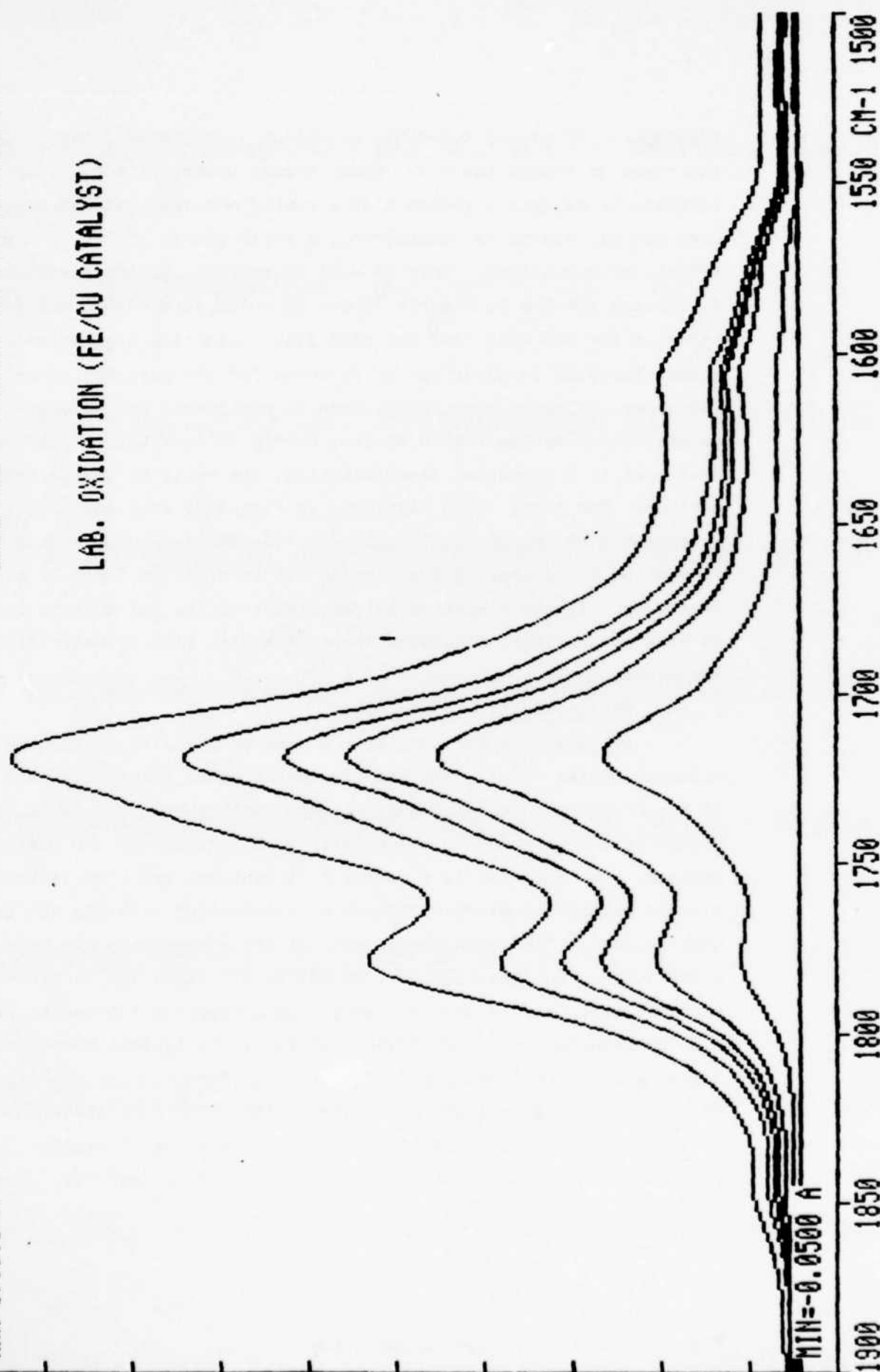
breakdown. If at any time this situation is detected, then it is important to change the oil. Under normal operating conditions a steady increase in oxidation products at a nearly constant rate is expected. Once the oil starts to deteriorate, a rapid change in the rate of oxidation is observed. This is well illustrated by the series of difference spectra in Figures 18 and 19 which show normal and failing behavior for two oils from the ASTM IIID, oxidative engine test. A very steady increase in oxidation is observed for the passing, normal oil. The other oil shows signs of failure by changes in the increased rate of deterioration by the fourth sample, barely halfway through the test. When seen in a graphical representation, the rates of change become more obvious. The three rates displayed in Figure 20 were obtained by integration of the carbonyl region for two failing and one passing oil. It must be noted that in practice an oil very seldom fails by oxidative breakdown. If the condition is detected then the oil must be withdrawn as soon as possible, otherwise there is a high risk of wear failure in the engine.

   6. Nitro-oxidation of an oil.

   As indicated earlier, some of the products of combustion are nitrogen oxides (NOx). American engines produce relatively high levels of NOx because of emission control requirements and this is an important factor in oil degradation, especially with gasoline or LPG fueled engines. The material is a powerful oxidant and can produce both nitrate esters and nitro compounds by interaction with the oil and unburnt fuel. The formation of some of these compounds has been correlated to the generation of undesirable sludges and varnishes. A standard test that is used for screening automotive lubricants is the ASTM VD sequence test. This subjects an oil to typical stop-start motoring conditions which are ideal for the formation of the nitrated species and the generation of sludges. The difference spectra obtained for scheduled samples from this test serve as a useful example for indicating the presence of nitrated compounds in a used oil. Figure 21*

*Courtesy of Perkin-Elmer Corporation

29

FIGURE 18

AUTOMOTIVE LUBRICANT : ASTM IIID TEST
SERIES FROM "PASS" SAMPLE

MAX=0.3250 A

MIN=-0.0750 A

FIGURE 19

MAX=1.6000 A

AUTOMOTIVE LUBRICANT : ASTM IIID TEST
SERIES FROM "FAIL" SAMPLE

MIN=-0.1000 A
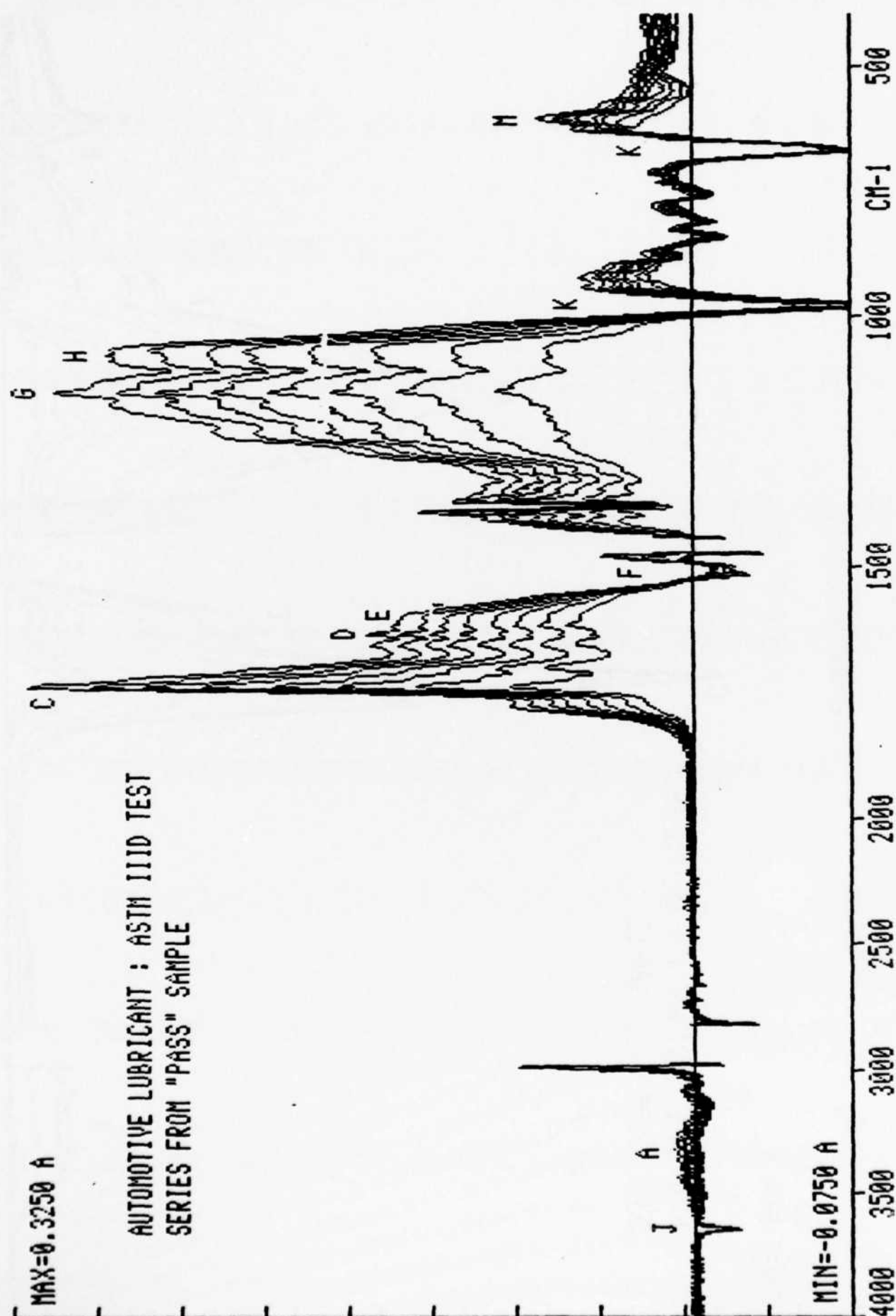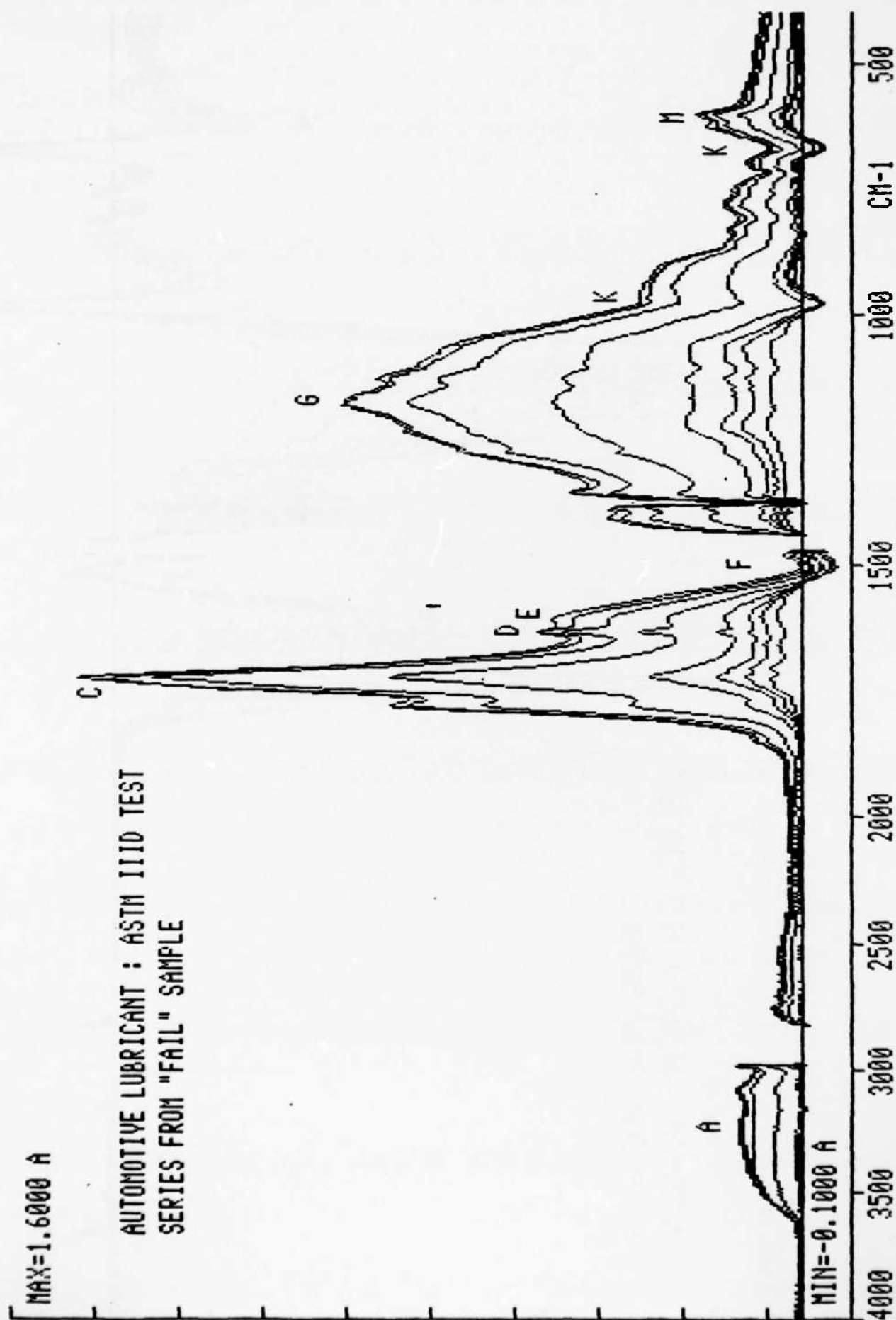
FIGURE 20

OXIDATION RATES FOR PASS/FAIL OILS

TEST: ASTM IIID, INTEGRATION LIMITS: 1880-1650 CM⁻¹

A: FAIL (WEAR)
B: FAIL (SLUDGE)
C: PASS

32

FIGURE 21

AUTOMOTIVE LUBRICANT : SAMPLES FROM ASTii VD ENGINE TEST

MAX=0.7500 A

MIN=-0.0500 A

1 : 3608 CM^{-1}
2 : 3253 CM^{-1}
3 : 3047 CM^{-1}
4 : 1718 CM^{-1}
5 : 1630 CM^{-1}
6 : 1605 CM^{-1}
7 : 1553 CM^{-1}
8 : 1336 CM^{-1}
9 : 1274 CM^{-1}
10 : 1155 CM^{-1}
11 : 1097 CM^{-1}
12 : 979 CM^{-1}
13 : 855 CM^{-1}

33
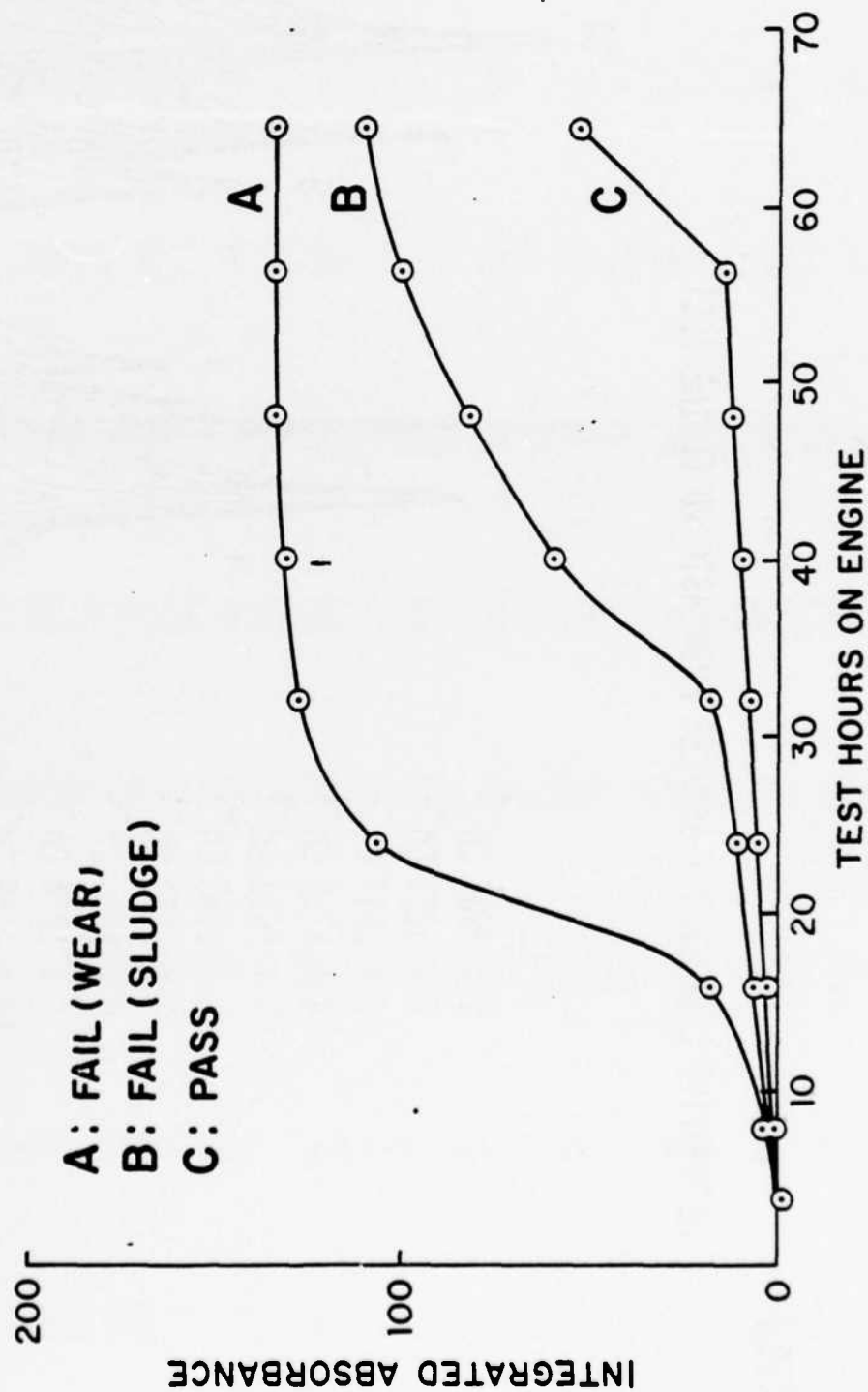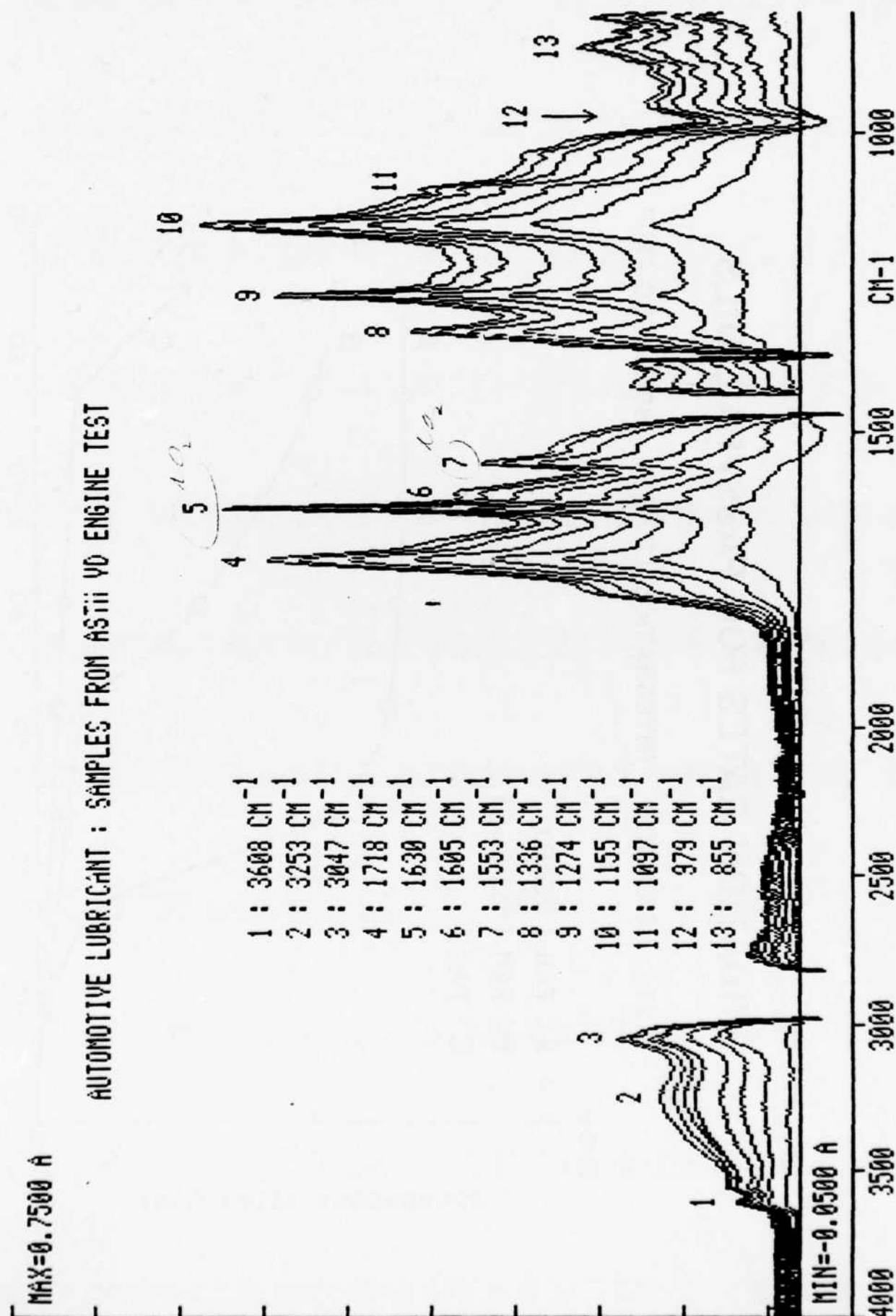
shows the progression of difference spectra with a general net increase
in overall band intensities caused by the formation of oil degradation
products. In these data, the bands at 1630 cm^{-1} (5) and 1553 cm^{-1} (7)
indicate the formation of nitroesters and nitro compounds respectively.
The intensities of these absorptions are on the high side of normal for
a modern, high performance gasoline engine equipped with positive
crankcase ventilation. LPG propelled vehicles generally show higher
levels of nitration because there is a higher air to fuel ratio in these
engines.

It is unusual to see excessively large nitration in most heavy
diesel engines. There are some exceptions as indicated by Figure 22*
which shows a high level of nitrate ester (1) in the used oil. Note
that the upper spectrum is a background corrected version of the
original, lower spectrum. If abnormally high levels of nitro-oxidation
are observed in a diesel oil then bad engine tuning is suspected. This
condition should be rectified if detected, otherwise it can lead to
excessive sludging and/or lacquer formation. Either of these situations
can result in mechanical failure.

7. Soot Formation.

The soot contamination effect that is measured in this study is
the result of a combination of light absorption and light scattering.
The main absorption of carbon is really in the visible region of the
spectrum, but the envelope is broad and its wings extend into the
infrared spectrum. This accounts for the general lowering of the back-
ground of the spectrum. The scattering of the soot particles contri-
butes to this lowering but also accounts for the slope that is observed.

The magnitude of the slope is related to the particle size. As
a rule, the larger the particles, the greater the scattering and hence
the greater the slope. This effect is demonstrated in Figure 23* by
three spectra of oils containing dispersed carbon of different average
particle sizes. The slope is appreciated in the difference spectra
generated by subtraction of the clean oil, Figure 24*. The results
shown illustrate an important feature of the analysis. A qualitative
measure of the carbon has to assume that the average particle size

*Courtesy of Perkin-Elmer Corporation

34

FIGURE 22

USED DIESEL LUBRICANT : EVIDENCE OF HIGH NOX + SO$_4$

1 : 1631 CM-1
2 : 1160 CM-1
3 : 606 CM-1

MAX=100.00 T

MIN=0.00 T
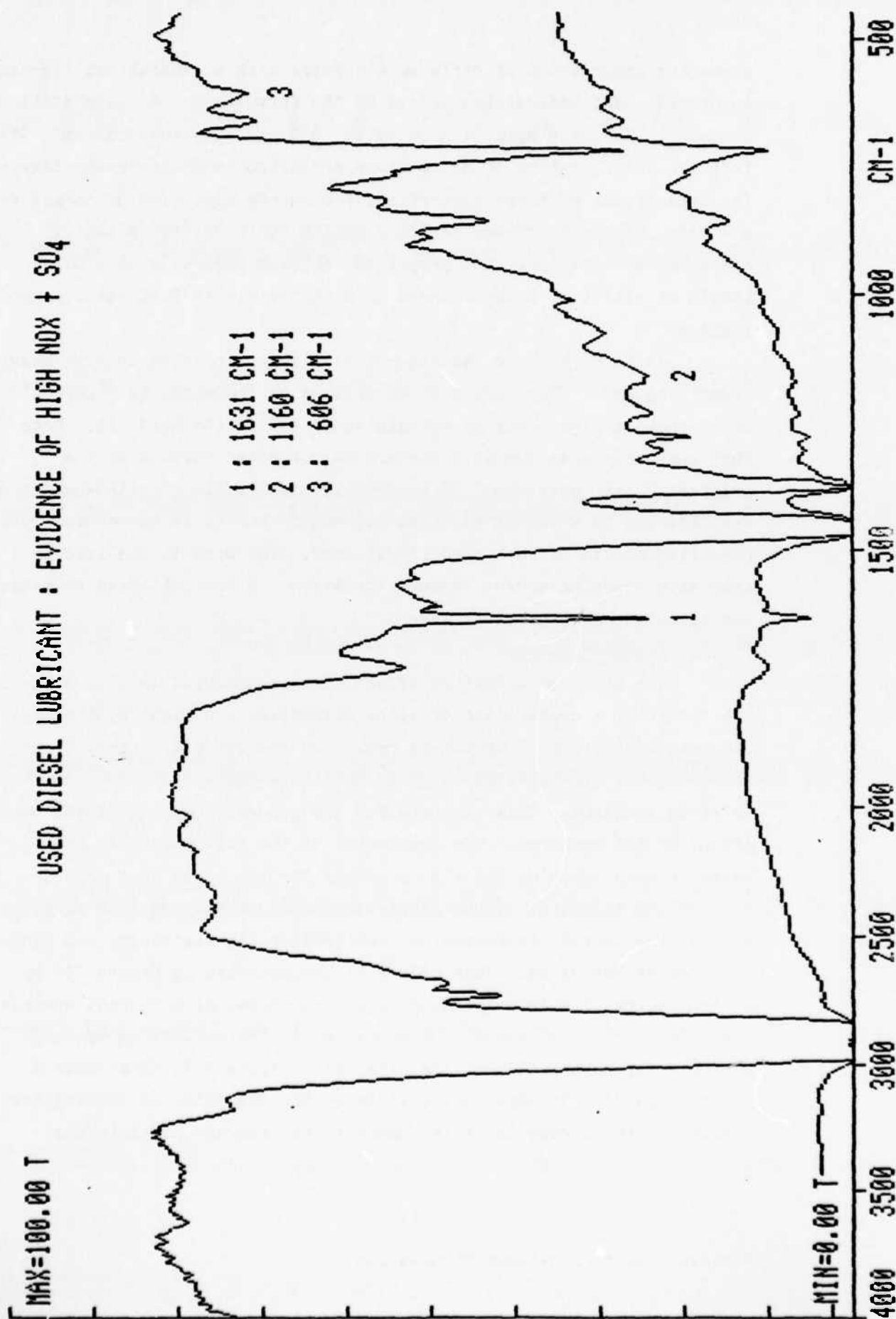
FIGURE 23

EFFECTS OF DISPERSED CARBON ON IR TRANSMISSION

COMPUTED DIFFERENCE DATA
(ABSORBANCE), 0.5% DISPERSED CARBON

B 0.13 MICRONS
C 0.25 MICRONS
D 0.50 MICRONS
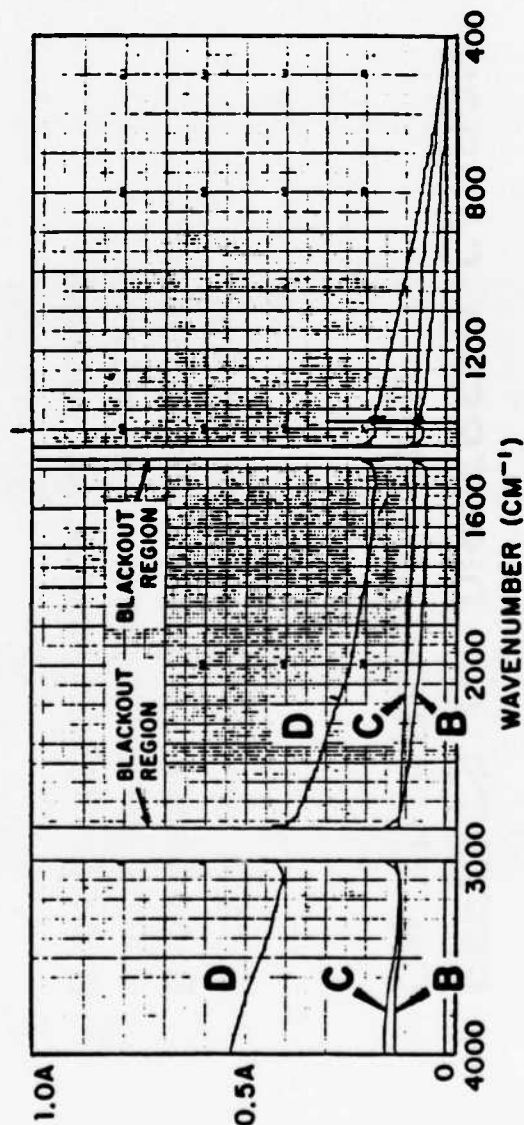
FIGURE 24

EFFECTS OF DISPERSED CARBON
ON IR TRANSMISSION

A FRESH OIL (TEXACO URSA 30 SAE HD)
B 0.5% DISPERSED CARBON, 0.13 MICRONS
C 0.5% DISPERSED CARBON, 0.25 MICRONS
D 0.5% DISPERSED CARBON, 0.50 MICRONS
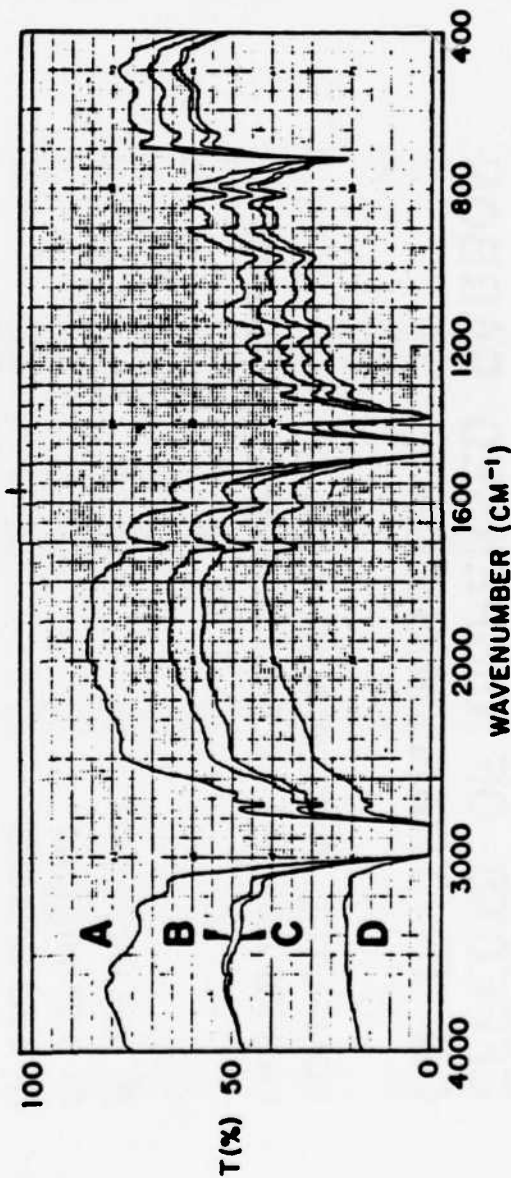
remains nearly constant. Any change in size caused by filter or additive failure obviously could have a significant effect on the measured values.

In a well-tuned diesel engine, it is normal to observe a gradual increase in carbon loading with increase in useage (hours). A typical example is provided by Figure 25 where a general decrease in transmission follows a corresponding increase in hours. Any major deviations from this rate of change can be an indication of a change in engine performance. Figure 26 shows data from the same engine but with a different oil change. The early samples in the series show a normal trend. The 18 hour sample shows a sudden drop in transmission that continues downward with the 51/52 hour samples. This is a clear indication of change in performance and in this example was probably caused by failure of the fuel injection system or over-choking caused by a blocked air filter. The whole story is well illustrated by a trend chart of the CL2 values (taken at 1990 cm^{-1} for this example) for the combination of the sample series, Figure 27.

8. Sulfate Formation.

The existence of sulfur compounds in fuels is of major concern for engine manufacturers and lubrication engineers. The main problem occurs with the combustion process where sulfur compounds are converted into sulfur dioxide and trioxide. These combine with water vapor, also formed in the combustion, to produce sulfuric acid. If unchecked this would produce a major corrosion problem in the engine. Crankcase lubricants are formulated with a base reserve to neutralize any of the corrosive acids formed by combustion. Typically, these are the hydroxide or carbonate overbased detergent additives. A normal sulfur level for diesel fuel is 0.4%-0.5%. Certain geographical regions of the world, such as South America, can have sulfur levels as high as 2.0%.

As part of an oil monitoring program, it is important to consider monitoring the rate of consumption of the overbased additives and/or the rate of formation of sulfate neutralization products. This is especially important if a high sulfur fuel is to be used. The effect

FIGURE 25

M35 MULTI-FUEL TRUCK   OIL GRADE : 30

OIL :   1.   422 HRS
        2.   425 HRS
        3.   445 HRS
        4.   481 HRS
        5.   496 HRS

MAX=100.00 T

MIN=0.00 T

OILS 1 - 3

OIL 4

OIL 5

CM-1

39

FIGURE 26

MAX=100.00 T

M35 MULTI-FUEL TRUCK   OIL GRADE : 30

OIL : 7.   2 HRS
      8.   5 HRS
      9.   7 HRS
      10.   15 HRS
      11.   18 HRS
      12.   51 HRS
      13.   52 HRS

OILS 7 - 10

OIL 11

OILS 12/13

MIN=0.00 T

4000   3500   3000   2500   2000   1500   1000   500

CM-1

40
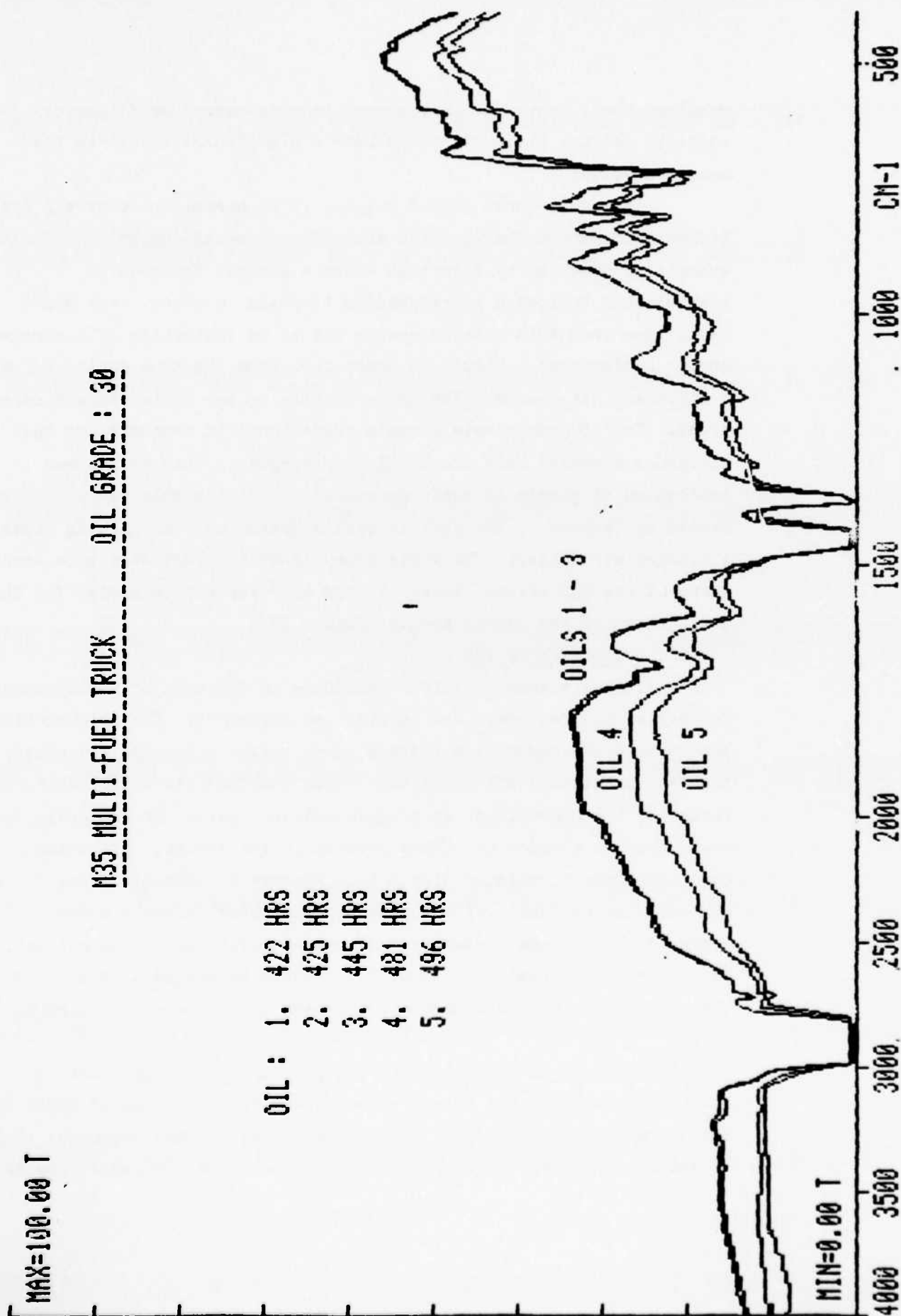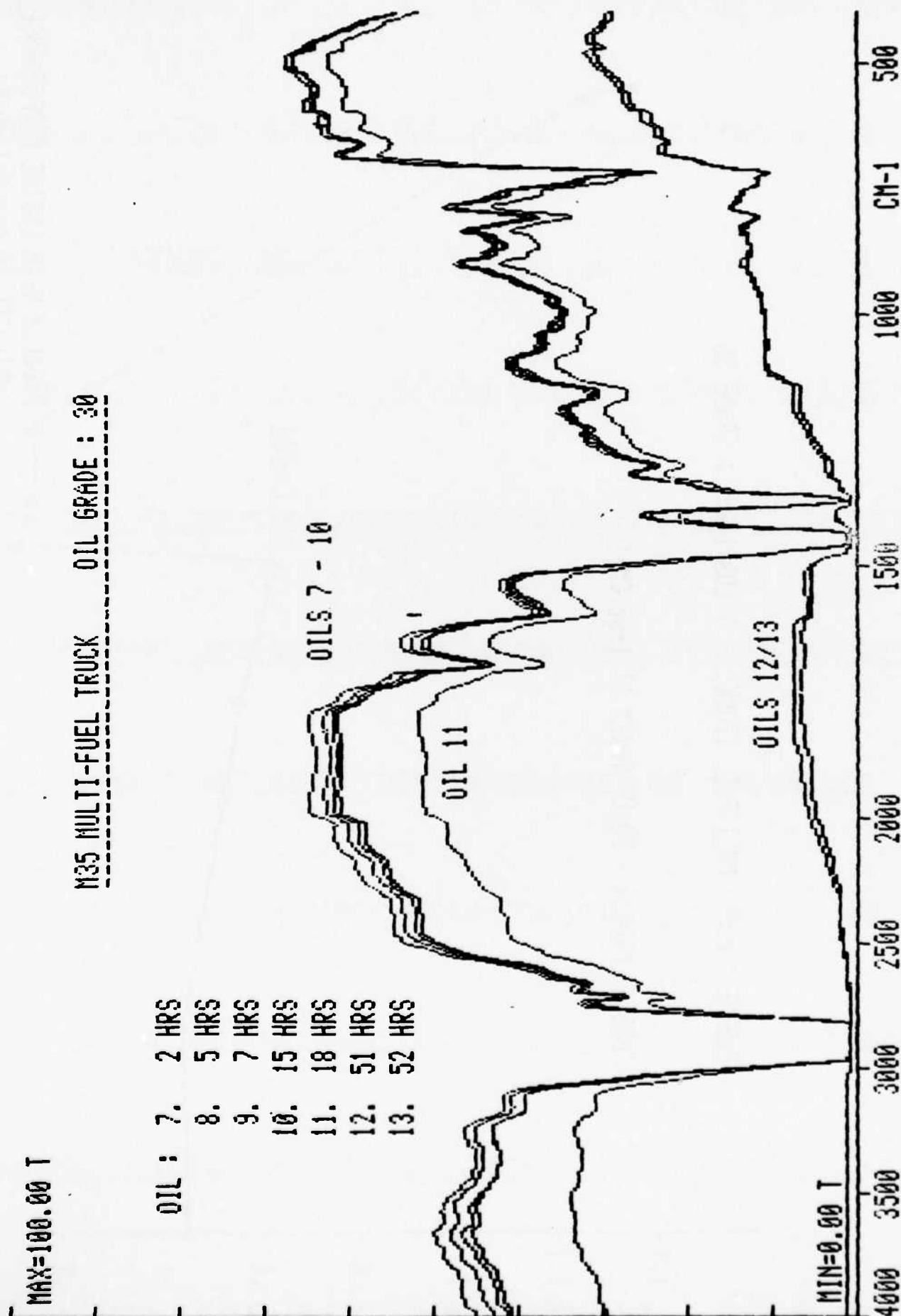
FIGURE 27

ENGINE : M35 - MULTIFUEL TRUCK   LUBRICANT : GRADE 30

CARBON LOADING - POINT TAKEN AT 1990 CM-1

41
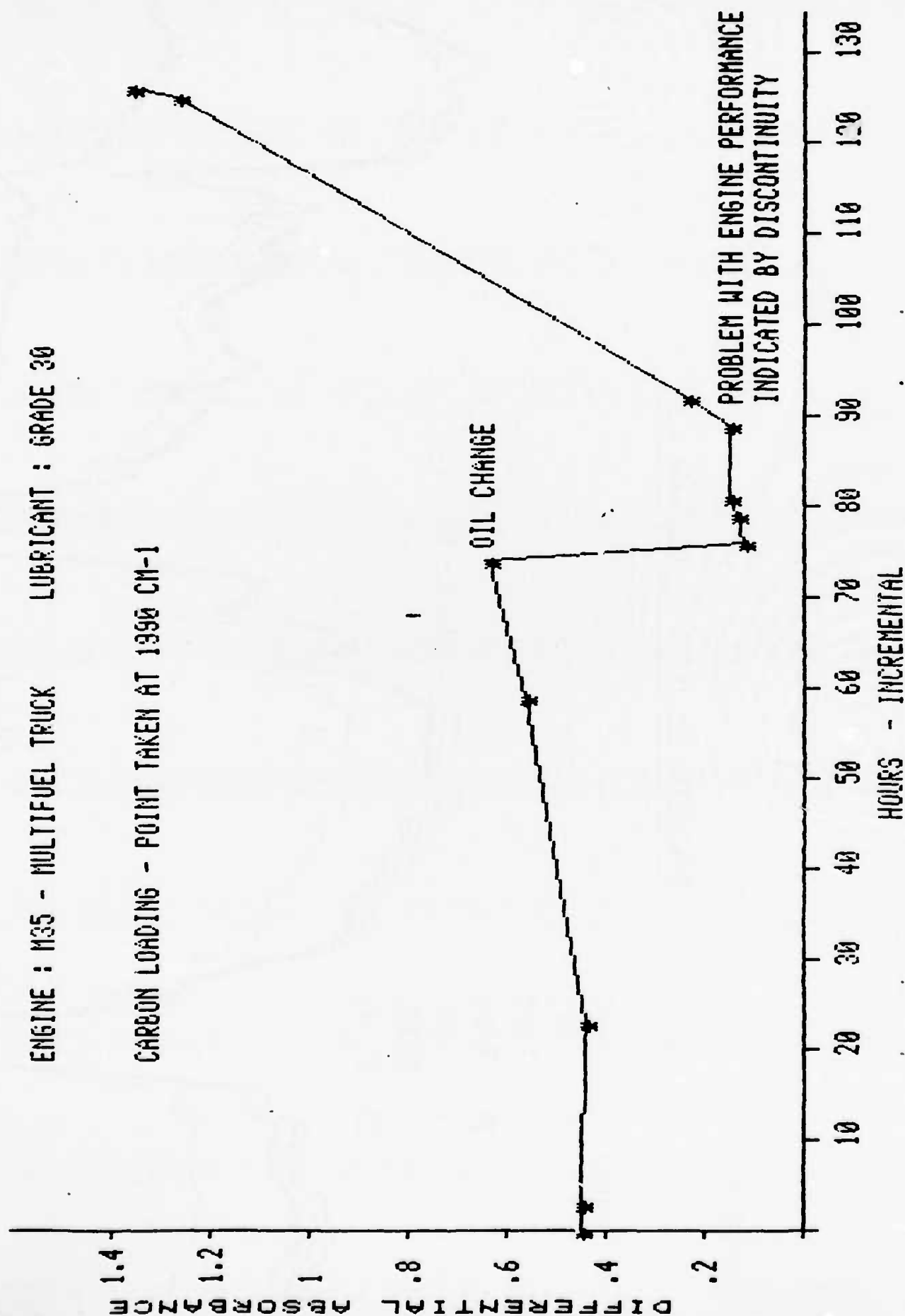
of sulfation on an average HD diesel oil (TBN=7) is shown in Figures 28*
and 29*. The asterisks in Figure 28 are intended to indicate possible
sulfate peaks in the used oil. The difference spectrum, Figure 29,
helps to demonstrate the consumption of overbased material and the
formation of metal sulfates. This particular example was generated from
a marine diesel engine operating with a fuel containing nominal 2%
sulfur.

E. <u>Summary</u>.

This section has covered the major areas of used oil analysis that
can be monitored by infrared spectroscopy. Based on the factors
discussed for condition monitoring, it has been possible to devise a
methodology for the general evaluation of the infrared spectrum. This
methodology involves the measurement of integrated areas and key
absorptions in different regions of the spectrum. It is this basic
methodology that was adopted for the work program outlined in this
report, and it is disucssed in detail in the next section.

*Courtesy of Perkin-Elmer Corporation

FIGURE 28

MARINE DIESEL : SAE 30 / TBN = 7   (FUEL CONTAINS HIGH SULFUR)

A : FRESH OIL
B : USED OIL - 713 HOURS

* CALCIUM SULFATE BANDS

MAX=100.00 T

MIN=0.00 T

43

FIGURE 29

MARINE DIESEL LUBRICANT : HIGH SULFUR FUEL

* CALCIUM SULFATE BANDS

ADDITIVE LOSS :
OB1 - HYDROXIDE OVERBASE
OB2/OB3 - CARBONATE OVERBASE
Z1/Z2 - ZDDP

MAX=0.2800 A

MIN=-0.1200 A

44
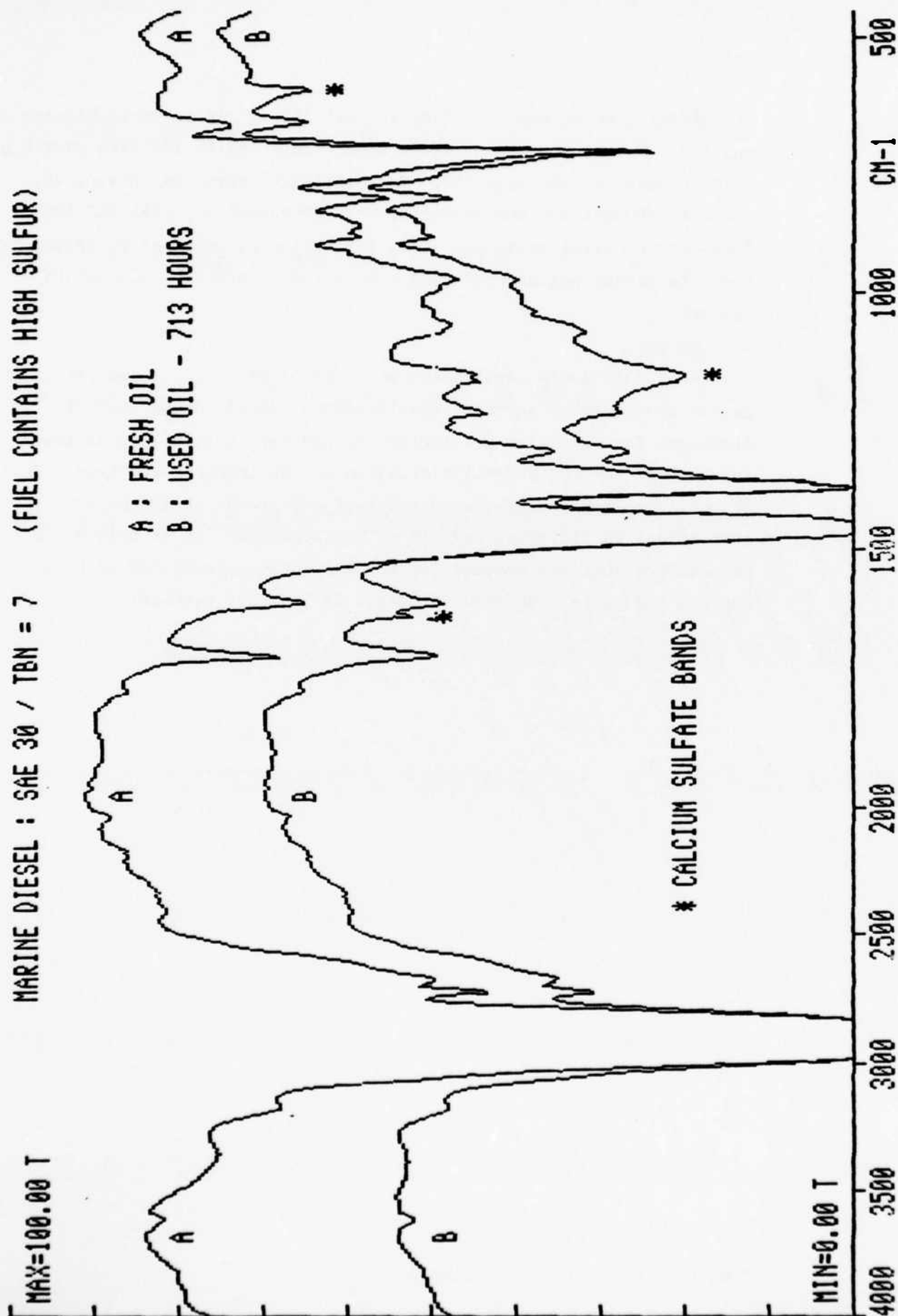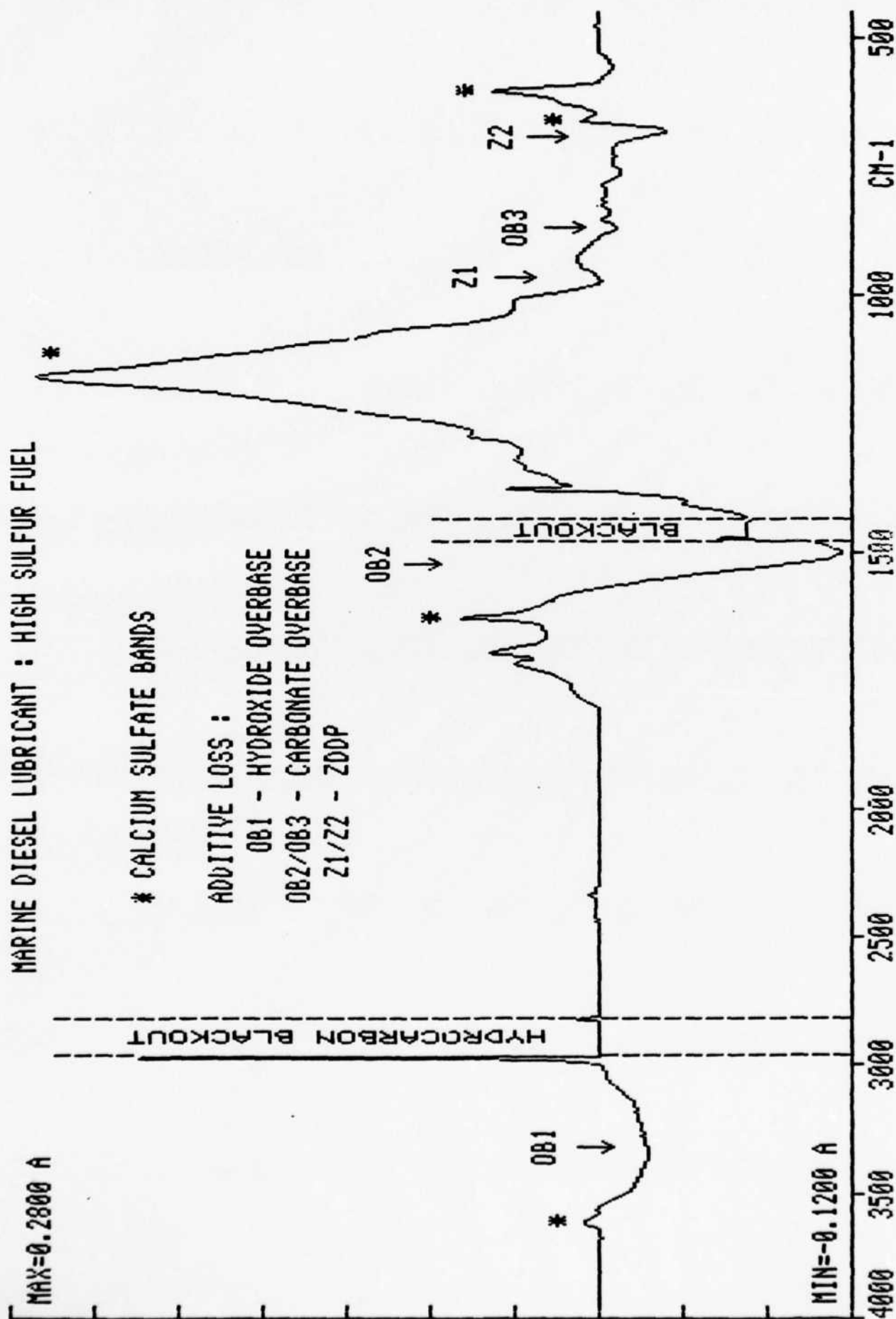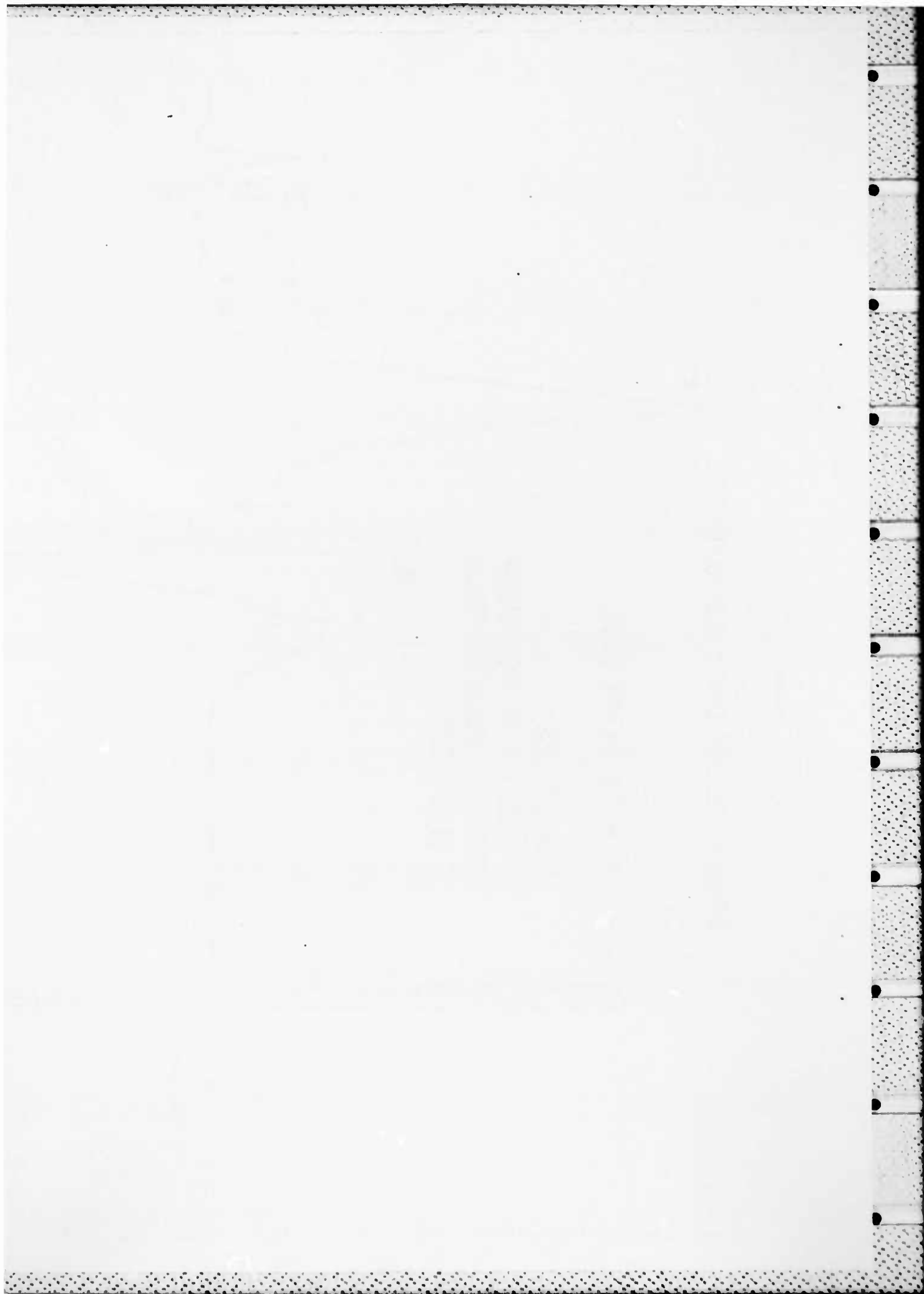
SECTION III
PROCEDURES

A. <u>Infrared Analysis Technique.</u>

1. <u>Instrument.</u>

The infrared spectrophotometer used in this study has its own
local microprocessor which carries out the functional control for
operation of the instrument. It also provides an intelligent inter-
face for communication with an external computer. The data system
has the necessary software for external control of the instrument, data
acquisition, and full data processing. Magnetic hard and/or soft disk
storage is used for bulk storage of data and programs. Using a
computer-based method, a differential infrared experiment can be
produced efficiently at any time independently of the infrared
instrument. The spectra of the fresh oil reference and the used oil
sample are obtained independently; however, in the same sealed cell.
Both spectra are recorded into the computer then compared by a program
specifically written for producing differential data. The methodology
operates by converting both spectra into absorbance format and then
carrying out a subtraction. The result, the differential spectrum, is
stored in the computer in absorbance format. It is available for
further calculation and, if required, archival storge on floppy disk.

Two types of sealed cells were used for the experiments in this
study: potassium bromode (KBr) for samples with zero or low water
content and barium fluoride (BaF_2) in cases of known coolant and/or
water contamination. A pathlength of 0.1 mm (100 microns) was used
throughout. The use of the same cell for both sample and reference is
important for a number of reasons. Obviously, it eliminates the need
for matched cells, which can be expensive, especially in the case of
barium fluoride. Also matched cells invariably do not exactly match
even with the best manufacturing processes. Any cell imperfections that
could result in photometric errors tend to be compensated by the use of
the same cell. The software does allow for variations in sample thick-
ness or pathlength in the difference calculation; and, therefore, in

45

principle a demountable cell could be used. The only occasion where a demountable cell may need to be used is when the sample is too viscous to be transferred into a standard fixed pathlength cell. In such cases, if no problems are experienced with the fresh oil, then it is likely that the sample is badly degraded or heavily contaminated. Therefore, any errors attributed to the use of the demountable cell are masked by the gross problems of the sample or the engine involved.

    2. <u>Selection of Peaks and Regions.</u>

       Selection of appropriate peaks and regions from the infrared spectra to be monitored was a primary, though implied, objective of this study. Generally speaking the regions and peaks of the infrared spectrum of hydrocarbon oils are well defined. It has been obvious from previous studies of oil condition that the degradation process varies as a function of oil formulation, engine type, operating conditions, and the frequency of top-off. Any successful monitoring program and this infrared methodology must account for continuous chemical changes in the oil. Accordingly, selection of the exact regions and areas to be monitored during this study was an iterative process, very much dependent upon judgement.

       Table 1 depicts the regions and peaks used during the final data reduction stage of the study for the LDS-465 engine and Figure 30 shows these regions and peaks on an infrared spectrum. In fact, these regions and peaks are different from those used earlier in the study when references A-1 and A-2 were written, and they include the supplemental variables for the LDS-465 engine -- Det I5, SO4, and FD4 -- not utilized in the analysis of the other engines in this study. These supplemental variables were added late in the study to account for the acidic/ketonic oxidation, sulfation, and fuel dilution that were unique to the LDS-465 engine. The earlier peaks and regions reflect an attempt to tailor the data collection to narrow regions and several specific peaks we could observe in the sequential spectra of a specific type of engine. However, as the study matured, we broadened the integrated areas in order to include all type oils and engines in a single methodology. Therefore, Table 1 reflects more a universal approach that applies to the infrared spectra of all hydrocarbon oils and engines than a highly specific approach that might be tailored to a precise oil formulation or specific engine type. Thus, the methodology collects some data that may

TABLE 1

PEAKS AND REGIONS OF THE INFRARES SPECTRA

CL2	Carbon Loading	1980 cm^{-1}
Det I1	Hydroxyl (moisture and/or organic acids)	$3600\text{-}3150 \text{ cm}^{-1}$
Det I2	Oxidation (organic carbonyl compounds)	$1810\text{-}1714 \text{ cm}^{-1}$ $(1810\text{-}1660 \text{ cm}^{-1})$[a]
Det I3	Nitration/Carboxylates[b]	$1650\text{-}1538 \text{ cm}^{-1}$ $(1650\text{-}1535 \text{ cm}^{-1})$[a]
Det I4	Sulfation/Oxidation/Glycol	$1300\text{-}1000 \text{ cm}^{-1}$
Det I5	Oxidation (mainly carboxylic acids and ketones)	$1725\text{-}1670 \text{ cm}^{-1}$ [a]
FD1	Aromatic Fuel	3040 cm^{-1} (3050 cm^{-1})[a]
FD2	Aromatic Fuel	1595 cm^{-1} (1610 cm^{-1})[a]
FDI3	Aromatic Fuel	$905\text{-}685 \text{ cm}^{-1}$
FD4	Aromatic Fuel	473 cm^{-1} [a]
ZN1	Additive, Zinc Peak	670 cm^{-1}
Coolant Leak	Glycol Peak[c]	1079.8 cm^{-1}
Coolant Leak	Glycol Peak[c]	1032.8 cm^{-1}
SO4	Sulfates	602 cm^{-1} [a]

a Modification or supplementary variables for the LD/LDS/LDT 465 Engines only

b No attempt was made to discriminate between organic nitrates (NOx) and carboxylates in this work. The predominant species detected will be indicated in the discussion provided for each engine. (Different types of engines do form NOx at different rates and therefore it may be possible to determine a characteristic "norm" for a given engine type. The NOx level and hence the potential level of organic NOx is strongly dependent of the air/fuel rates for any given engine. If an engine is running lean, a higher level of NOx is usually encountered.)

c Highlighted when observed in samples

FIGURE 30

MAIN SPECTRAL REGIONS ASSIGNED FOR USED OIL ANALYSIS

48
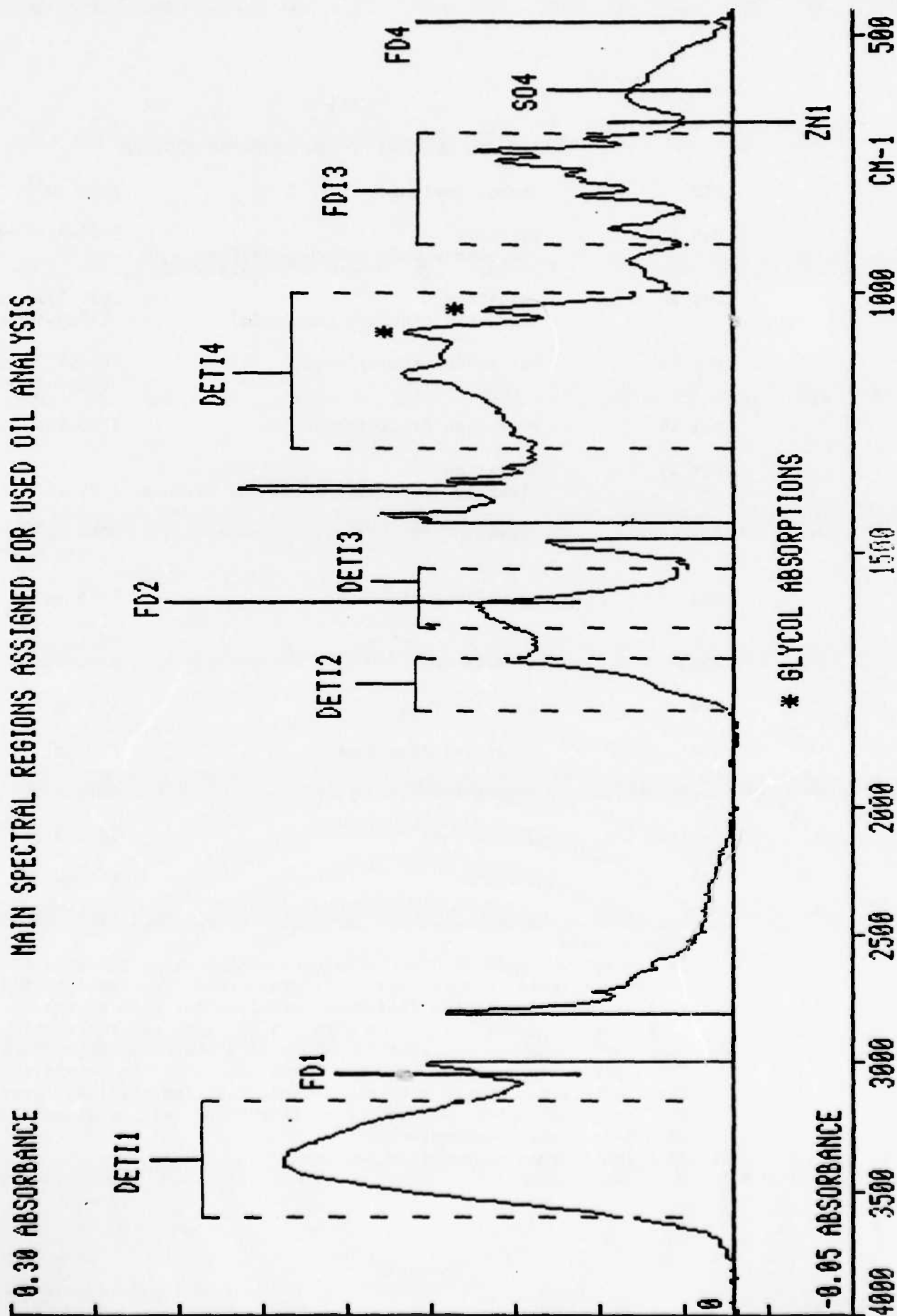
be superfluous for any specific oil formulation and engine but does collect sufficient data to profile oil degradation for most hydrocarbon oils and engines. Computer software prepared by Mr. Coates automatically calculates the area under the differential spectra for the regions of interest and measures the height of peaks of interest to obtain the necessary quantitative data.

3. Monitoring Program.

The approach described above formed the basis for our analyses of lubricants in service. To be successful, the methodology requires a sample of fresh oil. In any continuous service monitoring, it is necessary to have well-defined sampling intervals and to form a documented series of samples. This procedure enables a trend to be monitored that provides the most sensitive measure of oil and engine performance. When dealing with large scale fleet operations and field engines, these requirements present certain problems. The most difficult problem we had to accommodate was unannounced mixing of oil formulations and complete oil changes to different formulations. This circumstance is not uncommon in military operating conditions, and it adversely effects the reference oil data used in the differential calculations. We capitalized on the fact that fresher oils tend to contain less carbon to solve this problem, and incorporated a check routine into the software that compared carbon loading values of reference and test samples. Whenever a test sample contained less or nearly equal carbon relative to a reference sample, and the key regions of interest produced negative calculations, a flag was initiated. Judgement then was exercised to decide whether to accept the data as calculated or to select a new reference sample and recalculate. As a practical matter, whenever a new reference was required, the first sample in the series of samples causing the flag was selected as a new reference.

Another problem was encountered when grossly contaminated samples were analyzed. When military field engines were monitored, water and carbon contamination are occassionally so gross that the infrared radiation is absorbed by these constituents. Normally, a carbon loading correction is applied to the data to accommodate noncritical carbon build up and to isolate carbon effects from the other variables monitored. However, when carbon content exceeded

49

120 absorbance/cm, a gross level of carbon loading, the methodology
switched to measurement of carbon loading only, and no other values were
recorded.

A related, though somewhat different problem exists for high
water contamination. Like carbon, water is a very strong absorber and
can absorb all or most of the infrared energy in the hydroxyl band and
thereby adversely effect the carbon loading measurement. This causes an
incorrect carbon loading correction factor. However, the methodology
will still produce values for the other variables because of the
differential calculations. Accordingly when the hydroxyl values exceed
7500 integrated absorbance/cm relative to the reference sample, a flag
is initiated which warns that all other variables may be meaningless.
In this study we recorded only the Det I1, CL2 and the physical test
data when a high water flag was observed.

As a practical matter the appearance of these flags and the
subsequent loss of data should not adversely affect a routine monitoring
program because they are only activated when the contamination becomes
so gross that the infrared spectra are no longer useable as a diagnostic
monitoring tool. Certainly engines with this level of contamination
require immediate corrective action regardless of other indications of
degradation in the spectra. Nonetheless, for this study, we desired to
collect as much data from degraded oil samples as possible in order to
develop statistically significant evaluation guidelines.

4. <u>Analysis of Oil Samples.</u>

We obtained oil samples from US military operating activities,
and from independent test stands and laboratory experiments as shown in
Table 2. Using the technique described above, we conducted differential
infrared analyses of these samples. Table 1 shows regions and peaks of
the infrared spectra selected to be monitored during this study.
Figure 30 graphically depicts a typical infrared spectra and the regions
and peaks of interest.

In order to relate infrared data to standards more or less
recognizable to the oil analysis community, certain traditional
properties of oil condition were measured for each sample. These are
outlined in Table 3. Additionally iron wear metal was measured spectro-
metrically for each sample. These tests in Table 3, excepting COBRA
measurements, are commonly performed by many laboratories in the Joint
Oil Analysis Program (JOAP).

TABLE 2

INFRARED STUDY DATA EVALUATED

BASE	END ITEM	NO. OF END ITEMS	ENGINE TYPE	NO. OF SAMPLES
Ft. Carson	M-35 Truck	15	LDS-465	215
	M-920 Tractor	17	NTC-400	153
	M-113 APC	15	6V53T	134
	M-109 SP HOW	15	8V71T	177
	M-60 Tank	17	AVDS-1790	129
Peterson AFB	Flightline Trucks (Propane)	6	Ford 300	61
	(Ford, GM,	3	Ford 360	28
	Dodge)	2	GM 350 Chev	18
		2	Dodge 225	17
AFLRL/SWRI[a]	Diesel Test Stand,	4	6V-53T	46
	Endurance Test	1	LDT-465	14
SWRI[b]	Gasoline Test Stand Engines, IIID	6	GM 350 Olds V8	60
			TOTAL	1,052

a US Army Fuels and Lubricants Research Laboratory at Southwest Research Institute

b Engine Fuels and Lubricants Division at Southwest Research Institute

51

TABLE 3

TRADITIONAL JOAP PHYSICAL PROPERTY TESTS

1. Total Acid Number (TAN)

    - ASTM Method D664

    - Milligram KOH to neutralize all acidic materials in 1.0 gram of sample

2. Total Solids (TS)

    - Modified ASTM Method D893

    - Percent Solid Contamination

3. Viscosity (JOAP) (VIS)

    - Direct Reading Nametre Viscometer

    - Centipoise Grams/cm^3 at 75.5 $\pm$ .5°F

4. Crackle for Water Contamination (JOAP)

    - Limit exceeded/not exceeded

5. Diesel Fuel Dilution

    - Gas Chromatograph (GC)

    - Percent fuel contaminant

6. Complete Oil Breakdown Rate Analyzer (COBRA)

    - COBRA units (dimensionless)

7. Wear Metal (Fe)

The crackle test was used as a screening test for water to determine which cell to use for a given sample: BaF_2 for water contaminated samples and KBr for water-free samples. Gas chromatograph tests for fuel dilution were conducted for only those samples with viscosity measurements below 150 centipoise grams/cm^3. COBRA measurements were included solely because of JOAP interest in the COBRA and a JOAP desire to correlate COBRA measurements with other physical property tests.

B. Data Reduction.

Both the infrared derived data and the physical property data collected from each oil sample were subjected to extensive data analysis. For this study, degradation characteristics were assumed to be dependent on engine type. Accordingly data from a single engine type were grouped and analyzed independently. That is, all LDS-465 engines from the M35 truck were grouped and analyzed independently of other data. In some instances data from both field engines and bench test engines of a single engine type were available. In this case data from each source were analyzed first independently and then compared.

Simple coefficients of correlation between all possible pariwise combinations of all data variables were calculated for each engine type. These calculations were displayed as correlation matrices in the appendices and are arranged in decreasing value. Correlations of 0.5 or higher between physical property variables and infrared variables were of interest and judged to support our basic hypothesis that the infrared spectra contains information that will characterize degradation of in-service crankcase oils.

Additionally stepwise, multiple linear regression techniques were used to relate multiple variables in the infrared spectra to selected physical properties. These physical properties were viscosity (VIS), total solids (TS), total acid number (TAN), and, for selected engines, gas chromatograph percent fuel dilution (GC). The stepwise procedure was based on maximizing the coefficient of multiple determination (R^2) for candidate models. An R^2 of .75 or higher was considered significant. Initially, we had hoped to design regression models that would accurately predict these physical properties. Our intent was to use evaluation criteria existing for the physical properties with these models to judge oil condition. This goal was

53

pursued in reference A-2. As demonstrated in reference A-2, some physical properties could be accurately predicted from the infrared spectra. However, these properties are different for different engines, and the models tend to be very complex. Furthermore the chemical changes recorded in the infrared spectra may be a more generic indication of oil degradation than the traditionally measured physical properties. Accordingly we opted to develop evaluation criteria by engine type for each of the critical infrared variables independently of the physical properties. Consequently, the goal of developing predictive models for physical properties was abandoned. The regression analysis was retained, however, to identify highly significant variables, compute multiple correlation, and support our basic hypothesis concerning the relationship of infrared data to oil condition. In all cases, the physical property of interest was assumed to be the dependent variable and independent variables were assumed to be the first order, first order interactions, and second order terms derived from the infrared spectra. Stepwise development of these models are shown in the appendices. Best models were judged by maximizing R and minimizing mean square error. These models were all developed early in the study and are based on a slightly different data collection methodology than that outlined in Table 1.

Finally univariate statistics consisting of basic moments, stem leaf plots (an approximation of the data frequency distribution), normal probability plots, and frequency tables were developed for each variable for each engine type. These statistics were used to estimate tentative evaluation guidelines for significant variables by engine type. Generally the 95th percentile of the distribution of a given variable was considered to be the limit of normal occurrences, and occurrences above this point were considered abnormal. However, this judgement varied depending upon the shape of the distribution, skewness, length of tails, and secondary modes.

54

SECTION IV
RESULTS

A. Continental LD/LDS/LDT 465 Engine.

1. Background.

The LD/LDS/LDT 465 engine is a six cylinder, multi-fuel engine manufactured by Teledyne Continental Motors and used extensively by the Army in 2 1/2 and 5 ton cargo and special purpose trucks. It is normally fueled with diesel fuel. Historically, the LD-465 engine family has increased the viscosity of some lubricants and produced high blow-by which stresses the lubricant additive package. The TSC collected 215 samples from 15 engines over the course of this study. These engines were mounted in M35 trucks and operated under normal-use conditions by the 4th Supply and Transport Battalion, 4th Infantry Division, Ft. Carson, CO. The engines monitored did exhibit significant oil degradation and we added the supplemental infrared variables Det I5, SO4, and FD4 shown in Figure 1 to the data collected for this engine in an attempt to account for all the degradation effects that were occurring. These variables were not included for the other engines analyzed in this study. Additionally, the TSC collected samples from one LDT-465 engine used in a 210-hour endurance test conducted by the Army Fuels and Lubricants Research Laboratory at Southwest Research Institute (SWRI), San Antonio, TX. Fourteen samples were collected from this engine. Viscosity measurements were not performed on these bench test samples because we were unable to obtain sufficient sample volume for the Nametre viscometer. Data for the LDS field engines from Ft. Carson are in Appendix B, Table B-1, and data for the LDT test engine from SWRI are in Appendix C, Table C-1.

2. Significant Correlation.

Coefficients for correlation were computed between all possible variable pairs for the combined Ft. Carson data and separately for the single engine tested at SWRI. The correlation matrices are also included in the appendices in Tables B-2 and C-2. Correlations between infrared variables and physical property variables greater than or equal

55

to 0.5 for both the field data and the 210-hour endurance test are shown
in Table 4. These simple correlations are typically very high for the
test engine because the endurance test severely stresses the oil creating
measureable variation in the variables and because only a single engine
in a time sequence is involved. Note that gas chromatograph and
viscosity measures were not made on the test engine samples. The weaker
correlations among the field data occur because data from many engines
are combined and several interacting and possibly counteracting effects
confound the data. Between the test and field engines each of the
infrared variables except FDI3 is significantly correlated with at least
one of the physical properties.

3. <u>Regression Analysis.</u>

Stepwise regression was used to design predictive models for
viscosity, total acid number, total solids and percent fuel by gas
chromatograph from field data. These models, except the model for
percent fuel dilution, are discussed in detail in reference A-2. The
stepwise development of all models are included in Appendix B. The best
model for viscosity is in Table B-3. It has an R^2 of .66 and the
following 7 independent variables:

$(Det\ I2)^2$	FD1	FD1 x Det I3
Det I3	$(FD1)^2$	
Det I4	FD1 x Det I4	

The best model for total acid number is in Table B-4. It has an R^2 of
.76 and the following 7 independent variables:

$(Det\ I3)^2$	Det I4 x FD2	Det I3
FD1	Det I4 x FD3	
$(FD3)^2$	Det I4 x Det I3	

The best model for total solids is in Table B-5. It has an R^2 of .86
and the following 7 independent variables:

CL2	FD2	FD3
$(Det\ I3)^2$	CL1 x Det I4	
Det I4	CL1 x Det I3	

The best model for fuel dilution is in Table B-6. It has an R^2 of .77
and the following 10 independent variables:

FDI3	$(FD4)^2$	FDI3 x FD4	ZN1 x SO4
ZN1	$(ZN1)^2$	FDI3 x ZN1	
$(FDI3)^2$	$(SO4)^2$	FDI3 x SO4	

TABLE 4. SIGNIFICANT CORRELATIONS: LD/LDS/LDT-465 ENGINES

PHYSICAL PROPERTY VARIABLES

IR VARIABLE	HOURS		FE		VIS		TAN		SOLIDS		COBRA		GC	
	FIELD	TEST	FIELD	TEST	FIELD	TEST	FIELD	TEST	FIELD	TEST	FIELD	TEST	FIELD	TEST
CL2	0.502	0.984		0.969				0.918	0.803	0.970		0.688		
Det I1										-0.675				
Det I2		0.997		0.995				0.950		0.924		0.767	0.547	
Det I3		0.993		0.992				0.972		0.939	0.515	0.779	0.585	
Det I4		0.998	0.617	0.990			0.580	0.947	0.544	0.951		0.747		
Det I5		0.998		0.996				0.954		0.930		0.770	0.535	
FD1		0.547		0.847				0.828		0.942				
FD2		0.906		0.894					-0.578		0.503	0.811		
FDI3														
FD4		-0.739		-0.789				-0.654	-0.658			-0.727		
SO4		0.927		0.925				0.832	0.542	0.959		0.536		
ZN1										-0.615				

This model will be discussed further in paragraph 4 below.

The best models for total acid number, total solids, and percent fuel all had an R^2 value above .75, and we considered them to be significant in this study. The models are complex involving second order effects and first order interactions and do not account for all variation in the data. However, the total solids model is exceptionally good and as seen in Table B-5, certainly predicts solid contamination for this engine within the tolerances necessary for an oil monitoring program. The model for viscosity is somewhat less efficient than the others (R^2=.66); however, even this model has a multiple correlation of .81 and shows the strong relationship between viscosity and the infrared spectra. Our inability to design a better model for viscosity was most likely due to our lack of control in this experiment. Oil make-up and oil changes were not documented with fresh oil samples, and this affected the accuracy of the reference oil in the infrared differential experiment. Predictions from the best total acid number and percent fuel models are also in Appendix B and they show generally good results.

4. Fuel Dilution.

This engine has a characteristic fuel dilution problem that is caused by cross-over fuel lines that are routed through the engine lubricant. Accordingly, gas chromatograph (GC) analysis was performed to determine fuel dilution of 93 samples with viscosity values below 150 centipoise grams/cm^3. The variables FD1, FD2, FDI3, and FD4 were included in this methodology to monitor this fuel dilution characteristic. Unfortunately, none of these variables individually were highly correlated with percent fuel. Accordingly we sought optimal linear combination of these variables to account for the fuel dilution. As described earlier, stepwise regression analysis was used to design the best model using the complete data set to predict fuel dilution for this engine. This model included terms with ZN1 and SO4. This best fuel dilution model is used to predict fuel dilution for every observation in this data set and the results are in Table B-6. For those observations that included a gas chromatograph analysis of fuel dilution, the difference between observed and predicted values is also included. Finally, 90% confidence limits for the individual predictions are listed. Although this model does not account for all or nearly all of the variation in fuel dilution in this data set, the predictions are

58

sufficiently good to make oil monitoring decisions, and they support our basic hypothesis that fuel dilution may be measured from the infrared spectra.

5. Representative Engine.

A single engine from the field engines was selected to highlight the change in infrared data over sequential samples. Data from this engine are shown in Table 5. Spectra in Figures 31 and 32 are plotted for samples CD07A through CD12A. These samples are sequential without oil change and range from 2 through 51 hours on the oil. Figure 31 shows the sequence of simple infrared transmittance spectra. Note the spectra changes slowly but progressively through sample CD10A, changes noticeably for CD11A, and changes drastically for CD12A. This phenomenon is typical for these field engines and is indicative of pro-gressive build up of carbon in the oil sample. In fact carbon is so extensive in oil sample CD13A and so little infrared radiation is trans-mitted that the methodology is unable to accurately measure the remaining infrared variables (see Table 5). Figure 32 shows the sequence of differential absorbance spectra. Note that the carbon loading correction algorithm in the differential spectra software is working for these examples, and samples CD07A through CD11A show a small, gradual increase from the fresh or reference oil. However, in sample CD12A a drastic change is apparent, notwithstanding the carbon loading correction. The high water content of CD13A effects the carbon-loading values and causes the carbon-loading correction algorithm to be incorrect. The methodology produced a warning for this sample and remaining variables were not calculated. Aquatest IV (Karl Fisher Reagent) analysis of this sample indicates .12% water, and gas chroma-tograph analysis indicates 10% fuel. The drastic change in the differ-ential spectrum for sample CD12A is the key to an abnormal condition and would alert an evaluator during routine monitoring; however, at this point in the study abnormal thresholds for infrared variables have not been postulated. Interestingly total acid number, total solids, and crackle are within industry tolerances for this sample. Only viscosity of the physical properties indicates an abnormal condition.

6. Bench Test Data.

The SWRI bench test of the LDT-465 engine family was in accordance with the US Army, Coordinating Research Council, 210-hour

TABLE 5

PHYSICAL AND INFRARED TEST DATA - M35 TRUCK, LDS - 465 ENGINE

SAMPLE	HRS	FE PPM	VIS	TAN	%SOLIDS	COBRA	GC %	CRACKLE N	CL2	DET 11	DET 12	DET 13	DET 14	DET 15	FD1	FD2	FD13	FD4	ZN1	SO4
CD01A	422	94	130	3.16	6.8	16.5	10	N	38.99	321.12	612.66	845.70	2076.95	258.29	10.30	2.70	676.84	-0.96	0.24	1.56
CD02A	425	93	121	2.64	6.8	21.5	12	N	38.49	103.54	570.12	849.54	2228.22	254.69	11.77	0	711.17	-0.97	0.04	1.60
CD03A	445	103	96	2.61	8.8	18.0	18	N	38.43	536.55	636.26	851.01	1883.65	272.02	10.65	3.86	635.97	0.20	-0.09	2.01
CD04A	481	93	80	2.82	6.4	20.1	22	N	49.06	1669.50	707.59	1042.14	2441.57	353.56	3.86	2.48	821.30	0.09	0.22	2.13
CD05A	496	105	74	2.93	7.2	20.0	22	N	54.90	-1223.07	650.12	1014.04	2399.39	313.88	0	2.18	907.51	0.41	-0.46	2.16
CD07A	2	25	134	2.18	1.6	8.9	6	N	8.90	1076.63	159.36	352.11	723.64	89.43	2.04	1.25	596.23	-0.16	0.30	0.49
CD08A	5	29	122	2.00	2.0	6.2	9	N	10.12	606.31	150.74	352.09	713.12	79.81	2.41	1.34	603.82	0.13	0.13	0.54
CD09A	7	26	114	1.93	2.0	6.0	6	N	10.86	926.34	178.65	382.89	758.18	94.74	2.26	1.06	673.20	0.20	0.46	0.56
CD10A	15	27	112	2.00	2.0	6.1	10	N	11.31	641.58	191.27	414.23	858.03	101.00	2.68	0.99	699.71	0.20	0.28	0.41
CD11A	18	27	99	2.21	2.0	9.6	3	N	19.05	325.98	193.88	455.56	970.14	103.14	4.03	1.62	842.41	0.06	0.35	0.86
CD12A	21	42	69	2.18	9.6	15.0	14	N	112.22	5209.39	-831.57	-129.39	230.81	-450.38	0	0	771.02	0.88	0.11	1.47
CD13A	52	48	66	1.76	8.8	13.9	10	N	120.84	-------CARBON LOADING TOO EXCESSIVE-------										
CD15A	7	9	255	1.88	2.8	--	--	N	0.36	-783.60	-17.67	-47.62	35.05	-5.44	1.68	0.38	1.91	0.06	-0.63	0.47
CD16A	12	23	142	2.11	2.8	--	6	N	9.13	-1047.84	-6.23	33.71	47.41	-6.33	2.47	1.23	293.64	0.39	-1.28	0
CD17A	16	23	115	2.25	2.8	--	10	N	9.15	-1135.66	16.86	50.52	41.40	8.69	2.27	1.61	383.42	0.60	-1.40	0.49
CD18A	19	21	104	1.90	2.8	--	15	N	11.93	-904.79	100.50	121.41	103.23	21.02	4.70	2.70	411.65	0.76	-1.55	0.47

*Sample CD06A discarded as bad sample
*Sample CD14A used as reference for remaining samples

FIGURE 31

IR SPECTRA - 6 SAMPLES
US ARMY M-35 TANK ENGINE

MAX=100.00 T

SAMPLE SERIES : LDS465
SAMPLES : CD07A THROUGH CD12A
CD07A--2 HOURS
CD08A--5 HOURS
CD09A--7 HOURS
CD10A--15 HOURS
CD11A--18 HOURS
CD12A--51 HOURS

CD07A THRU CD10A

CD11A

CD12A

MIN=0.00 T

4000   3500   3000   2500   2000   1500   1000   500

CM-1

61
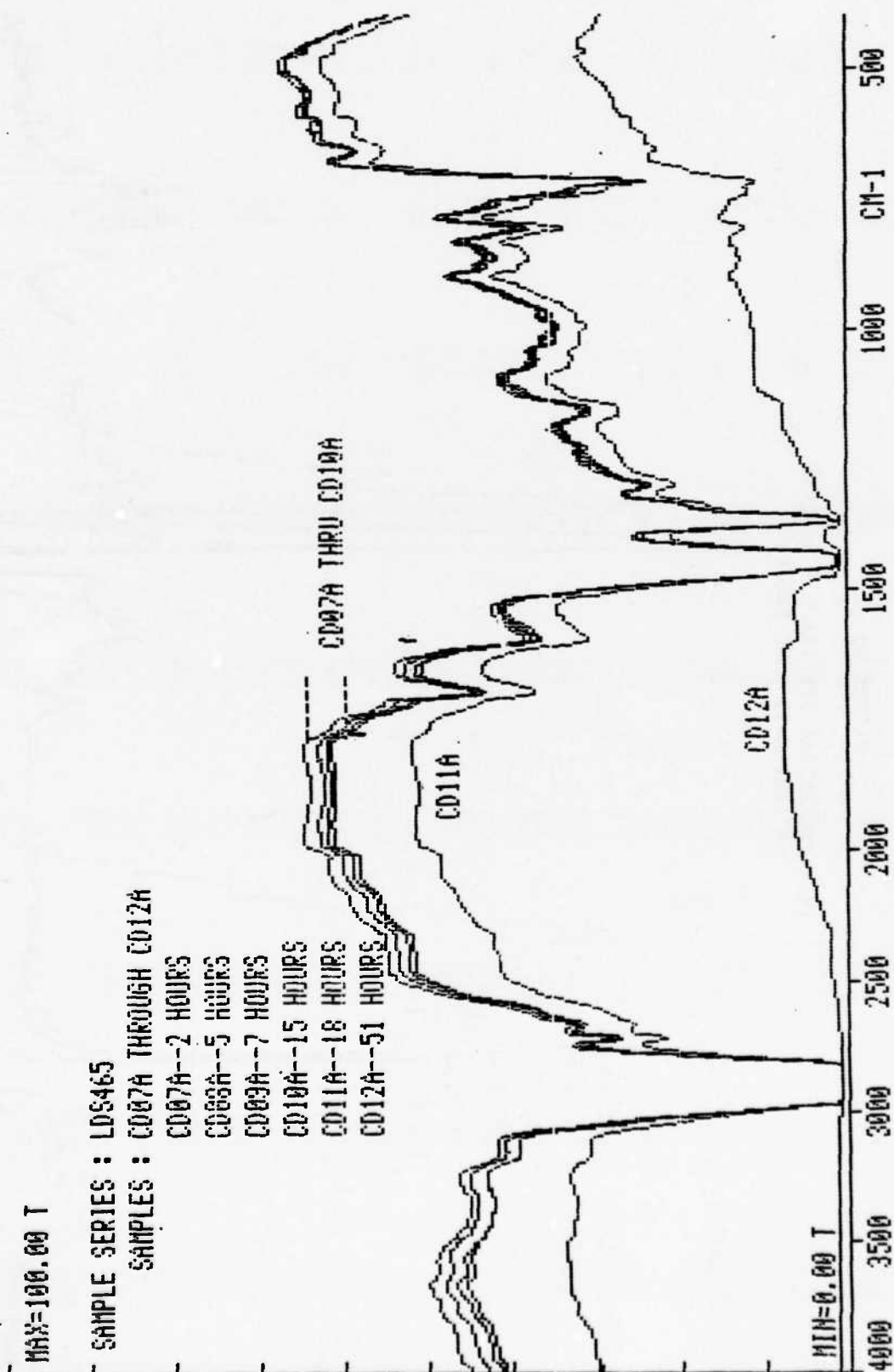
FIGURE 32

IR DIFFERENTIAL SPECTRA - 6 SAMPLES
US ARMY M-35 TANK ENGINE

MAX=0.3000 A

SAMPLE SERIES : LOS465
SAMPLES : 7=C007A
8=C008A
9=C009A
10=C010A
11=C011A
12=C012A

MIN=-0.0500 A

62
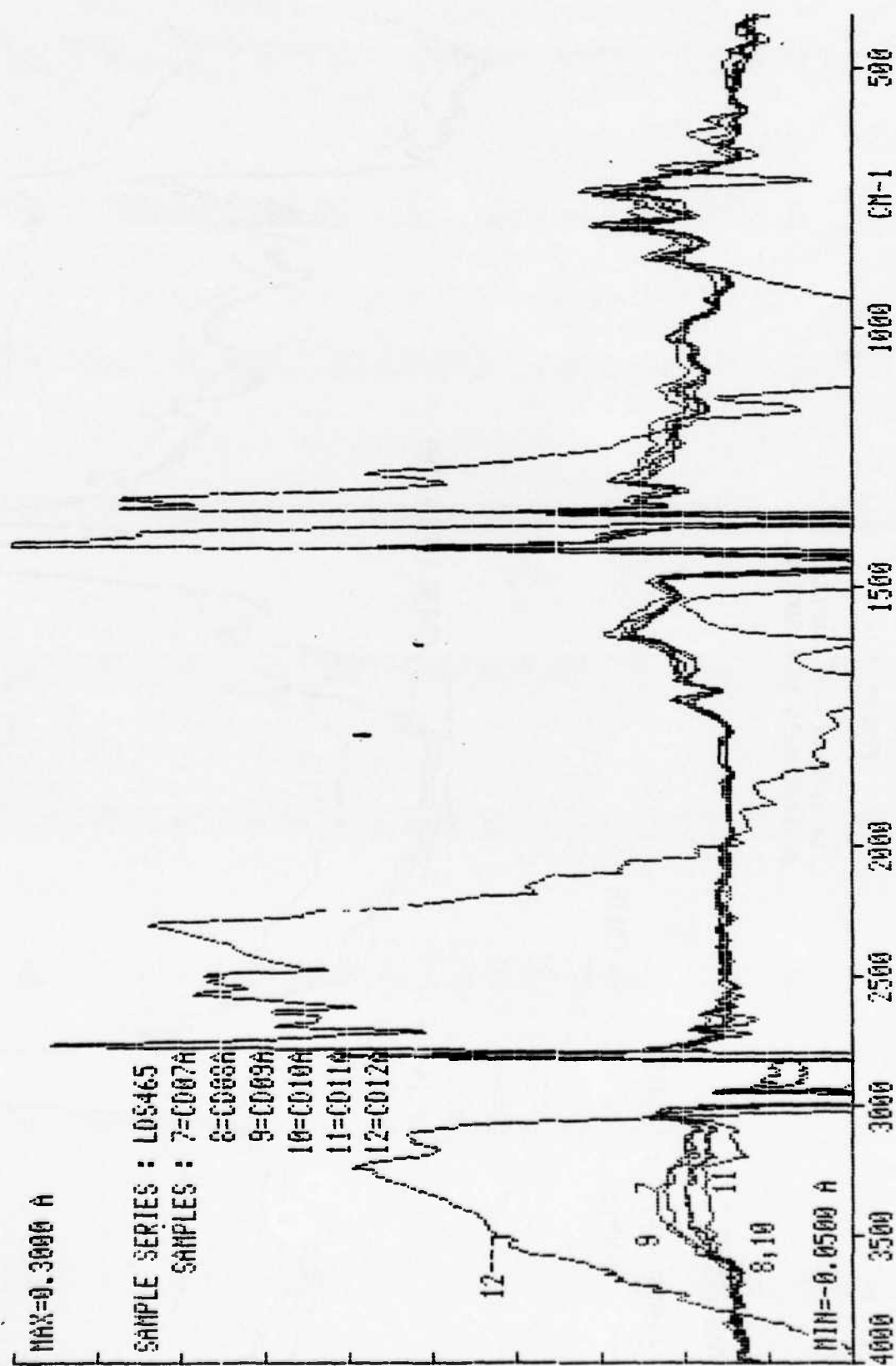
Wheeled-Vehicle Endurance Cycle Test. This test has been correlated with 20,000 miles of proving ground operation. Oil samples from this test were supplied by SWRI, and the TSC performed its analyses on these samples independently. The test cycles are outlined in Table 6, and the TSC measured data are in Table 7. These data show a progressive increase in all variables throughout the duration of the test. The simple infrared transmittance spectra in Figure 33 shows a progressive and steady change. The infrared differential absorbance spectra, Figure 34, shows a steady and continuous increase in Det I2 (oxidation, 1810-1660 cm^{-1}), Det I3 (degradation 1650-1535 cm^{-1}), Det I4 (oxidation/sulfation/glycol, 1300-1000 cm^{-1}), and Det I5 (oxidation, 1725-1670 cm^{-1}). The one positive reading for Det I1 (hydroxyl, 3600-3150 cm^{-1}) for sample RD015 is more likely due to the formation of organic acids rather than to water. There are no glycol/antifreeze peaks (1079.8 and 1032.8 cm^{-1}). There was a continuous increase in sulfates (SO4, 602 cm^{-1}) and total acid number; however, these increases were likely due to the time sequencing of the test data. The test oil contained approximately .32% sulfur and the test fuel contained approximately .42% sulfur. The origin of the sulfate formation is usually linked to the fuel sulfur but recent results have provided speculation about oxidation of the lubricant sulfur. Degradation of the oil is progressive; however, the additive package appears to still be working because each successive spectrum reflects a steady rate of oil degradation.

7. <u>Selection of Threshold Levels.</u>

Univariate statistics were performed on each variable in the field data for the combined set of engines. These data are also in Appendix B. By examining the frequency distribution for approximately normally distributed variables, an indication of typical behavior for LD-465 family field engines may be inferred as follows:

a. Table B-7 contains a frequency table and plots for CL2 (1980 cm^{-1}), a measure of carbon loading in the oil for these engines. There is a distinct bimodal nature in the frequency distribution of these data. Examination of the stem leaf plot and frequency table suggest that there is a distribution of normally performing engines with a mode at approximately 1.26 absorbance units/cm, and there is a distribution of abnormally performing engines with a mode at approximately

TABLE 6

ARMY/CRC 210-HOUR WHEELED VEHICLE ENDURANCE CYCLE

Period[a]	Time, hr.	Rack/Throttle Setting	Coolant Jacket-Out Temp, $^{o}C(^{o}F)$
1	2	5 min idle followed by slow acceleration to maximum power[b]	82(180)
2	1	idle	38(100)
3	2	Maximum Power	82(180)
4	1	idle	38(100)
5	2	Maximum Power	82(180)
6	1	idle	38(100)
7	2	Maximum Power	82(180)
8	1	idle	38(100)
9	2	Maximum Power	82(180)
10	10	5 min idle followed by shutdown	------

[a] These 10 periods yield 14 hours of running with a 10-hour shutdown; this cycle is repeated 15 times for a total test time of 210 hours.

[b] For the LD-465 series engines, Maximum Power occurs at 2600 rpm.

TABLE 7

PHYSICAL AND INFRARED TEST DATA - 210 HOUR ENDURANCE LDT-465 TEST ENGINE

SAMPLE	HRS	FE PPM	VIS*	TAN	%SOLIDS	COBRA	GC %	CL2	DET 11	DET 12	DET 13	DET 14	DET 15	FD1	FD2	FD13	FD4	ZN1	SO4
RC001	0	4	67	2.6	0.4	--	--	--	--				--REFERENCE OIL--						
RC002	14	12	--	2.8	0.8	13	--	1.45	-1343.61	131.78	228.92	686.99	82.15	0.97	14.95	-6.39	-0.06	-2.87	0.45
RC003	42	25	--	3.2	1.6	9	--	6.07	-1143.03	308.87	477.14	1651.50	201.06	2.91	38.49	-165.83	0.17	-3.40	1.70
RC004	56	30	--	3.3	1.6	9	--	8.00	-2511.23	392.69	555.01	2125.55	241.77	3.18	0	-223.76	0	-5.11	2.39
RC005	70	41	69	3.5	3.2	10	--	10.16	-2550.26	463.77	630.85	2544.42	299.43	4.20	0	-217.88	0	-4.68	2.62
RC006	84	46	--	3.6	3.6	11	--	12.04	-2577.44	518.59	697.81	2932.42	333.14	5.32	1.14	-217.29	-0.03	-4.66	3.14
RC007	98	59	--	3.8	3.6	12	--	13.70	-2656.85	612.85	792.36	3403.94	393.46	7.06	1.19	-253.79	-0.07	-4.85	3.29
RC008	112	65	--	4.2	4.0	12	--	15.42	-2612.92	702.62	929.99	3923.83	446.38	8.98	0	-204.77	-0.12	-5.12	3.46
RC009	126	72	--	4.4	4.0	12	--	17.29	-2504.16	750.33	970.61	4199.25	489.27	10.20	1.48	-198.68	-0.05	-4.72	1.65
RC010	140	86	75	4.1	4.4	12	--	18.38	-2598.23	797.12	1045.35	4455.79	517.64	9.17	1.50	-232.50	-0.09	-5.08	3.51
RC011	154	97	--	4.5	4.8	13	--	19.94	-2579.41	996.17	1204.74	5128.11	631.75	0	1.25	-192.81	-0.07	-4.87	4.32
RC012	168	103	--	4.5	5.2	13	--	23.45	-2608.15	1052.27	1277.38	5411.12	668.64	0	1.74	-165.84	-0.11	-4.89	4.32
RC013	182	118	--	5.1	4.8	14	--	21.92	-2345.27	1157.07	1350.13	5815.88	736.52	0	2.22	-188.14	-0.26	-4.44	4.58
RC014	196	123	79	4.9	4.8	14	--	21.42	-2196.53	1215.92	1412.98	5978.65	766.43	0	2.40	-159.40	-0.25	-4.30	4.35
RC015	210	--	79	6.2	---	17	--	23.50	357.99	1297.83	1706.84	6531.45	817.52	0	2.04	-116.98	-0.12	-3.15	4.16

*Viscosity results are in centistokes (cSt) at 104°F. Sample volumes were too small for the Nametre Viscometer.

FIGURE 33

IR SPECTRA - 15 SAMPLES
216 HOUR ENDURANCE TEST, LDS-465 ENGINE

SAMPLE SERIES : LDS-465
SAMPLES : R6001 THROUGH R6015

SPECTRA - ALL IN DESCENDING ORDER
FROM UPPER SPECTRUM TO
LOWER SPECTRUM.

MAX=100.00 T

MIN=0.00 T

MAX=100.00 T

MIN=0.00 T
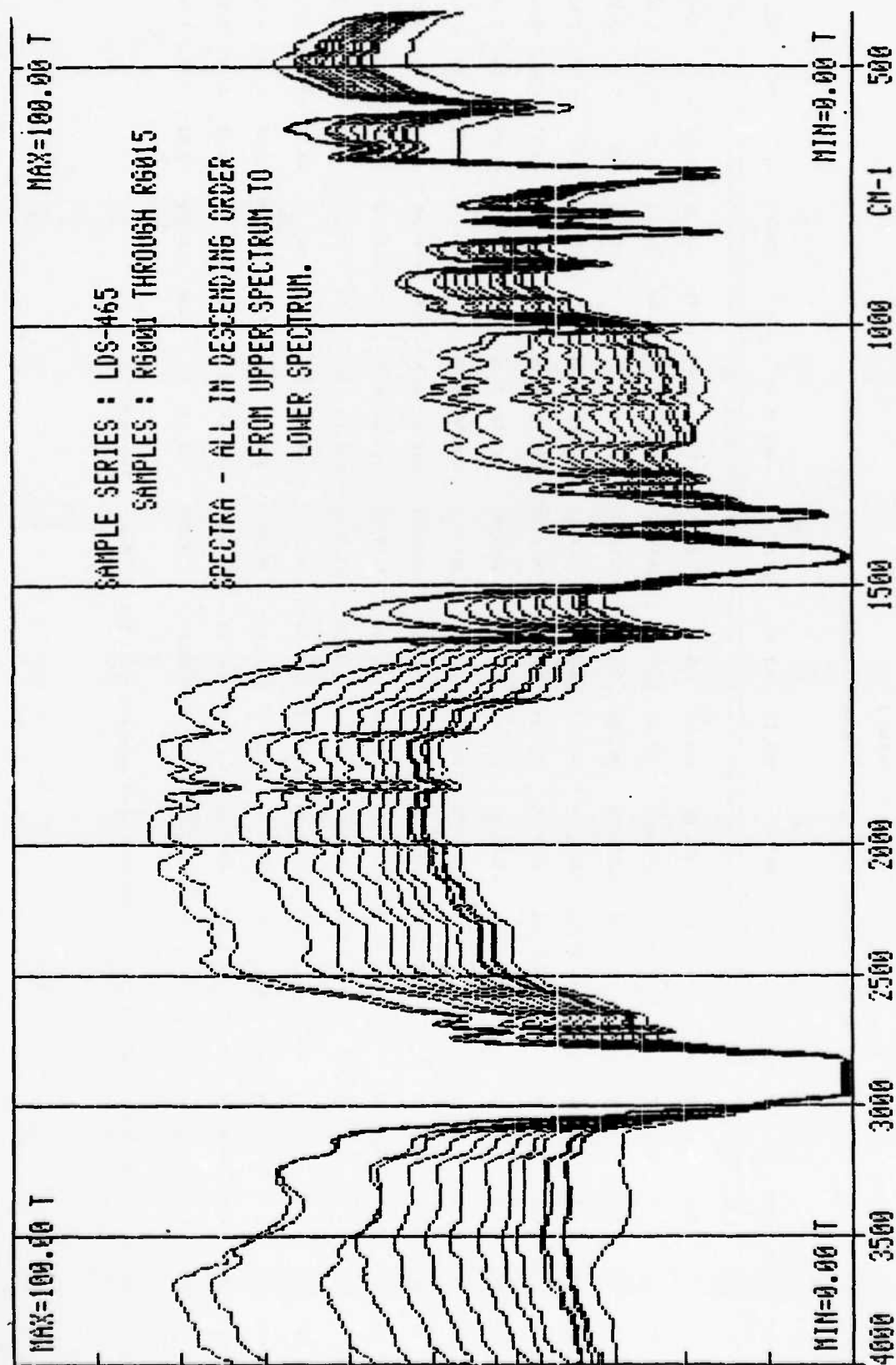
FIGURE 34

IR DIFFERENTIAL SPECTRA – 14 SAMPLES
210 HOUR ENDURANCE TEST, LDS-465 ENGINE

67
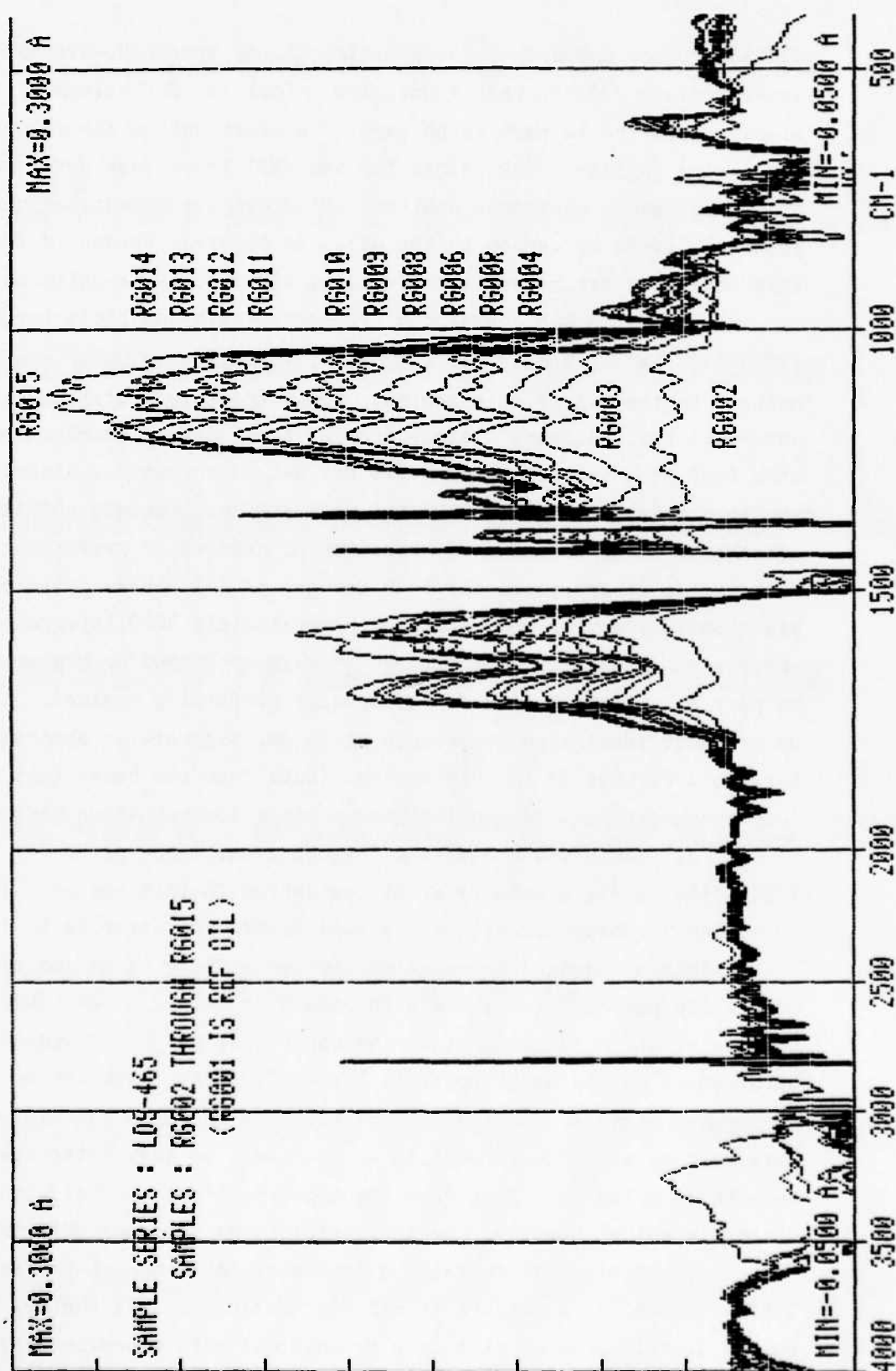
170 absorbance units/cm. These distributions appear to overlap at approximately 130 absorbance units/cm. That is, CL2 values of 130 or higher appear to be part to be part of a distribution for abnormally performing engines. CL2 values for the SWRI bench test never exceeded 23.50 absorbance units/cm; however, this test should not produce abnormal levels of carbon in the oil. An abnormal threshold for CL2 in this engine is estimated, therefore, at 130 absorbance units/cm.

b. Table B-8 contains a frequency table and plots for Det I1 (3600-3150 cm^{-1}), a measure of hydroxyl (principally water contamination) in the oil of this engine. Again there is a distinct bimodal nature in the frequency distribution of these data. Examination of the stem leaf plot and frequency table for Det I1 suggests a distribution of normally performing engines with a mode at approximately 900 integrated absorbance units/cm and a distribution of abnormally performing engines with a mode at approximately 5400 integrated absorbance units/cm. These distributions appear to overlap at approximately 4000 integrated absorbance units/cm. That is, Det I1 values of 4000 or higher appear to be part of a distribution for abnormally performing engines. This value, 4000 integrated absorbance units/cm, suggests an abnormal threshold for Det I1 in this engine. Data from the bench test are mostly negative and do not indicate a water contamination problem.

c. Table B-9 contains a frequency table and plots for Det I2 (1810-1660 cm^{-1}), a measure of oil oxidation in this engine. This distribution is unimodal, slightly skewed toward the upper tail, and less peaked than a standard normal distribution. There is no indication of abnormally performing engines with regard to Det I2. The lower tail of the distribution is larger than the upper tail and this suggests that occurrences in the small upper tail are all part of the set of normally performing engines. Accordingly we estimate an upper evaluation threshold at the 99th percentile of this data or 1299 integrated absorbance units/cm. Data from the bench test are all below this threshold value; however, the last sample does approach this value.

d. Table B-10 contains a frequency table and plots for Det I3 (1650-1535 cm^{-1}), a measure of oil degradation in this engine. The frequency distribution of this data is unimodal with approximately equal tails. The curve is broad, skewed slightly toward the lower tail and less peaked than a standard normal distribution. Data in the extreme

tails appear to be outliers or abnormal occurrences.
Accordingly an abnormal threshold for Det I3 is assumed
to be at the 98.9th percentile or 2090 integrated absorbance
units/cm. This value is consistent with the test engine data, but the
last sample in the test engine series does approach this threshold.

     e. Table B-11 contains a frequency table and plot for Det I4
($1300-1000$ cm^{-1}), a measure of oil oxidation, sulfation, and/or glycol.
The frequency distribution of this data is essentially unimodal except
that there are several occurrences with low or near zero values. This
distribution is skewed slightly toward the lower tail, and less peaked
than a normal distribution. This distribution clearly peaks in the
2500-3000 integrated absorbance units/cm range, and there are scattered
outliers in the upper tail. We would normally estimate an abnormal
threshold at the 95th percentile; however, the bench test engines
demonstrated Det I4 values well above this value without serious changes
in the rate of oil degradation. Accordingly we estimate the abnormal
threshold at the 98.9th percentile of the field data or 5222 integrated
absorbance units/cm. The last four test engine samples are above this
value and would be rejected by this methodology.

     f. Table B-12 contains a frequency table and plots for Det I5
($1725-1670$ cm^{-1}), a subset of Det I2 and further measure of oil oxi-
dation in this engine. The distribution of this data is unimodal,
skewed slightly toward the upper tail, and slightly less peaked than a
standard normal distribution. We would normally estimate the abnormal
threshold for Det I5 at the 95th percentile; however, the last five
observations of the test engine exceed this value. Accordingly we chose
the 99th percentile or 770 integrated absorbance units/cm for the
abnormal threshold of Det I5. The last observation from the test engine
exceeds this value and would be rejected by this methodology.

     g. Table B-13 contains a frequency table and plots for FD1
(3050 cm^{-1}), a measure of aromatics in the oil at a single peak. Forty
percent of the field data is less than one. Any occurrences above zero
should be cause to consider fuel dilution. We estimate the abnormal
threshold at the 75th percentile or 5.8 absorbance units/cm.
Interestingly, four observations from the middle of the test engine data
fail this criterion; however, subsequent samples are zero. At this time
we are unsure of the cause of this phenomenon.

h.   Table B-14 contains a frequency table and plots for FD2 (1610 cm^{-1}), a measure of aromatics in the oil at a single peak. Sixty percent of these values are concentrated below one. The range of normal occurrence probably includes only random values above zero. We estimate the abnormal threshold for these data at the 75th percentile or 2.4 absorbance units/cm. The second to last sample from the test engine fails this criteria.

i.   Table B-15 contains a frequency table and plots for FDI3 (905-685 cm^{-1}), a measure of aromatics in the oil. This distribution is strongly skewed to the upper tail and sharply peaked. Abnormal occurrences probably are not seen in the upper extremes of the data. We estimate the abnormal threshold at the 99th percentile, 2346 integrated absorbance units/cm. The test engine values are all negative.

j.   Table B-16 contains a frequency table and plots for FD4 (473 cm^{-1}), a measure of aromatics in the oil. The distribution of this data is unimodal, skewed slightly toward the lower tail, and much flatter than a standard normal distribution. All observations appear to be part of a single distribution tightly clustered about a single mode near zero. We estimate the abnormal threshold at the 99th percentile or 1.16 absorbance units/cm. All the bench test values for this variable are at or near zero.

k.   Table B-17 contains a frequency table and plots for ZN1 (670 cm^{-1}), a measure of the oil additive ZDDP. This distribution is well behaved, skewed to the upper tail, and slightly less peaked than a standard normal distribution. Normal occurrence are close to zero. The lower tail is of interest for this variable because depletion of the additive is of concern. This tail is long and contains obvious outliers. The abnormal threshold is, therefore, assumed to be at the 3.8th percentile or -4 absorbance units/cm. The positive values are all small and are considered random noise occurrences about zero. The test engine showed depletion of this additive in nearly all samples; however, there was not an increasing depletion through the last sample. This was probably due to small amounts of make up oil that easily improved the ZDDP additive levels.

l.   Table B-19 contains a frequency table and plots for SO4 (602 cm^{-1}), a measure of sulfates in the oil. The distribution is unimodal, skewed slightly toward the lower tail, and much flatter than a

70

standard normal distribution. There is a slight change in this distribution at the 98.4th percentile and this value, 2.81 absorbance units/cm, is assumed to be the abnormal threshold for SO_4 in this engine. Interestingly nearly all the test engine samples fail this criterion.

m. Table B-20 contains distribution for iron wear metal in parts per million (PPM). The distribution is unimodal, skewed slightly toward the lower tail, and much less peaked than a standard normal distribution. The upper tail is large but continuous. The abnormal threshold is estimated at the 99th percentile or 199 PPM. Two occurrences, 200 and 210 PPM, fall above this threshold.

n. Table B-21 contains the distribution for viscosity measured on the Nametre viscometer in centipoise grams/cm^3. The distribution is unimodal, skewed toward the lower tail and less peaked than a standard normal distribution. The upper tail is larger than the lower tail. The upper abnormal threshold is estimated at the 97th percentile or 316 centipoise grams/cm^3 because the distribution appears to become discontinuous at this point. A lower threshold is estimated at the 5th percentile or 74.3 centipoise grams/cm^3.

o. Table B-22 contains the distribution for total acid number measured in milligrams of KOH to neutralize. The distribution is unimodal, skewed toward the lower tail, and sharply peaked. The upper tail contains apparent outliers, thus the abnormal threshold is estimated at the 98.6th percentile or 5 milligrams, the last point before the apparent outliers.

p. Table B-23 contains distribution for total solids measured in percent solid contaminates. The distribution is unimodal, skewed toward the lower tail and slightly less peaked than a normal distribution. The upper tail contains three apparent outliers. The abnormal threshold is estimated at approximately the 98.6th percentile or 25%. Three samples were above this threshold, and they all failed the high carbon loading threshold.

q. Table B-24 contains the distribution for COBRA. The distribution is bimodal with a primary mode in the 6 to 9 range and a secondary mode in the 15 to 15.8 range. Since COBRA tends to decline as mineral oils degrade, the lower tail is important. The abnormal threshold is estimated at the 5th percentile or 5 COBRA units. Three samples have

71

COBRA values below this threshold. Extremely high values for COBRA indicate severe water contamination.

B. Detroit Diesel Allison 6V-53T Engine.

   1. Background.

      The 6V-53T engine is a six cylinder two-cycle, multi-fuel engine manufactured by Detroit Diesel Allison, Division of GMC. It is used extensively by the US Army in personnel carriers, combat vehicles, and other special purpose vehicles. It is normally fueled with diesel fuel. The TSC collected 131 samples from 15 engines over the course of this study and used 119 observations in this analysis. These engines were mounted in M-113 personnel carriers and were operated under normal training conditions by the 1st Battalion of the 22nd Field Artillery at Ft. Carson, CO.

      Additionally the TSC collected samples from 6 stationary test engines used in a 240-hour engine test conducted by the Army Fuels and Lubricants Research Laboratory at SWRI to evaluate piston deposits, wear, ring and valve distress and skirt scuffing. Forty-six samples collected from four of these 6V-53T bench test engines were used in this study. Nametre viscosity measurements were not made on these samples because the TSC was unable to obtain sufficient sample volume. Data from the Ft. Carson samples and the SWRI samples are listed in Appendices D and E, Tables D-1 and E-1 respectively.

   2. Significant Correlation.

      Coefficients of correlation were computed between all possible variable pairs for the combined Ft. Carson engine data and separately for the combined SWRI engine data. The correlation matrices are also at Appendices D and E, Tables D-2 and E-2, respectively. Correlation coefficients between infrared variables and physical test variables greater than or equal to 0.5 for both the field data and bench test data are shown in Table 8. There is at least one significant correlation among the infrared variables except Det I1 for each of the physical properties. The infrared variables from the test engines are more strongly correlated to the physical properties than the field engine but not to the extent observed for the LDT-465 engine. These simple correlations are less universal and more exclusive to specific pairs of variables than for the LD-465 engines. These simple correlations are sufficient to support our basic hypothesis that data in the infrared spectra are correlated to degradation of the crankcase oils.

TABLE 8. SIGNIFICANT CORRELATIONS: 6V-53T ENGINE

PHYSICAL PROPERTY VARIABLES

IR VARIABLE	HOURS		FE		VIS		TAN		SOLIDS		COBRA		GC	
	FIELD	TEST	FIELD	TEST	FIELD	TEST	FIELD	TEST	FIELD	TEST	FIELD	TEST	FIELD	TEST
CL2	0.598			0.790					0.675				-0.532	
DET I1														
DET I2					0.549			0.521						
DET I3				0.696									-0.508	
DET I4				0.580										
FD1				-0.705										
FD2										0.763		-0.591	-0.668	
FDI3				-0.571									-0.621	
ZN1				-0.622										

73

3. Regression Analysis.

We used stepwise regression to design predictive models for viscosity, total acid number, total solids, and percent fuel dilution by GC. These models for the field engines are in Appendix D. The best model for viscosity is in Table D-3. It has an R^2 of .88 and the following 10 independent variables:

CL1	CL2 x Det I2
Det I1	CL2 x Det I3
Det I3	CL2 x Det I4
(Det I2)^2	Det I1 x Det I2
CL1 x Det I1	Det I2 x Det I4

The best model for total acid number is in Table D-4. It has an R^2 of .24 and the following 3 independent variables:

CL2

(CL2)^2

CL1 x Det I2

The best model of total solids is in Table D-5. It has an R^2 of .85 and the following 14 independent variables:

CL1	(Det I3)^2
CL2	CL1 x Det I1
Det I1	CL1 x Det I2
Det I2	CL2 x Det I1
Det I3	Det I1 x Det I2
Det I4	Det I1 x Det I3
(CL1)^2	Det I1 x Det I4

The best model for percent fuel is in Table D-6. It has an R^2 of .91, and the following three independent variables:

CL2

(Det I3)^2

Det I3 x Det I4

The models for viscosity and total solids, though large and complex, are quite good. They show strong correlation and account for most of the variability in the data. The model for total acid number, on the other hand, is poor, probably because there was little variation in total acid number in the data. Likewise fuel dilution problems with this engine are rare. Only 14 samples were screened for possible fuel dilution, and these were found to have fuel levels below 7 percent. The

stepwise procedure for percent fuel did produce a surprisingly good model; interestingly, none of the independent variables were the aromatics specifically included in the methodology to monitor fuel. Owing to the small population, we have little confidence in the percent fuel model.

4. Representative Engine.

Field data from a single 6V-53T engine was selected to highlight the change in infrared data over four sequential samples. Data from this engine are shown in Table 9. Figure 35 shows the simple transmittance spectra for samples CC10K through CC13K and the fresh oil. Gross contamination or deterioration is not evident; however, spectra of the used oil samples are suppressed by carbon (CL2) and contain moderate water contamination. In one sample, CC13K, one can detect the presence of glycol peaks at 1079.8 and 1032.8 cm^{-1}. Figure 36 compares the differential spectra of the four samples containing moisture with the reference oil. The moisture content of sample CC13K was found to be approximately 0.25% using the Aquatest IV analyzer and Karl Fisher reagent. The drastic change in the differential spectrum for sample CC13K is the key to an abnormal condition and would alert an evaluator during routine monitoring.

5. Bench Test Data.

The Southwest Research Institute bench test of the 6V-53T engine family was in accordance with the US Army, Coordinating Research Council (CRC) 240-hour Tracked-Vehicle Endurance Cycle Test and with Federal Test Method Standard No. 791B, Method 355T. This test has been correlated to 6437 kilometers (4000 miles) of proving ground operation. Oil samples from this test were supplied by SWRI. We performed its analyses on these samples independently. The test cycles are outlined in Table 10. The TSC measured data for one test engine are in Table 11. After the 120-hour oil sample is taken, the engine is shut down, the oil is drained from the filter housing and crankcase, new test oil is added, and a new oil filter and new air cleaners are installed. The data in Table 11 shows a progressive increase in all variables, except solids, Det I1 and FD1. The simple infrared transmittance spectra are shown in Figures 37 and 38. A progressive and steady change for each of the 120-hours of operation is seen. The infrared differential spectra, Figures 39 and 40, show a steady and continuous increase for

75

TABLE 9

PHYSICAL AND INFRARED TEST DATA - M113 PERSONNEL CARRIER, 6V53T ENGINE

SAMPLE	FE PPM	VIS	TAN	SOLIDS %	GC %	CRACKLE	COBRA	CL2	DET I	DET 12	DET 13	DET 14	FD1	FD2	FD13	ZN1	HRS
CC01K	94	173	2.22	4.0	--	N	10.5	43.44	-91.63	121.52	114.31	1006.21	-3.66	0.13	378.48	1.43	unk
CC02K	98	191	2.34	6.0	--	N	6.2	35.15	371.80	131.60	57.86	826.69	-2.76	0	156.33	0.90	"
CC03K	124	190	2.41	8.0	--	N	6.5	37.14	-126.28	116.34	51.02	807.18	-3.14	0	151.25	1.10	"
CC04K	112	191	2.02	7.2	--	N	7.1	42.86	4827.09	75.16	273.07	775.91	1.92	0	290.70	2.74	"
CC05K	110	169	3.61	4.8	--	N	6.0	43.48	511.72	1.60	31.45	1511.19	-4.27	0	387.60	1.30	"
CC06K	109	166	2.88	4.8	--	N	5.0	43.48	949.74	21.45	15.27	1316.19	-3.31	0	316.50	1.28	"
CC07K	106	146	2.71	4.8	2	N	6.0	43.50	864.41	-5.01	57.25	1238.00	-3.62	0	256.64	0.92	"
CC08K	103	143	2.29	4.8	3	N	6.3	42.86	520.14	4.18	72.62	1304.17	-3.72	0	293.97	0.90	"
CC09K	111	143	2.23	6.0	3	N	6.0	44.89	950.58	14.92	70.17	1301.72	-3.21	0	285.21	0.78	"
CC10K	62	184	2.36	4.0	--	P	7.0	36.44	1550.93	-138.73	41.71	488.36	-0.78	0	211.12	1.54	"
CC11K	67	208	1.74	3.2	--	N	7.5	36.91	2417.00	-158.04	12.78	410.11	0.97	0	170.89	1.40	"
CC12K	122	205	2.18	10.0	--	N	6.0	59.23	-170.62	-183.92	13.09	402.88	-8.11	0	-145.30	-0.53	"
CC13K	80	224	1.38	6.0	--	P	---	39.71	6278.68	61.65	861.63	2926.55	7.96	0	1634.54	4.24	"
CC14K	127	271	1.87	7.2	--	N	6.5	50.38	949.91	55.26	758.57	2223.97	-2.77	0	1196.55	1.32	"
CC15K	113	280	1.60	8.0	--	N	6.0	49.77	1152.67	92.15	805.95	2236.54	-2.39	0	1331.72	1.29	"

76

FIGURE 35

IR SPECTRA, 5 SAMPLES

US ARMY M-113 PERSONNEL CARRIER ENGINES

MAX=100.00 T

SAMPLE SERIES : 6V-53T
SAMPLES : FRESH OIL
CC16K
CC11K
CC12K
CC13K

MIN=0.00 T
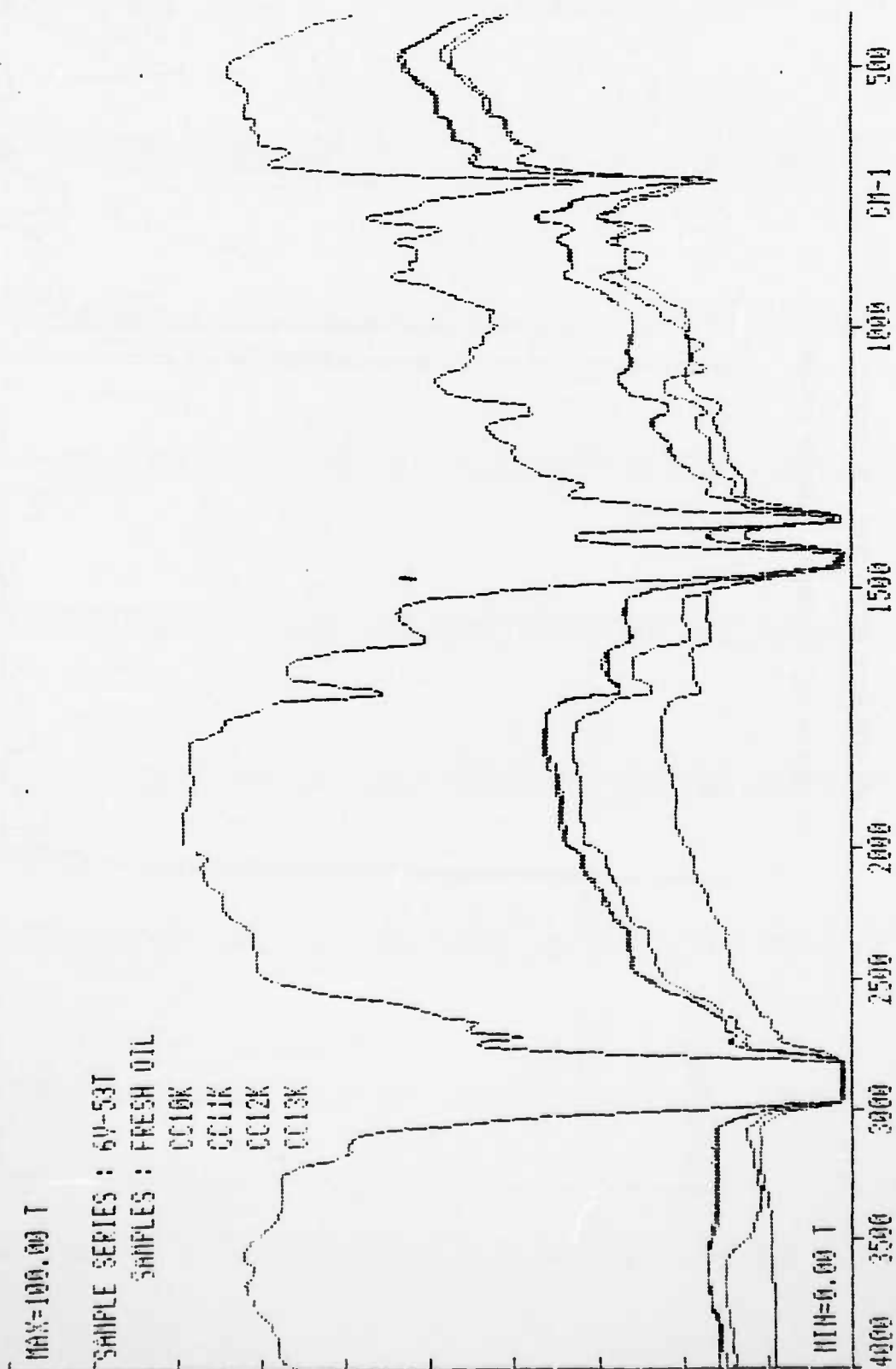
FIGURE 36

IR DIFFERENTIAL SPECTRA – 5 SAMPLES

US ARMY M-113 PERSONNEL CARRIER ENGINES
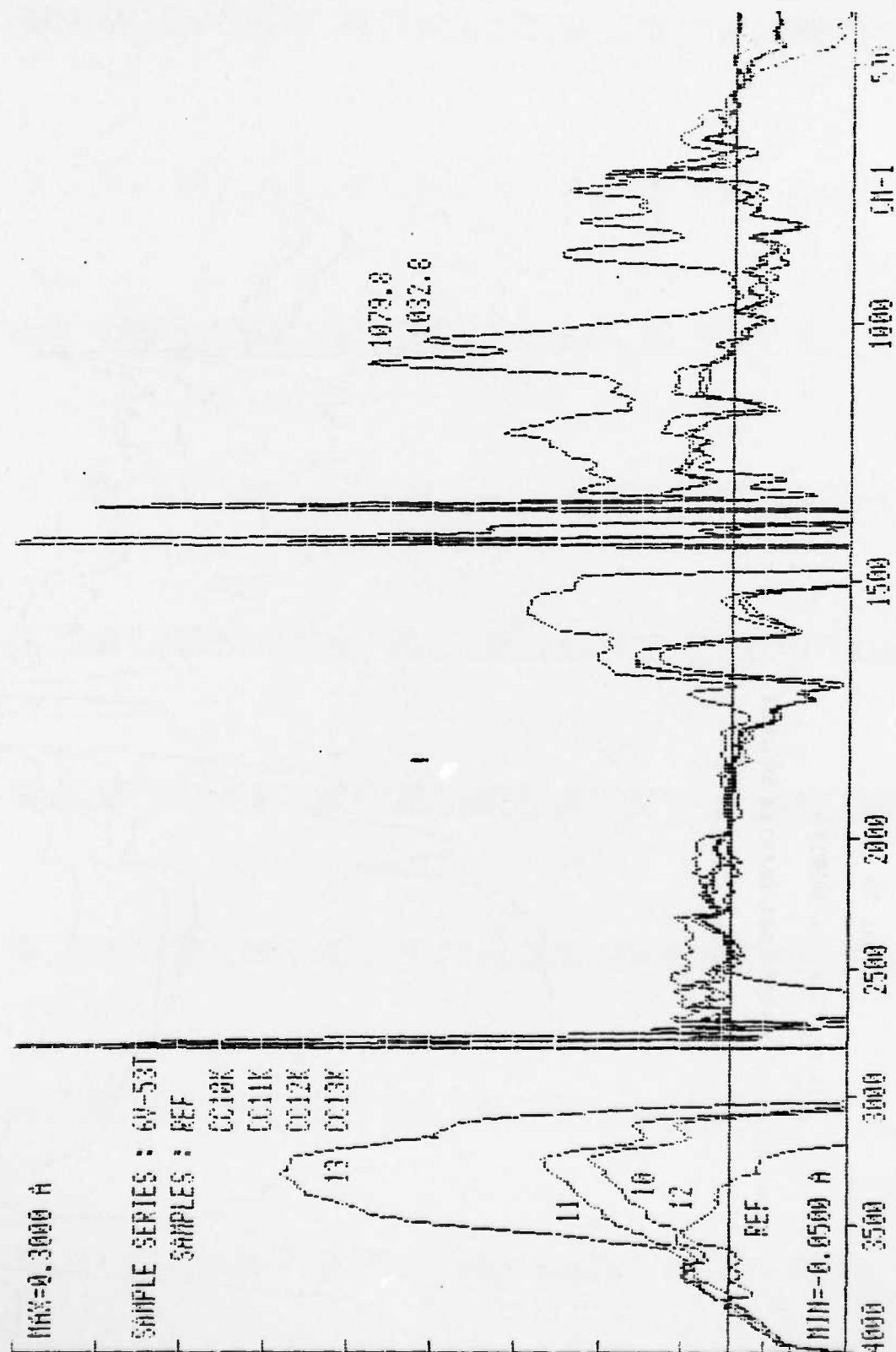
TABLE 10

ARMY/CRC 240-HOUR TRACKED-VEHICLE ENDURANCE CYCLE

Period [a]	Time, hr	Rack/Throttle Setting	Coolant Jacket-Out Temp, $^{\circ}C(^{\circ}F)$
1	0.5	idle	38(100)
	2.0	Maximum Power [b]	77(170)
	0.5	idle	38(100)
	2.0	Maximum Torque[b]	77(170)
2	0.5	idle	38(100)
	2.0	Maximum Power	77(170)
	0.5	idle	38(100)
	2.0	Maximum Torque	77(170)
3	0.5	idle	38(100)
	2.0	Maximum Power	77(170)
	0.5	idle	38(100)
	2.0	Maximum Torque	77(170)
4	0.5	idle	38(100)
	2.0	Maximum Power	77(170)
	0.5	idle	38(100)
	2.0	Maximum Torque	77(170)
5	4	5 min idle, followed by shutdown	---

a These five periods yield 20 hours of running with a 4-hour shutdown; this cycle is repeated 12 times for a total test time of 240 hours.
b For the 6V-53T, Maximum Power occurs at 2800 rpm and Maximum Torque occurs at 2200 rpm.

TABLE 11

PHYSICAL AND INFRARED TEST DATA - 6V53T TEST ENGINE

SAMPLE	FE PPM	VIS*	TAN*	SOLIDS %	GC %	CRACKLE	COBRA	CL2	DET 11	DET 12	DET 13	DET 14	FD1	FD2	FDI3	ZN1	HRS
RC01F	74	---	---	0.4	---	N	40.0	3.79	-1534.89	- 4.63	92.17	198.13	-1.48	0	25.65	-1.78	20
RC02F	97	---	---	0.4	---	N	33.0	7.65	-1497.67	25.56	206.56	739.30	-2.77	0	-104.39	-2.20	40
RC03F	114	13.64	2.35	0.4	---	N	31.50	12.00	-1469.48	95.25	368.78	1262.13	-3.22	0	-177.47	-2.92	60
RC04F	131	---	---	0.4	---	N	33.50	15.97	-1588.45	145.38	474.32	1717.25	-3.64	0	-218.32	-3.47	80
RC05F	127	---	---	0.4	---	N	32.00	17.07	-1679.01	172.67	551.11	1930.88	-3.71	0	-232.42	-3.39	100
RC06F	129	14.83	2.79	0.4	---	N	32.50	19.58	-1648.75	202.99	629.91	2288.18	-4.09	0	-266.58	-3.56	120
RC07F	44	---	---	0.4	---	N	34.50	7.33	-1547.24	73.71	244.48	845.27	-2.89	0	-111.85	-2.09	140
RC08F	59	---	---	0.4	---	N	39.50	11.67	-1627.50	121.08	369.87	1270.25	-3.50	0	-158.63	-2.77	160
RC09F	89	14.68	2.63	0.4	---	N	34.00	14.74	-1668.07	156.61	463.61	1615.69	-3.60	0	-186.68	-2.86	180
RC10F	116	---	---	0.4	---	N	35.0	16.79	-1686.22	182.81	530.47	1839.61	-3.85	0	-213.42	-3.38	200
RC11F	123	---	---	0.4	---	N	33.0	19.51	-1628.91	205.68	604.48	2123.84	-4.16	0	-258.31	-3.64	220
RC12F	139	15.28	3.07	0.4	---	N	29.0	23.11	-1307.77	213.76	684.44	2420.88	-3.77	0	-277.78	-3.71	240

*Data reported by Southwest Research Institute; insufficient sample for TSC to obtain VIA and TAN

VIS, centistokes (cSt) at 100°F
TAN, ml 0.1N KOH per gram of sample

FIGURE 37

IR SPECTRA, 6 SAMPLES

240-HOUR ENDURANCE TEST, 6V-53T ENGINE

81
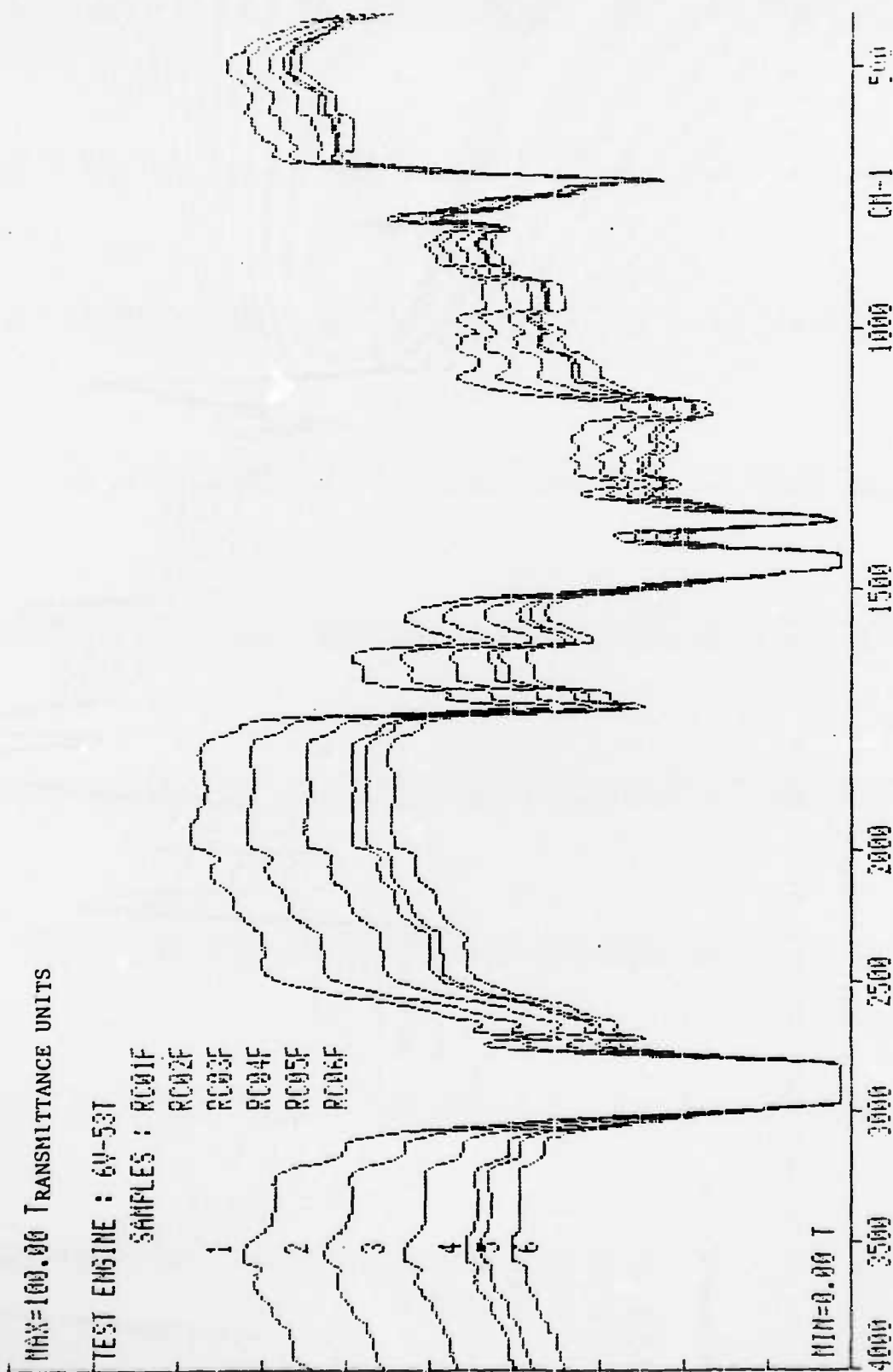
FIGURE 38

IR SPECTRA, 6 SAMPLES
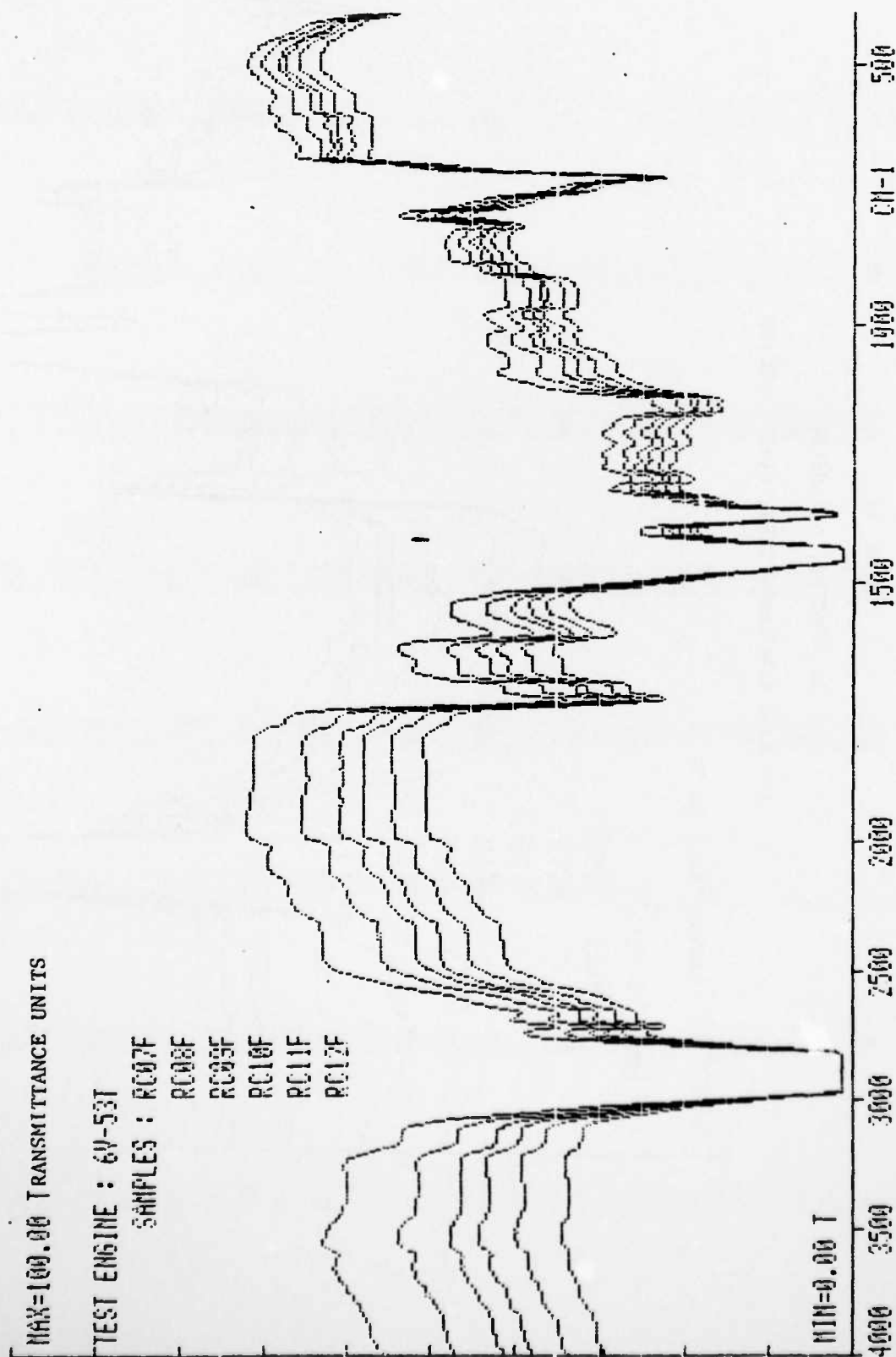
240-HOUR ENDURANCE TEST, 6V-53T ENGINE

MAX=100.00 TRANSMITTANCE UNITS

TEST ENGINE : 6V-53T

SAMPLES : RC07F
RC08F
RC09F
RC10F
RC11F
RC12F

MIN=0.00 T
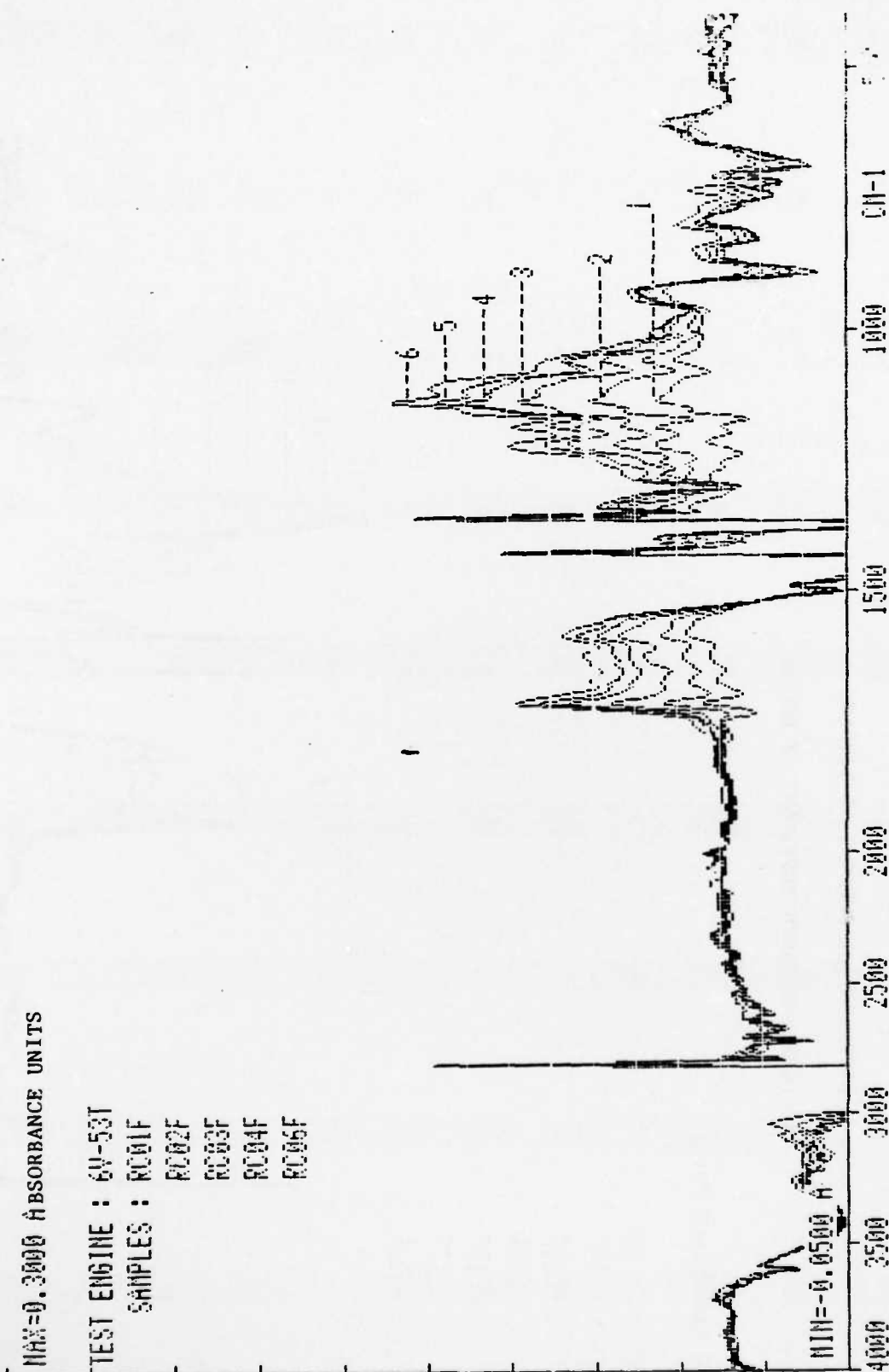
4000 3500 3000 2500 2000 1500 CM-1 1000 500

DIFFERENTIAL SPECTRA, 6 SAMPLES

240-HOUR ENDURANCE TEST, 6V-53T ENGINE

MAX=0.3000 ABSORBANCE UNITS

TEST ENGINE : 6V-53T
SAMPLES : RC01F
RC02F
RC03F
RC04F
RC05F

MIN=-0.0500 A

FIGURE

DIFFERENTIAL SPECTRA, 6 SAMPLES

240-HOUR ENDURANCE TEST, 6V53-T ENGINE
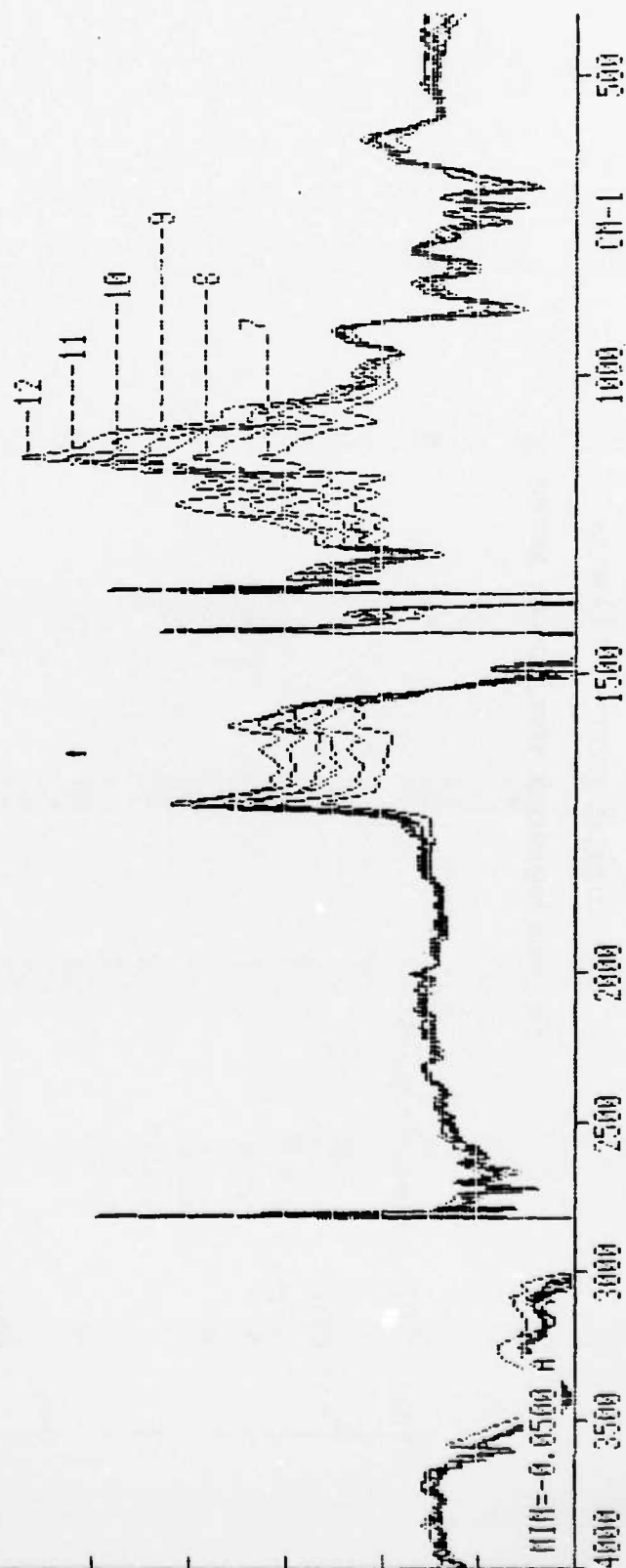
CL2 (carbon loading, 1980 cm^{-1}), Det I2 (oxidation, 1810-1714 cm^{-1}), Det I3 (nitration, 1650-1538 cm^{-1}), and Det I4 (oxidation, glycol, sulfation, 1300-1000 cm^{-1}). A continuous decrease is noted for FD1 (aromatics, 3040 cm^{-1}). The negative values for Det I1 (hydroxyl, 3600-3150 cm^{-1}) indicate the absence of water and glycol relative to the fresh oil during the test. Degradation of the oil in this engine is progressive but not extreme.

6. Selection of Threshold Levels.

Univariate statistics were performed on each variable in the field data and test engines independently. These data are also in Appendices D and E. By examining the frequency distribution of each variable, an indication or normal behavior for the 6V-53T engine may be inferred as follows:

a. Tables D-7 and E-3 contain a frequency table and plots for CL2 (1980 cm^{-1}), a measure of carbon loading in the oil for the field engines and test engines respectively. The distribution for the field engines is unimodal, skewed slightly toward the lower tail, and is much less peaked than a standard normal distribution. The abnormal threshold may be estimated at the 95th percentile of the distribution or 67 absorbance units/cm. Carbon loading for the test engines are all well below this limit. We consider this consistent since the test engine is operated on the laboratory bench and the test does not create particularly high carbon producing conditions.

b. Tables D-8 and E-4 contain a frequency table and plots for Det I1 (3600-3150 cm^{-1}), a measure of hydroxyl (principally water contamination) in the oil for the field engines and test engines respectively. The field engine distribution is unimodal, skewed to the lower tail and is sharply peaked. Most normal occurrences fall close to the median value, and the upper tail contains obvious outliers. Accordingly, an abnormal threshold may be estimated at the 97.3rd percentile, 2417 integrated absorbance units/cm where the first break in continuity of the upper tail occurs. The test engines' extreme values are well below this limit. Thse results are intuitively expected since water contamination generally is a yes or no condition. The test engines obviously did not experience water contamination.

c. Tables D-9 and E-5 contain a frequency table and plots for Det I2 (1810-1714 cm^{-1}), a measure of oil oxidation for the field

engines and test engines. The field engine distribution is unimodal, has a very light skew toward the upper tail and is much less peaked than a standard normal distribution. Overall the distribution approximates a normal distribution. The abnormal threshold may be estimated at the 95th percentile of the data or approximately 220 absorbance units/cm. Since there is oxidative stressing of the oil in the 240 hour test, we would expect the test engine distribution to approximate the field engine distribution, and it does. The 95th percentile for the test engines falls at 218 integrated absorbance units/cm.

     d. Tables D-10 and E-6 contain a frequency table and plots for Det I3 (1650-1538 cm^{-1}), a measure of oil degradation for the field engines and test engines. The distribution for the field data is unimodal, very slightly skewed to the lower tail and less peaked than a standard normal distribution. The distribution is a reasonable approximation of a normal distribution, and the abnormal threshold may be assumed at the 95th percentile or 780 absorbance units/cm. The bench test similarly, closely approximates a normal distribution; however, its extreme values are slightly below this threshold.

     e. Tables D-11 and E-7 contain a frequency table and plots for Det I4 (1300-1000 cm^{-1}), a measure of oil oxidation, sulfation, and glycol, for the field engines and test engines. The field engine distribution is nearly normal in shape with only slight skew toward the lower tail. The abnormal threshold may be estimated at the 95th percentile or 2228 integrated absorbance units/cm. The test engines have a very similar distribution and the 95th percentile is at 2231 integrated absorbance units/cm. As with Det I2 this value is indicative of the oil stressing that occurs during this test and entirely consistent with the estimated threshold.

     f. Tables D-12 and E-8 contain a frequency table and plots for FD1 (3040 cm^{-1}), a measure of aromatics in the oil for the field engines and test engines. The field data is unimodal, skewed toward the lower tail and sharply peaked. Normal occurrences appear to fall near the median value. There are several outliers in the upper tail, and these break the continuity of the distribution at about the 97th percentile. Interestingly, the test engine data are bimodal with a small secondary mode below the primary mode. Our estimate for the abnormal threshold for FD1 is the 97th percentile, 3.62 absorbance units/cm. The test engine data are well below this level as would be expected.

86
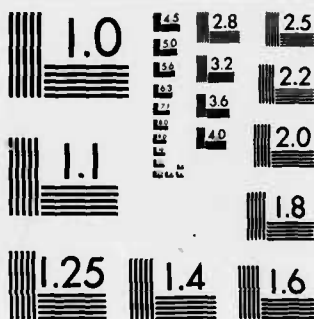
MICROCOPY RESOLUTION TEST CHART
NATIONAL BUREAU OF STANDARDS-1963-A

g. Tables D-13 and E-9 contain a frequency distribution and
plots for FD2 (1595 cm^{-1}), a measure of aromatics in the oil for the
field engines and test engines. Eighty-eight percent of the field
values are zero. There are several outliers in the upper tail and these
probably are abnormal occurrences. The test engine data are again
bimodal and the upper portion of the distribution is symmetric about its
mode while the lower mode, and 35% of the occurrences, is at zero. An
abnormal threshold is difficult to estimate from these data because one
does not expect fuel contamination in the test engines and because the
fuel measurement (GC) had a significant negative correlation while one
would expect a positive correlation. Since the distribution is heavily
concentrated at or near zero, we estimate the abnormal threshold at the
90th percentile, 2.8 absorbance units/cm. If we assume the upper mode
in the test engine data indicates a distribution of abnormal
occurrences, the above threshold woulf fall in the lower tail and thus
be an intuitively appropriate criterion.

h. Tables D-14 and E-10 contain a frequency distribution and
plots for FDI3 (904-685 cm^{-1}), a measure of aromatics, in the oil for
the field engines and test engines. The field data are unimodal,
strongly skewed to the lower tail, and sharply peaked. Most normal
occurrences will fall close to the median value. An estimate of an
abnormal threshold is the 90th percentile or 657 integrated absorbance
units/cm. The occurrences above this point appear to be outliers. The
test engine data are mostly negative and well below this criterion.
Again the problem associated with a negative correlation with GC exists
for this variable. We assume that other degradation products exist
which affect this variable in this engine.

i. Tables D-15 and E-11 contain a frequency distribution and
plots for ZN1 (670 cm^{-1}), a measure of the ZDDP additive, in the oil for
the field and test engines. The field data are unimodal, slightly
skewed toward the lower tail and sharply peaked. This additive should
deplete during normal operation and the abnormal threshold should be in
the lower tail. The test engine data are also unimodal; however, it is
slightly skewed toward the upper tail. Its peak is wide and flat and
the 5th percentile is -4.39 absorbance units/cm. Based on the test
engine data, the 5th percentile for the field data is probably too

87

conservative for the abnormal threshold for this distribution, and we have chosen the 1st percentile, -3.44 absorbance units/cm as the abnormal threshold. This value is intuitively compatable with the test engine data.

j. Tables D-17 and E-13 contain a frequency table and plots for iron wear metal, contamination in parts per million (PPM) for the field and test engines. The distribution of the field data is unimodal, slightly skewed toward the lower tail, and near normal in shape. The data are clustered tightly until the 99th percentile or 194 PPM. The last occurrence, 200 PPM, appears to be abnormal and this sample indeed was heavily contaminated with water. The iron values in the test engines were all well below this threshold.

k. Table D-18 contains a frequency table and plots for viscosity of these oils in centipoise grams/cm^3 for the field engines. The field data are unimodal, skewed slightly toward the lower tail and much less peaked than a normal distribution. The upper tail is continuous with no apparent outliers, thus the abnormal limit is estimated at the 99th percentile or 342 centipoise grams/cm^3. Only one value exceeds this limit with a viscosity of 346, and it is the water contaminated sample noted for excess iron in paragraph j. above. The abnormal lower limit is estimated at the 1st percentile or 102 centipoise grams/cm^3. One sample has approximately this value; however, it does not fail any of the infrared criteria.

l. Tables D-19 and E-14 contain a frequency table and plots for total acid number in milligrams of KOH to neutralize in the oil for the field and test engines respectively. The distribution in unimodal, skewed toward the lower peak, less peaked than a normal distribution, and contains apparent outliers in the upper tail. The outliers in the upper tail begin at the 96.7th percentile or 3.22. Four occurrences fall above this threshold. One sample with TAN of 3.6 also fails the study criteria for Det I2 (nitration), FD1 and FD2. One sample with TAN of 3.61 also fails FD1. Interestingly, the sample with TAN 3.73 passes all other criteria. The final sample with TAN of 3.78 also fails the FD2 criteria. The test engines are all within this threshold.

m. Tables D-20 and E-15 contain a frequency table and plots for total solids contamination in the oil in percent solid contamination for the field and test engines. The field data are unimodal, strongly

88

skewed toward the lower tail, very sharply peaked, and has a long upper
tail with an apparent outlier. The last apparent natural occurrence is
at about the 97.5th percentile or 14% solids; the outlier is at 36%
solids. Three abnormal occurrences fall above this value, and these
samples also fail Det I1 for high water contamination. The test engine
samples are all well below this threshold.

        n. Table D-21 and E-16 contain the distribution for COBRA
measurement of the oil for the field and test engines. This distri-
bution is unimodal, strongly skewed toward the lower tail, very sharply
peaked, and has one apparent outlier. The abnormal threshold is assumed
to be at the 1st percentile or 3 units since this variable tends to
decline with oil degradation. The one sample with an abnormal value of
3 units also is contaminated with water. The test engines sample values
are all well above this threshold. The extremely high value in the
upper tail is normally indicative of free water or extreme water
contamination; however, in this case, the sample shows no contamination
or other severe deterioration.

C. Cummins NTC-400 Engine.

    1. Background.

        The NTC-400 engine is a six cylinder, diesel engine manufactured
by Cummins Engine Company and used by the US Army in the M920 tractor
truck. It is fueled with diesel fuel. The TSC collected 153 samples
from 17 engines over the course of this study. A total of 142 samples
were used for this report. These engines were mounted in M920 tractor
trucks and operated under normal use conditions by the 52nd Engineer
Battalion, Ft. Carson, CO. We were unable to obtain samples from any
NTC-400 test engines. Data for the NTC-400 field engines from
Ft. Carson are listed in Appendix F, Table F-1.

    2. Significant Correlations.

        Coefficients of correlation were computed between all variable
pairs for the combined Ft. Carson data. The correlation matrix is also
included in Appendix F at Table F-2. Correlation coefficients between
the infrared variables and the physical property variables are all less
than 0.5 except the pair FDI3 and HRS which had a simple correlation of
-.77.

    3. Regression Analysis.

        Stepwise regression was used to design predictive models for
viscosity, total acid number, total solids, and percent fuel by gas

chromatograph. These models are in Appendix F. The best model for viscosity is at Table F-3. It has an R^2 of .65, and the following 16 independent variables:

CL2	$(Det\ I1)^2$	CL2 x Det I3	Det I3 x Det I4
Det I1	$(Det\ I2)^2$	Det I1 x Det I3	
Det I3	$(Det\ I3)^2$	Det I1 x Det I4	
Det I4	$(Det\ I4)^2$	Det I2 x Det I3	
$(CL2)^2$	CL1 x Det I4	Det I2 x Det I4	

The best model for total acid number is at Table F-4. It has an R^2 of .59 and the following 10 independent variables:

Det I1	CL2 x Det I2
$(Det\ I2)^2$	CL2 x Det I3
CL1 x Det I2	Det I1 x Det I3
CL1 x Det I1	Det I1 x Det I4
CL2 x Det I1	Det I2 x Det I3

The best model for total solids is at Table F-5. It has an R^2 of .45 and the following 6 independent variables:

Det I1	CL2 x Det I1
$(CL2)^2$	Det I1 x Det I2
$(CL2)^2$	Det I2 x Det I3

The best model for percent fuel dilution is at Table F-6. It has an R^2 of .60 and the following 10 independent variables:

Det I2	$(FD2)^2$
FDI3	CL2 x Det I3
$(Det\ I1)^2$	Det I2 x Det I3
$(Det\ I3)^2$	FD2 x CL2
$(Det\ I4)^2$	FD2 x Det I2

We consider these regression models to be poor. Examination of the physical properties show little variation and suggests that these engines did not degrade their crankcase oils. The viscosity of the lubricating oil in these engines were below 150 centipoise g/cc for 40% of the samples received. However, only one sample was contaminated with 5% fuel. Accordingly, the regression models show weak relationships among physical properties and infrared variables.

4. Representative Engine.

A single engine from the field data was selected to highlight the change in infrared data over sequential samples. Data from this

90

engine are shown in Table 12. Spectra in Figure 41 show the sequence of simple infrared transmittance for each sample. Note the spectra of two samples, CG08D and CG13D, show a small dip in the hydroxyl area (3600-3150 cm^{-1}) indicating moisture contamination. Although these two samples show similar amounts of moisture, the second transmits considerably less infrared radiation because of its increased carbon loading as shown by CL2 values. Otherwise these spectra show that the oil did not deteriorate or become contaminated. The iron (Fe) wear metal readings indicate an oil change probably occurred after sample CG02D. The differential spectra for samples CG13D and CG14D, Figure 42, shows a very small amount of hydroxyl in sample CG13D and a small increase in sulfation (1300-1000 cm^{-1}) in sample CG14D.

5.   Selection of Threshold Levels.

Univariate statistics were performed on each variable in the field data for the combined set of engines. These data are also in Appendix F. By examining the frequency distribution for these data, an indication of normal behavior for the NTC-400 engine may be inferred as follows:

a.   Table F-7 contains a frequency table and plots for CL2 (1980 cm^{-1}), a measure of carbon loading, in the oil for this engine. The distribution is severely skewed toward the lower tail and sharply peaked. One apparent outlier is at 66.84 absorbance units and is assumed to be an abnormal occurrence. Because this distribution differs significantly from the normal, it is difficult to estimate an abnormal threshold; however, there is a clear break in the data between the two extreme occurrences. Accordingly we estimate the abnormal threshold at this point or 16 absorbance units/cm.

b.   Table F-8 contains a frequency table and plots for Det I1 (3600-3150 cm^{-1}), a measure of hydroxyl (principally water contamination), in the oil for this engine. The distribution is strongly skewed toward the lower tail and sharply peaked. Normal values are tightly clustered about the median. The upper tail is large and contains probable outliers. An abnormal threshold is estimated at the 95th percentile of the distribution, 2878 integrated absorbance units/cm.

c.   Table F-9 contains a frequency table and plots for Det I2 (1810-1714 cm^{-1}), a measure of oil oxidation, for this engine. The

91

TABLE 12

PHYSICAL AND INFRARED TEST DATA - M 920 TRACTOR, NTC 400

SAMPLE*	FE PPM	VIS	TAN	SOLIDS %	GC %	CRACKLE	COBRA	CL2	DET I1	DET I2	DET I3	DET I4	FD1	FD2	FD13	ZN1	HRS
CG01D	41	134	2.41	3.2	4	N	12.5	8.81	183.42	178.28	426.53	1354.09	1.73	5.11	86.62	-2.89	unk
CG02D	45	128	2.49	3.6	4	N	14.1	9.16	-174.87	213.60	499.00	1817.64	2.54	6.15	258.66	-3.09	"
CG03D	15	166	2.16	1.2	--	N	12.1	0.61	25.74	4.33	- 9.42	- 110.64	3.78	0.35	- 31.18	-0.79	"
CG05D	1.	161	2.18	1.2	--	N	9.1	2.72	170.50	- 12.93	179.96	721.66	0.34	0	194.08	-0.22	"
CG06D	16	203	2.14	1.6	--	N	8.9	3.01	329.16	- 22.10	189.19	721.12	0.24	0	194.28	-0.18	"
CG07D	22	163	2.17	1.6	--	N	7.0	4.68	615.81	- 2.97	278.41	910.56	0.11	0	164.29	-0.64	"
CG08D	19	160	2.14	2.0	--	N	6.9	4.34	1591.64	70.47	384.01	868.18	3.56	4.62	224.48	-0.46	"
CG09D	25	169	2.53	2.0	--	N	6.0	8.89	95.90	84.80	412.50	1762.43	-0.30	4.58	235.06	-1.70	"
CG10D	39	156	2.24	2.0	--	N	--	10.95	239.69	131.66	489.32	1741.87	0.51	5.32	189.60	-2.39	"
CG11D	36	150	2.39	3.2	--	N	--	11.04	22.59	139.84	483.00	1773.32	0.36	5.26	199.12	-2.68	"
CG12D	44	157	2.71	3.2	--	N	--	13.67	251.42	126.12	492.63	1905.20	-0.66	0	173.36	-2.50	"
CG13D	44	154	2.32	4.0	--	N	--	13.70	1553.95	124.98	577.23	1871.47	0.62	0	219.31	-2.20	"
CG14D	50	160	2.64	3.2	--	N	--	15.60	12.21	148.67	519.74	2090.94	-0.67	6.01	158.85	-3.06	"

*Sample CG04D used as reference.

92

FIGURE 41

IR SPECTRA, 14 SAMPLES
US ARMY M-920 TRACTOR TRUCK ENGINE

MAX=100.00 T

SAMPLE SERIES : MTC-400 ENGINE
SAMPLES : CG01D THROUGH CG14D

MIN=0.00 T

93
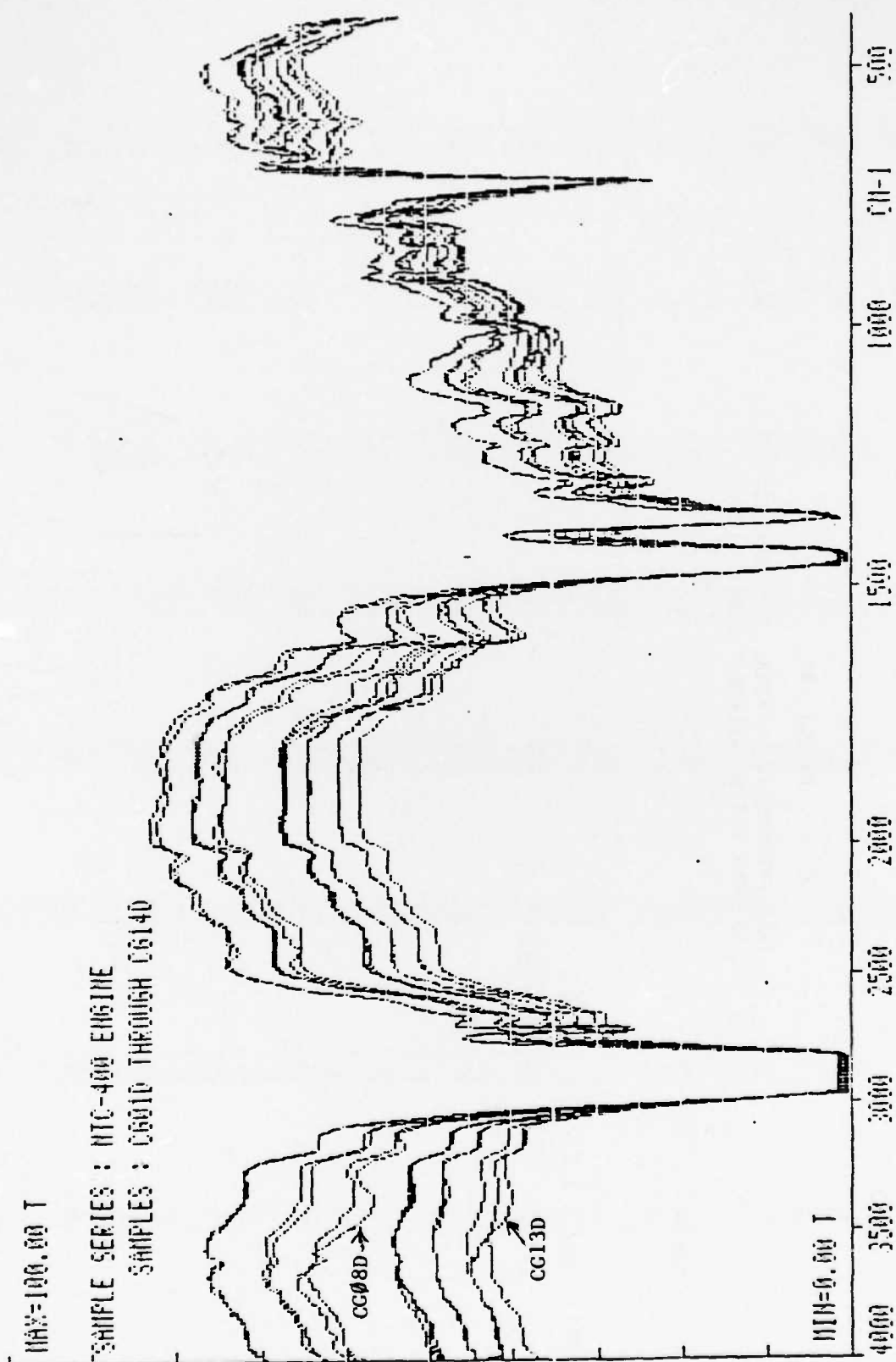
FIGURE 42

IR DIFFERENTIAL SPECTRA, TWO SAMPLES
US ARMY M-920 TRACTOR TRUCK ENGINE
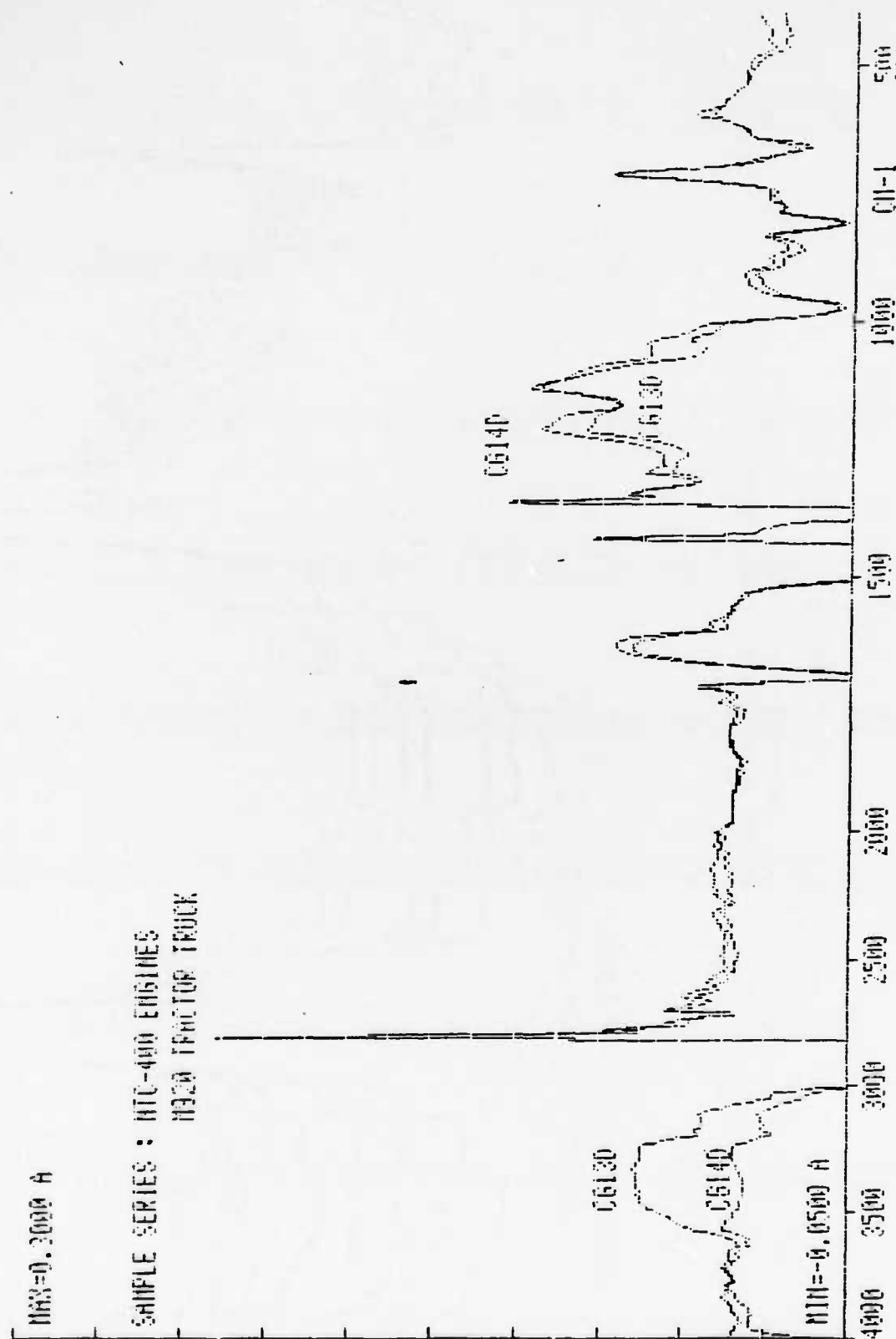
frequency distribution is unimodal, skewed toward the lower tail, and sharply peaked. The upper tail contains apparent outliers above the 98.6th percentile. The abnormal threshold is estimated at the 98.6th percentile of the distribution of 456 integrated absorbance units/cm.

d. Table F-10 contains a frequency table and plots for Det I3 (1650-1538 cm^{-1}), a measure of carboxylates, for this engine. The frequency distribution is unimodal, skewed slightly toward the lower tail, and sharply peaked. The upper tail contains apparent outliers above the 98.6th percentile. The abnormal threshold is estimated at the 98.6th percentile or 860 integrated absorbance units/cm.

e. Table F-11 contains a frequency table and plots for Det I4 (1300-1000 cm^{-1}), a measure of oil oxidation, sulfation, and glycol. This distribution is unimodal, skewed toward the lower tail, sharply peaked, and normal occurrences appear to cluster tightly about the median. There appears to be only one outlier which is probably an abnormal occurrence. The abnormal threshold is estimated at 3000 integrated absorbance units/cm which is at about the 98.6th percentile because the data below and including this value are all tightly clustered.

f. Table F-12 contains a frequency table and plots for FD1 (3040 cm^{-1}), a measure of aromatics, in the oil collected for this engine. The distribution is unimodal, skewed toward the lower tail, and sharply peaked. The upper tail is long relative to the lower tail. The abnormal threshold is estimated at the 95th percentile or about 7.1 absorbance units/cm.

g. Table F-13 contains a frequency table and plots for FD2 (1595 cm^{-1}), a measure of aromatics, in the oil collected for these engines. Sixty-seven percent of all occurrences for this variable are zero. The distribution has a long narrow upper tail and at least two occurrences that appear to be extreme outliers or abnormal occurrences. Since the data is so tightly concentrated at zero, nearly all occurrence above this value would appear abnormal. Therefore, the abnormal threshold is estimated at the 75th percentile or 2.2 absorbance units/cm.

h. Table F-14 contains a frequency table and plots for FDI3 (905-685 cm^{-1}), a measure of aromatics, collected for these engines. This distribution is unimodal, skewed toward the lower tail, and sharply peaked. There appear to be two clear outliers. The abnormal threshold

is estimated at the 95th percentile of the distribution or 882 absorbance units/cm.

i. Table F-15 contains a frequency table and plots for ZN1 (670 cm^{-1}), a measure of ZDDP additive, collected for these engines. Ninety-nine percent of this distribution is clustered between -4.07 and 1.73 absorbance units/cm. Since this variable measures depletion, negative values indicate an increase in degradation. The abnormal threshold is assumed at the 5th percentile which is -3.7 absorbance units/cm.

j. Table F-17 contains a frequency table and plots for iron wear metal, contamination in parts per million (PPM). The distribution is unimodal, skewed toward the lower tail, and slightly less peaked than a standard normal distribution. The upper tail contains a possible outlier. The abnormal threshold is estimated at the 99th percentile or 66 PPM. One sample exceeds this threshold, and it also exceeds the threshold for FD2.

k. Table F-18 contains a frequency table and plots for oil viscosity for this engine measured with the Nametre Viscometer in centipoise grams/cm^3. The distribution is unimodal, slightly skewed toward the lower tail, and less peaked than a standard normal distribution. Both the upper tail and the lower tail have one apparent outlier. The upper abnormal threshold is estimated at the 99th percentile or 243 centipoise grams/cm^3 and the lower threshold is estimated at the 1st percentile or 75 centipoise grams/cm^3. Both apparent outliers pass all the infrared criteria.

l. Table F-19 contains a frequency table and plots for total acid number of these oils, measured in milligrams of KOH to neutralize. The distribution is unimodal, skewed toward the upper tail, and similar to a standard normal distribution in peakedness. No apparent abnormal occurrences are in the distribution. The abnormal threshold is estimated at the 9^r h percentile or 3.27. Only one sample falls above the threshold, and it passes all the infrared criteria; however, its Det I2 value, 412 integrated absorbance units/cm, is approaching the abnormal threshold 456.

m. Table F-20 contains a frequency table and plots for total solids contamination measured in percent solid contamination. Twenty percent of all occurrence are at .4%. The abnormal threshold is

96

estimated at the 95th percentile which occurs at 3.94%. There are seven samples falling above this threshold. Three of these samples also failed the FD2 criterion; the other passed all the infrared criteria.

      n. Table F-21 contains a frequency table and plots for COBRA. The distribution is unimodal, slightly skewed toward the lower tail, and less peaked than a normal distribution. The lower tail is of interest since this variable tends to decrease as the oil degrades. The abnormal threshold is estimated at the 5th percentile or 4.9 units.

D. Detroit Diesel Allison 8V-71T Engine.

   1. Background.

      The 8V-71T engine is an eight cylinder, two-cycle, multi-fuel engine manufactured by Detroit Diesel Allison, Division of GMC. It is used extensively by the US Army in a self-propelled howitzer and other special purpose equipment. It is normally fueled with diesel fuel. The TSC collected 177 samples from 15 engines over the course of this study. A total of 152 samples were used for this report. These engines were mounted in M109 self-propelled howitzers and operated under normal training conditions by the 1st Battalion of the 29th Field Artillery, 4th Infantry Division at Ft. Carson, CO. We were unable to obtain samples from 8V-71T bench test engines. Data for the 8V-71T field engines from Ft. Carson are listed in Appendix G, Table G-1.

   2. Significant Correlations.

      Coefficients of correlation were computed between all variable pairs for the combined Ft. Carson data. The correlation matrix is at Table G-2. Correlation coefficients between the infrared variables and the physical property variables are all less than 0.5 except for the pair, total solids and carbon loading, which was .776.

   3. Regression Analysis.

      Stepwise regression was used to design predictive models for viscosity, total acid number, total solids, and percent fuel by gas chromatograph. These models are in Appendix G. The best model for viscosity is at Table G-3. It has a R^2 of .38 and the following 18 independent variables:

CL1	$(Det\ I1)^2$	CL2 x Det I3
CL2	$(Det\ I2)^2$	Det I1 x Det I2
Det I1	$(Det\ I3)^2$	Det I1 x Det I3
Det I4	$(Det\ I4)^2$	Det I1 x Det I4
$(CL1)^2$	CL1 x Det I1	Det I2 x Det I4
$(CL2)^2$	CL1 x Det I3	Det I3 x Det I4

The best model for total acid number is at Table G-4. It has an R^2 of .46 and the following 20 independent variables:

CL1	$(CL2)^2$	CL1 x Det I2	Det I1 x Det I2
CL2 ·	$(Det I1)^2$	CL1 x Det I4	Det I1 x Det I3
Det I3	$(Det I2)^2$	CL2 x Det I1	Det I1 x Det I4
Det I4	$(Det I3)^2$	CL2 x Det I2	Det I2 x Det I3
$(CL1)^2$	CL1 x Det I1	CL2 x Det I3	Det I2 x Det I4

The best model for total solids is at Table G-5. It has an R^2 of .74 and the following 16 independent variables:

CL1	$(CL1)^2$	CL1 x Det I3	CL2 x Det I3
CL2	$(CL2)^2$	CL1 x Det I4	CL2 x Det I4
Det I1	$(Det 2)^2$	CL2 x Det I1	Det I1 x Det I3
Det I2	CL1 x Det I1	CL2 x Det I2	Det I2 x Det I4

The best model for GC is at Table G-6. It has an R^2 of .75 and the following 10 independent variables:

Det I1	Det I1 x Det I2
Det I4	Det I1 x Det I4
FDI3	Det I2 x Det I3
$(Det I1)^2$	Det I3 x Det I4
$(Det I2)^2$	$(FD2)^2$

All of these regression models are poor except the models for total solids and fuel dilution. As we would expect, the physical properties show little degradation or change in the oil for this engine except for a slight accumulation in total solids and some fuel dilution. Since these engines experience a fuel dilution problem, we were able to design an effective model to predict fuel.

    4. Representative Engine.

        A single engine from the field engines was selected to highlight the change in infrared data over sequential samples. Data from this engine are shown in Table 13. A decrease in iron (Fe) wear metal, total acid number, solids, and CL2 show that an oil change probably occurred after samples CH03J and CH07J. Four samples, CH03J, CH05J, CH06J, and CH07J show moisture contamination (Det I1).

        The presence of small amounts of fuel was found in all samples from this engine. The low viscosity of these samples is probably due to this fuel dilution. The simple infrared transmittance spectra, Figure 43, does not show any appreciable deterioration but does show moisture

TABLE 17

PHYSICAL AND INFRARED TEST DATA - M109 SELF-PROPELLED HOWITZER, 8V71T ENGINE

SAMPLE	FE PPM	VIS	TAN	SOLIDS %	GC %	CRACKLE	COBRA	CL2	DET 11	DET 12	DET 13	DET 14	FD1	FD2	FDI3	ZN1	HRS
CH01J	117	138	2.62	4.8	3	N	9.0	23.69	- 107.54	191.08	279.93	1228.43	-0.48	Ø	216.67	-0.89	58
CH02J	187	133	2.97	4.8	3	N	8.5	24.56	- 366.20	188.66	334.67	1592.08	-0.23	3.32	331.75	-0.74	117
CH03J	116	85	2.84	1.6	3	P	16.1	21.08	6063.97	2.01	264.54	458.25	3.74	Ø	345.75	2.97	175
CH04J	190	88	2.86	3.6	3	N	12.0	27.53	- 24.82	186.15	284.16	980.46	0.81	Ø	29.69	-1.44	31
CH05J	201	84	3.92	6.4	2	P	12.0	33.30	1763.78	58.42	462.33	1511.25	-0.57	3.59	320.78	0.51	40
CH06J	214	87	3.15	7.6	4	N	9.5	37.59	1439.94	64.07	457.60	1538.12	-1.64	Ø	282.25	-0.09	88
CH07J	221	88	2.70	8.0	3	N	10.0	37.73	1637.84	77.50	470.32	1428.15	-0.91	3.84	161.25	-0.02	90
CH08J	71	121	1.96	0.8	2	N	4.5	10.86	891.64	5.12	146.6°	335.02	3.02	Ø	67.72	-0.82	2
CH09J	85	121	2.22	2.8	2	N	4.5	21.91	765.71	?1.??	279.14	622.65	0.79	Ø	56.41	-0.61	14
CH10J	90	127	2.34	0.4	2	N	5.0	25.31	213.98	31.05	239.68	603.95	0.03	Ø	65.81	-1.21	14
CH11J	81	129	2.58	0.4	2	N	4.5	25.08	396.51	0.03	179.67	462.46	0.33	Ø	48.91	-1.13	14
CH12J	90	125	2.69	0.4	2	?	4.5	27.??	445.52	9.77	191.37	513.05	-0.11	2.76	48.26	-1.44	16
CH13J	100	129	2.87	3.6	3	N	8.0	31.51	585.41	-84.27	181.88	673.64	-3.03	Ø	43.50	-0.71	27
CH14J	104	130	2.96	8.0	3	N	7.5	30.03	177.17	-90.32	162.75	616.31	-3.17	Ø	54.20	-0.79	29
CH15J	112	127	2.59	8.0	3	N	7.5	33.22	563.45	-35.04	206.06	731.50	-3.38	Ø	35.24	-1.04	38
CH16J	133	124	2.60	8.0	4	N	7.0	38.27	262.81	-42.44	270.04	881.62	-3.83	Ø	26.87	-1.73	47

99

FIGURE 43

IR SPECTRA, 4 SAMPLES

US ARMY M-109 SELF PROPELLED HOWITZER 8V71T ENGINE

SAMPLE SERIES : 8V-71T
SAMPLES : 1 = REF, NEW OIL
          3 = CH03J
          5 = CH05J
          7 = CH07J

MAX=100.00 T

MIN=0.00 T

CM-1

100
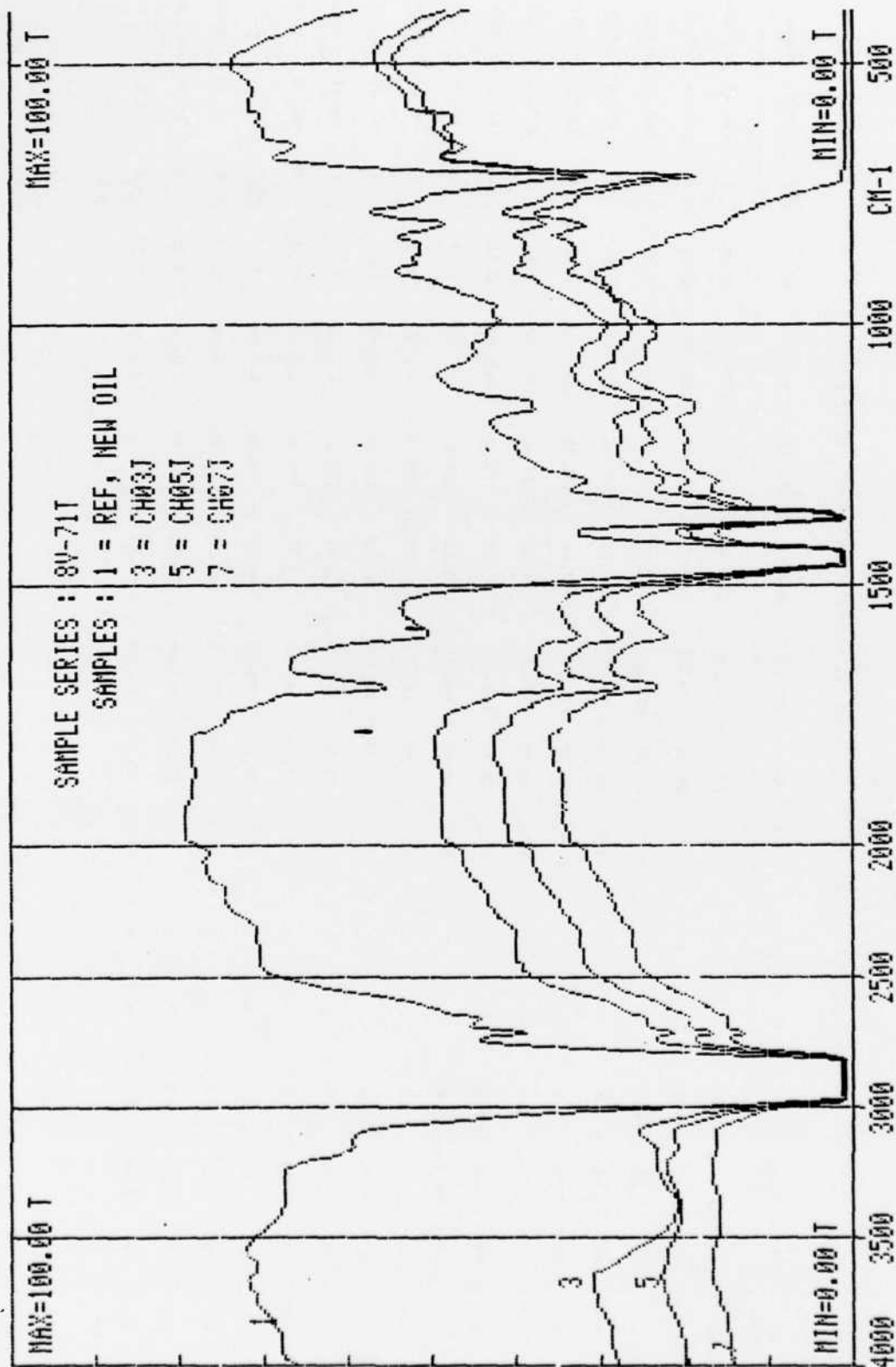
contamination in samples CH03J, CH05J, and CH07J. Glycol (antifreeze) was not detected in any sample. Carbon loading (CL2) is not a problem in this 8V-71T engine. The differential spectra, Figure 44, shows the presence of hydroxyl (Det I1) in three samples (CH03J, CH05J, CH07J). There is no evidence of glycol from a coolant leak, thus confirming that the moisture is probably from condensation.

5. Selection of Threshold Levels.

Univariate statistics were performed on each variable in the field data for the combined set of engines. These data are also in Appendix G. By examining the frequency distribution, an indication of normal behavior for 8V-71T field engines may be inferred as follows:

a. Table G-7 contains a frequency table and plots for CL2 (1980 cm^{-1}), a measure of carbon loading, in the oil collected for these engines. The distribution is unimodal, skewed slightly toward the lower tail, and less peaked than a standard normal distribution. Normal occurrences are distributed over a broad range. An abnormal threshold for CL2 is estimated at the 95th percentile or 53 absorbance units/cm.

b. Table G-8 contains a frequency table and plots for Det I1 (3600-3150 cm^{-1}), a measure of hydroxyl (principally water contamination), collected for these engines. The distribution is unimodal, skewed toward the lower tail, and sharply peaked. Normal occurrence cluster close to the median. An abnormal threshold may be assumed at the 95th percentile or 2116 integrated absorbance units/cm.

c. Table G-9 contains a frequency table and plots for Det I2 (1810-1714 cm^{-1}), a measure of oil oxidation, collected for these engines. This distribution is unimodal, skewed only slightly toward the lower tail, and is less peaked than a standard normal distribution. Overall the distribution closely approximates the normal distribution. The upper tail is very small, and there are no apparent outliers. An abnormal threshold for Det I2 may be assumed at the 99th percentile or 348 integrated absorbance units/cm.

d. Table G-10 contains a frequency table and plots for Det I3 (1650-1538 cm^{-1}), a measure of carboxylates (some nitration is noted in a few samples), in the oil for these engines. The distribution is unimodal, slightly skewed toward the upper tail, and less peaked than a standard normal distribution. The upper tail is small, and there are no apparent outliers. The abnormal threshold may be assumed to be at the 99th percentile or 855 integrated absorbance units/cm.

101

FIGURE 44

IR DIFFERENTIAL SPECTRA, 16 SAMPLES

US ARMY M-109 SELF PROPELLED HOWITZER 8V71T ENGINE
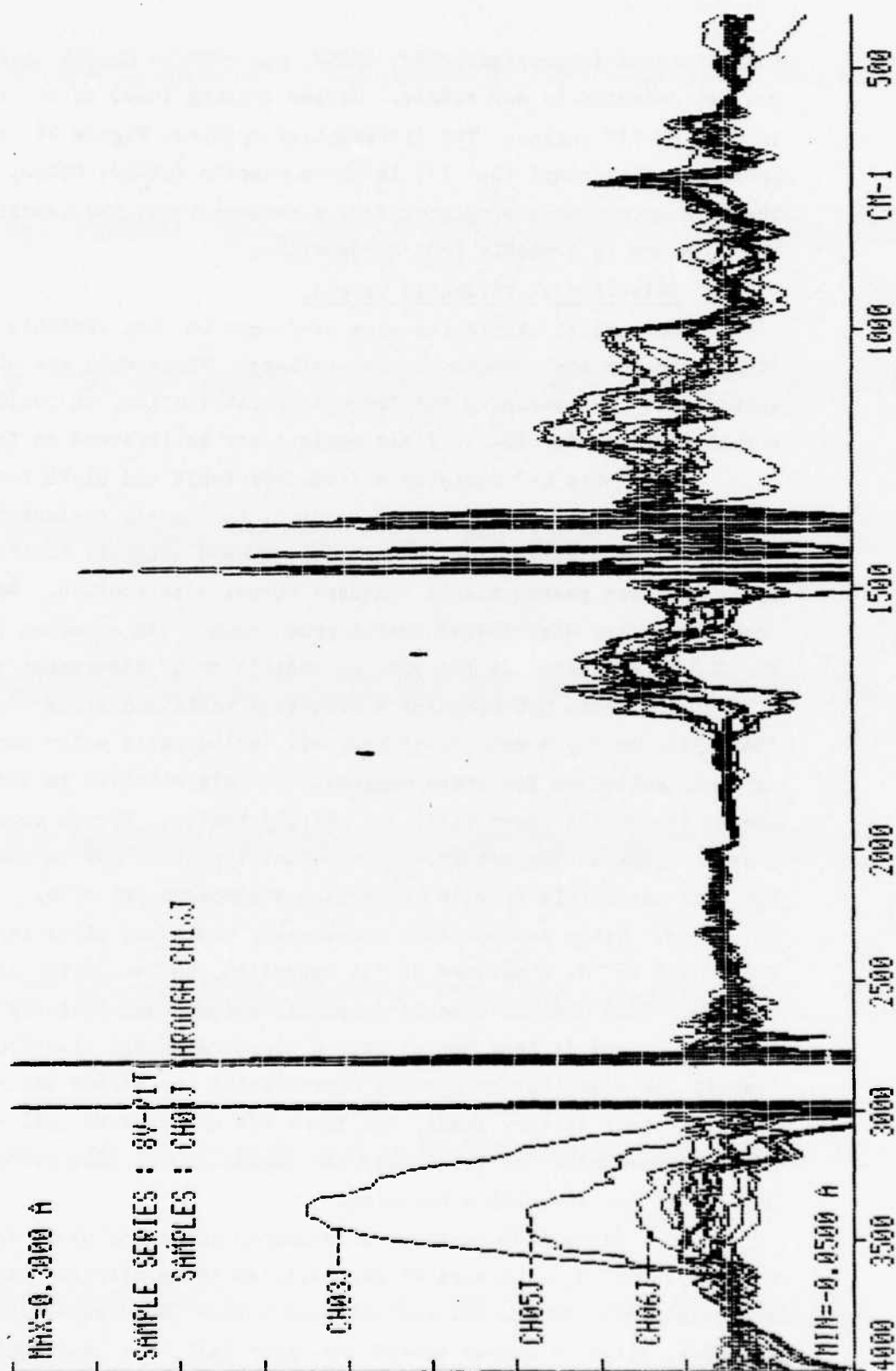
e. Table G-11 contains a frequency table and plots for Det I4 (1300-1000 cm^{-1}), a measure of oil oxidation, sulfation, and glycol, collected for these engines. The distribution is unimodal, slightly skewed toward the lower tail, and less peaked than a standard normal distribution. Most occurrences are tightly clustered about the median. There are no true outliers in the upper tail and we estimate the abnormal threshold at the 99th percentile or 2470 integrated absorbance units/cm.

f. Table G-12 contains a frequency table and plots for FD1 (3040 cm^{-1}), a measure of aromatics in the oil. The distribution is unimodal, slightly skewed toward the lower tail, and less peaked than a standard normal distribution. There is a small cluster of occurrences around the 95th percentile. This grouping of data appears to be a continuous part of the distribution and includes normal occurrences. Thus the abnormal threshold is assumed to be at the 99th percentile or 9.1 absorbance units/cm.

g. Table G-13 contains a frequency table and plots for FD2 (1595 cm^{-1}), a measure of aromatics, in the oil collected for these engines. Sixty-four percent of all occurrences are zero. There is a long upper tail and these occurrences are probably abnormal. Accordingly we estimate the abnormal threshold at the 75th percentile or 3.84 absorbance units/cm.

h. Table G-14 contains a frequency table and plots for FDI3 (905-685 cm^{-1}), a measure of aromatics in the oil. This distribution is unimodal, only slightly skewed toward the lower tail, and sharply peaked. Most normal occurrences are tightly clustered about the median. The curve is continuous through the 98th percentile; there is one possible outlier. Accordingly, the abnormal threshold is estimated at the 98th percentile. Its value is 903 integrated absorbance units/cm.

i. Table G-15 contains a frequency table and plots for ZN1 (670 cm^{-1}), a measure of the ZDDP additive, in the oil collected for these engines. This distribution is unimodal, skewed toward the lower tail, and sharply peaked. Since this variable measures additive depletion, the lower tail is significant. The lower tail is small, containing no outliers. Accordingly we estimate the abnormal threshold at the 1st percentile or -2.0 absorbance units/cm.

j. Table G-17 contains a frequency table and plots for iron wear metal contamination in parts per million (PPM). The distribution is unimodal, skewed strongly to the lower tail, and very sharply peaked. Normal occurrences are clustered tightly about the mode. There are two apparent outliers in the data which are assumed to be abnormal occurrences. These outliers occur above the 98th percentile; therefore, the abnormal threshold is estimated at about the 98th percentile or 325 PPM. Both outliers pass all criteria for the infrared variables.

k. Table G-18 contains a frequency table and plots for viscosity of the oil measured on the Nametre Viscometer in centipoise grams/cm^3. The distribution is unimodal skewed slightly toward the upper tail, and much less peaked than a standard normal distribution. The abnormal thresholds are estimated at the 5th percentile or 86.6 centipoise grams/cm and the 95th percentile or 206 centipoise grams/cm^3 Eight samples occur below the lower threshold, and all pass all infrared criteria except one which failed Det I1 due to water contamination. Eight samples occurred above the upper threshold. Three of these failed FD2; two failed FDI3, one also failed Det I1 and FD2; two others failed Det I1 because of water contamination. The most viscous sample, surprisingly passed all infrared criteria.

l. Table G-19 contains a frequency table and plots for total acid number of the oil measured in milligrams of KOH to neutralize. The distribution is unimodal, slightly skewed toward the lower tail, and less peaked than a standard normal distribution. There are no apparent outliers, and the upper threshold can be estimated at the 99th percentile or about 4 milligrams. One sample occurs slightly above this threshold; however, it passes all infrared criteria.

m. Table G-20 contains a frequency table and plots for total solids contamination in percent solid contaminates. There is a strong cluster of occurrences at .4%. The distribution is slightly skewed toward the lower tail and occurrences are broadly distributed. There are no apparent outliers. The abnormal threshold is estimated at the 95th percentile or 8.4%. Four samples occur above this value.

n. Table G-21 contains a frequency table and plots for COBRA. The distribution is unimodal, skewed slightly toward the lower tail, and slightly less peaked than a standard normal distribution. Most occurrence are tightly clustered about the median. Generally, the lower

tail is important because this variable declines as oil degrades; however, free or excessive water contamination will give very high COBRA readings. The lower threshold is estimated at the 1st percentile or about 2.7 units and the upper threshold is estimated at the 99th percentile or 14 units. One sample occurs below this threshold and one occurs above. The lower sample passes all the infrared criteria; the upper sample fails Det I1 and is contaminated with water.

E. Continental Diesel Engine AVDS-1790.

  1. Background.

       The AVDS-1790 engine is a 12 cylinder, four-cycle, multi-fuel engine manufactured by Teledyne Continental Motors. It is used extensively by the US Army in the M60 series tank. It is fueled with diesel fuel. The TSC collected 129 samples from 17 engines over the course of this study. A total of 128 samples were used in this report. One sample was discarded because it was apparently from another engine type. These engines were operated under normal training conditions by the 6th Battalion, 32nd Armored, 4th Infantry Division at Ft. Carson, CO. We were unable to obtain samples from AVDS-1790 test engines. Data for the AVDS-1790 field engines from Ft. Carson are listed in Appendix H, Table H-1.

  2. Significant Correlations.

       Coefficients of correlation were computed between all variable pairs for the combined Ft. Carson data. The correlation matrix is at Table H-2. Interestingly CL2, Det I2, Det I3, Det I4, FD2, and FDI3 were all highly correlated with GC measurements as shown in Table 14. These may be random effects due to the small number of GC measurements performed for this engine. The infrared variables were not significantly correlated with any of the other physical properties. This fact is surprising because the AVDS-1790 appears to degrade its crankcase oil.

  3. Regression Analysis.

       Stepwise regression was used to design predictive models for viscosity, total acid number, total solids, and percent fuel dilution by gas chromatograph. The models are in Appendix H. The best model for viscosity is at Table H-3. It has an R^2 of .46 and the following 17 independent variables:

105

TABLE 14. SIGNIFICANT CORRELATIONS: AVDS-1790 ENGINE

PHYSICAL PROPERTY VARIABLES

IR VARIABLE	HOURS FIELD	FE FIELD	VIS FIELD	TAN FIELD	SOLIDS FIELD	COBRA FIELD	GC FIELD
CL2							.878
Det I1							
Det I2							.912
Det I3							.902
Det I4							.899
FD1							
FD2							.708
FDI3	-.532						.757
ZN1							

```
CL1              CL1 x Det I2         CL2 x Det I4
Det I3           CL1 x Det I3         Det I1 x Det I2
Det I4           CL1 x Det I4         Det I1 x Det I3
(CL1)²           CL2 x Det I1         Det I1 x Det I4
(CL2)²           CL2 x Det I2         Det I2 x Det I3
(Det 2)²         CL2 x Det I3
```

The best model for total acid number is at Table H-4. It has an R^2 of .35 and the following 13 independent variables:

```
CL1              (CL2)²               CL2 x Det I2
CL2              (Det I1)²            Det I1 x Det I3
Det I2           (Det I2)²            Det I2 x Det I4
Det I3           (Det I3)²
Det I4           CL1 x Det I2
```

The best model for total solids is at Table H-5. It has an R^2 of .94 and the following 15 independent variables:

```
CL2              (CL2)²               CL1 x Det I3
Det I2           (Det I1)²            CL2 x Det I1
Det I3           (Det I3)²            Det I1 x Det I3
Det I4           CL1 x Det I1         Det I1 x Det I4
(CL1)²           CL1 x Det I2         Det I2 x Det I3
```

The best model for GC is at Table H-6. It has an R^2 of .94 and 3 independent variables:

```
CL2              Det I2               Det I3
```

This is the best model for fuel dilution we were able to design in the study. Interestingly, it does not contain any of the aromatics we had included specifically for this purpose. The model for total solids is also very good, though large and complex. The models for viscosity and total acid number are poor. This might be expected for total acid number because these data have only a few occurrences in which TAN is above 4.0. However, a good model for viscosity should have been feasible. There are apparently factors influencing viscosity for this engine for which we have not accounted sufficiently. A probable factor in this category is high water contamination.

4. <u>Representative Engine.</u>

A single engine from the field engines was selected to highlight the change in infrared data over sequential samples. Data for this engine are shown in Table 15. The iron wear metal is high in this

TABLE 15

PHYSICAL AND INFRARED TEST DATA - M60 TANK, AVDS 1790

SAMPLE	FE PPM	VIS	TAN	SOLIDS %	GC %	CRACKLE	COBRA	CL2	DET I1	DET I2	DET I3	DET I4	FD1	FD2	FD13	ZN1	HRS
CE01S	229	239	2.47	3.2	--	N	8.5	22.29	337.13	100.30	273.40	644.41	2.73	0	362.79	-0.73	unk
CE02S	203	234	2.58	3.6	--	N	8.1	22.83	51.18	87.09	260.21	594.76	2.19	2.63	328.53	-1.36	"
CE03S	403	232	2.58	3.6	--	N	8.2	23.75	1879.23	76.31	339.21	646.18	3.07	3.64	433.75	0.04	"
CE04S	157	217	2.22	3.2	--	N	--	16.28	772.32	220.01	378.64	917.56	0.44	0	-138.94	-0.39	"
CE05S	204	195	2.13	2.0	--	N	5.0	16.96	1593.17	265.68	650.09	1840.37	3.72	0	205.20	-0.29	"
CE06S	168	306	2.18	2.0	--	N	3.0	17.63	1087.05	121.71	601.98	1349.51	3.16	0	214.49	-0.12	"
CE07S	277	311	2.39	2.8	--	N	3.5	19.95	937.44	124.70	617.39	1302.43	1.98	7.25	227.30	-0.81	"
CE08S	153	202	2.69	2.0	--	N	6.1	5.76	1527.15	1.28	48.05	53.64	3.81	0	55.32	-1.24	"
CE09S	169	248	2.69	3.2	--	N	--	22.33	373.08	8.88	505.24	1224.50	-1.08	0	342.97	-0.40	"
CE10S	285	243	2.82	4.0	--	N	--	16.07	1505.00	62.91	515.19	1551.49	-0.16	0	150.60	0.79	"
CE11S	263	321	3.28	18.0	--	P	--	37.25	17958.95	------- HIGH WATER CONDITION -------								"
CE12S	142	297	2.02	8.0	--	P	--	8.66	26514.33	------- HIGH WATER CONDITION -------								"
CE13S	147	280	2.43	2.4	--	N	--	11.14	822.35	233.45	920.44	2554.91	6.49	0	1520.28	1.41	"
CE14S	225	275	2.42	2.4	--	N	--	12.54	1002.95	246.51	1016.29	2603.76	7.02	0	1444.52	1.20	"
CE15S	117	326	2.70	4.0	--	N	--	22.35	1864.41	370.48	1553.45	3917.90	5.77	0	1503.18	1.00	"
CE16S	153	263	3.24	4.8	--	N	--	31.77	1770.97	428.14	1595.63	4026.30	4.32	17.21	1409.88	0.31	"

108

engine, and this indicates some engine wear. The iron decrease in
samples CE04S, CE06S, CE08S, CE12S, and CE15S indicates that oil
additions and resultant dilution effects probably occurred. The data
show only light oil degradation. The only contamination noted was for
hydroxyl (Det I1, 3600-3150 cm^{-1}), particularly in two samples (CE11S
and CE12S). In fact the moisture was so extensive in both of these
samples that the other infrared variables were blocked. The infrared
spectra in Figure 45 show a comparison of six consecutive used oil
samples (CE11S through CE16S) from this engine and the reference oil.
There are no glycol peaks at 1079.8 and 1032.8 cm^{-1}. The hydroxyl found
in this engine is from condensation, not from a coolant leak. The
differential infrared spectra in Figure 46 of the same six consecutive
samples (Ce11S through CE16S) show high hydroxyl for two samples, light
oxidation (Det I2, 1810-1714 cm^{-1}), and light to moderate nitration
(Det I3, 1650-1538 cm^{-1}). Moderate oxidation/sulfation (Det I4,
1300-1000 cm^{-1}) is present in five of these samples. Sample CE12S shows
very light oxidation/sulfation, probably due to the very high concen-
trations of moisture. The differential spectrum of the reference oil is
included also, and it shows the location of the base line used.

5. Selection of Threshold Levels.

Univariate statistics were performed on each variable in the
field data for the combined set of engines. These data are also in
Appendix H. By examining the frequency distribution, an indication of
normal behavior for AVDS-1790 engines may be inferred as follows:

a. Table H-7 contains a frequency table and plots for CL2
(1980 cm^{-1}), a measure of carbon loading in the oil collected from these
engines. The distribution is bimodal with a small secondary mode
occurring in the upper tail. The distribution is skewed toward the
lower tail and is much less peaked than a standard normal distribution.
If one assumes that the secondary mode is from a distribution of
abnormal occurrences, the two distributions overlap at approximately 48
absorbance units/cm. This value is at the 90th percentile of the total
data set. Thus 48 absorbance units/cm is estimated to be the abnormal
threshold for CL2 in this engine.

b. Table H-8 contains a frequency table and plots for Det I1
(3600-3150 cm $^{-1}$), a measure of hydroxyl (principally water contami-
nation), collected from these engines. These data are skewed toward the

FIGURE 45

IR SPECTRA - 7 SAMPLES

US ARMY M-60 TANK ENGINE

SAMPLES : 1 = REF
11 = OE115
12 = OE125
13 = OE135
14 = OE145
15 = OE155
16 = OE165

MAX=100.00 T

SAMPLE SERIES : AMOS 1790

MIN=0.00 T
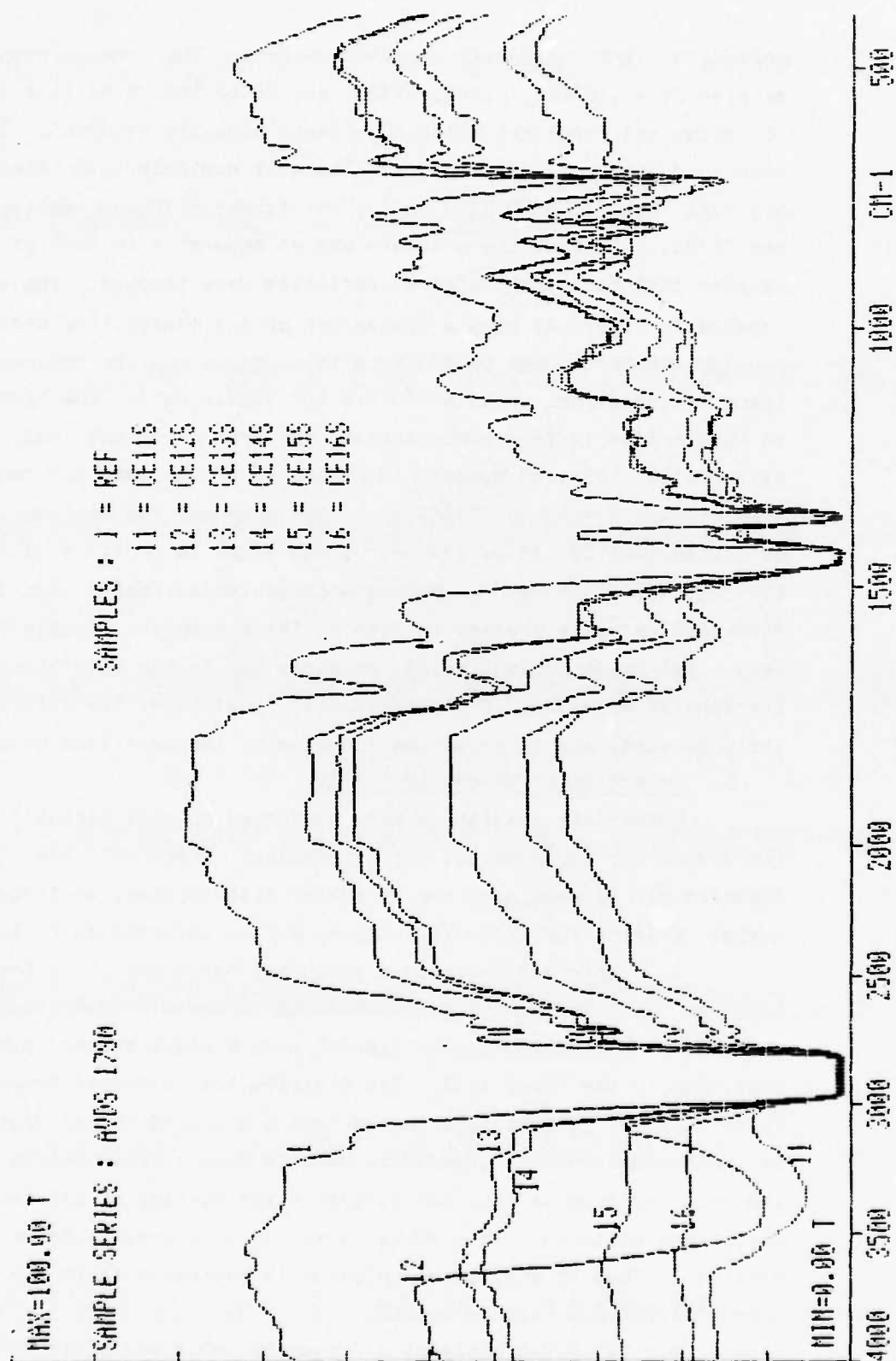
FIGURE 46

IR DIFFERENTIAL SPECTRA - 7 SAMPLES

US ARMY M-60 TANK ENGINE

111
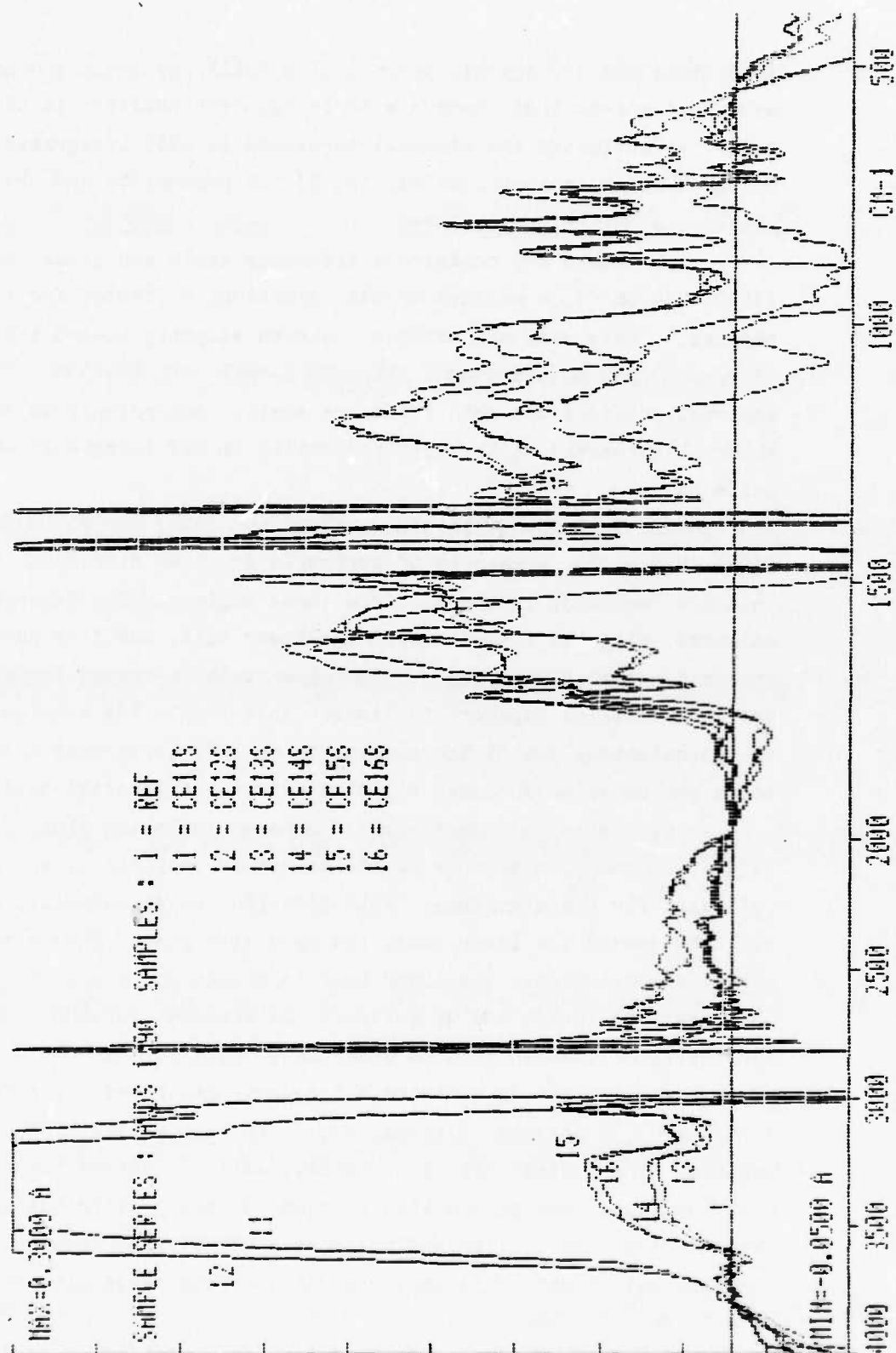
lower tail and are sharply peaked. The tails are small and nearly symmetric except that there are three apparent outliers in the upper tail. We estimated the abnormal threshold at 4800 integrated absorbance units/cm which is approximately the 97.5th percentile and the last· occurrence before the outliers.

      c. Table H-9 contains a frequency table and plots for Det I2 (1810-1714 cm^{-1}), a measure of oil oxidation, collected for these engines. These data are unimodal, skewed slightly toward the lower tail, and less peaked than a standard normal distribution. There are no apparent outliers and both tails are small. Accordingly we estimate the abnormal threshold at the 99th percentile or 527 integrated absorbance units/cm.

      d. Table H-10 contains a frequency table and plots for Det I3, (1650-1538 cm^{-1}), a measure of carboxylates (some nitration is observed in a few samples), in the oil from these engines. The distribution is unimodal, slightly skewed toward the lower tail, and less peaked than a standard normal distribution. The upper tail is larger·than the lower tail and contains apparent outliers. We estimate the abnormal threshold at approximately the 97.5th percentile or 1280 integrated absorbance units per cm which includes all data except the apparent outliers.

      e. Table H-11 contains a frequency table and plots for Det I4 (1300-1000 cm^{-1}), a measure of oil oxidation, sulfation, and glycol, collected for these engines. This distribution is unimodal, skewed slightly toward the lower tail, and much less peaked than a standard normal distribution. The lower tail is smooth and continuous. The upper tail is large, and we estimate the abnormal threshold at the 95th percentile or 3424 integrated absorbance units per cm.

      f. Table H-12 contains a frequency· table and plots for FD1 (3040 cm^{-1}), a measure of aromatics, in the oil collected for these engines. The distribution is unimodal, slightly skewed toward the lower tail, and much less peaked than a standard normal distribution. Overall, the distribution approximates a normal distribution very well. The abnormal threshold is estimated at the 95th percentile or 9.3 absorbance units/cm.

      g. Table H-13 contains a frequency table and plots for FD2 (1595 cm^{-1}), a measure of aromatics in the oil collected from these engines. Sixty-three percent of these occurrences were zero. The upper

112

tail is large with extreme values. All occurrences above zero may be abnormal. We estimate the abnormal threshold at the 75th percentile or 3.9 absorbance units/cm.

h. Table H-14 contains a frequency table and plots for FDI3 (905-685 cm^{-1}), a measure of aromatics, in the oil collected for these engines. This distribution is unimodal, skewed toward the lower tail, and less peaked than a standard normal distribution. The upper tail contains several apparent outliers. We estimate the abnormal threshold below these outliers at the 90th percentile or 1008 integrated absorbance units/cm.

i. Table H-15 contains a frequency table and plots for ZN1 (670 cm^{-1}), a measure of ZDDP additive, in the oil collected for these engines. The lower tail of this distribution is important because the ZDDP additive tends to deplete when in service. The distribution is unimodal, skewed slightly toward the lower tail, and less peaked than a standard normal distribution. The lower tail is small. The data is tightly clustered about the median. Accordingly, we estimate the abnormal threshold at the 1st percentile or -2.09 absorbance units/cm.

j. Table H-17 contains a frequency table and plots for iron wear metal, in parts per million (PPM). The distribution is unimodal, skewed toward the lower tail, and more peaked than a standard normal distribution. The upper tail is long and contains an apparent outlier. The apparent outliers fall above the 97.7th percentile and this point or 581 PPM is estimated as the abnormal threshold. There are three samples occurring above this threshold. The two lesser occurrances also failed the Det I4 criterion. The largest value, 867 PPM, failed CL2, Det I2, Det I4, and FDI3.

k. Table H-18 contains a frequency table and plots for viscosity measured on the Nametre Viscometer in centipoise grams/cm^3. The distribution is unimodal, slightly skewed toward the lower tail, and much less peaked than a standard normal distribution. Overall, the distribution closely approximates a normal distribution. The abnormal thresholds are estimated at the 5th percentile or 95 centipoise grams/cm^3 and the 95th percentile or 411 centipoise grams/cm^3. Six samples occur below this threshold. Of those falling below the threshold, four passed all infrared criteria, one failed the FD2 criteria, and one failed the Det I4 and FD2 criteria. Of those samples falling above the threshold,

113

three passed all infrared criteria, two failed the FD2 criterion, and one failed the Det I1 criterion because of water contamination.

l. Table H-19 contains a frequency table and plots for total acid number of the oil, measured in milligram of KOH to neutralize. The distribution is unimodal, skewed toward the lower tail and very sharply peaked. The upper tail is continuous to about the 98th percentile; and this point, 4.6 milligrams, is taken as the abnormal threshold. Three samples occur above this threshold. Of these, two pass all infrared criteria, and the middle sample failed the Det I4 criterion.

m. Table H-20 contains a frequency table and plots for total solids measured in percent solid contamination. The distribution is unimodal, strongly skewed toward the lower tail, and very peaked. Normal occurrence tightly cluster about the mode. The abnormal threshold is estimated at the 95th percentile or 10% solids. Six samples occur above this threshold, and all but one fail Det I1 because of water contamination. The sixth sample failed the FD2 criterion.

n. Table H-21 contains a frequency table and plots for COBRA. The distribution is bimodal, skewed toward the lower tail, and more peaked than a standard normal distribution. A secondary mode is in the lower tail and is of interest because this variable tends to decrease as oil degrades. The 1st percentile or 3 units is estimated as the abnormal threshold. No samples occur below this value; three occurrences are exactly 3 units. Infrared variables for these were examined; however, these samples passed all the infrared criteria.

F. Propane Fueled Engines.

1. Background.

Samples from several propane fueled engines used by the Air Force as administrative and flight line vehicles were also included in the study. These engines were Ford 6 cylinder and 8 cylinder engines, a General Motors V-8 engine, and a Dodge 6 cylinder engine operated in pick-up trucks, vans, and sedans. We collected 134 samples from 21 engines over the course of the study. We used 61 Ford 6 cylinder samples, 28 Ford 8 cylinder samples, 18 GM V-8 samples, and 17 Dodge 6 cylinder samples in this study. These data are in Appendix I in Tables I-1, I-18, I-21, and I-24. Barium fluoride (BaF_2) cells were used in obtaining the infrared spectra of the oil samples from the propane engines because these samples generally contain some amounts of

114

moisture. Further, since these samples are fueled with propane, we did not attempt to analyze for aromatics (FD1, FD2, FDI3) as an indication of fuel dilution. In fact, FDI3 and ZN1 could not be calculated because the BaF_2 cell is not operative at the low wavenumber range of these constituents. This discussion is limited generally to the Ford 6 cylinder engines because the engine population for the other type engine was too small for significant conclusions.

2. Significant Correlations.

Coefficients of correlation were computed between all possible variable pairs for each set of engines. The correlation matrices are in Tables I-2, I-19, I-22, and I-25. Correlations between infrared variables and physical properties greater than or equal to .5 for each set of engines are listed in Table 16. Det I4 (oxidation, sulfation, glycol) exhibited the most significant correlation with the physical properties. We believe this variable to be primarily a measure of oxidation for these engines because propane fuel is reasonably free of sulfur constituents. Carbon loading, oxidation, and nitration (CL2, Det I2, Det I3) also exhibited reasonably strong correlations.

3. Representative Engine.

Representatives of each type propane gas engine were not selected for detailed discussion; however, a single engine, a Ford V8-360 CID, was selected from the entire set of propane engines that exhibited engine wear, oil deterioration, and oil contamination. The data from the engine selected are shown in Table 17. Engine wear is evident because of high iron wear metal (Fe). The decrease in Fe for samples PB02J and PB08J are attributed to an oil change. We believe the continued increase in Fe after each oil change is caused by corrosion from moisture contamination. Note the positive crackle tests for four samples. The Fe content decreases for sample PB08J because of an oil change (Oct 82) but immediately shows an increase for sample PB09J. The moisture is probably the result of condensation. These engines are operated in a stop and go manner with high idle time and little or no sustained high revolutions per minute. This method of operation is conducive to moisture build-up from condensation. The decrease in TAN after sample PB07J is attributed to an oil and filter change. The COBRA values show no discernable trends.

115

TABLE 16

SIGNIFICANT CORRELATIONS : PROPANE GAS ENGINES

PHYSICAL PROPERTY VARIABLES

ENGINE	IR VARIABLE	MILES	FE	VIS	TAN	SOLIDS	COBRA
FORD 6	CL 2						
	DET I1						
	DET I2		-.521				-.599
	DET I3	.745				.566	
	DET I4						-.541
FORD 8	CL 2		.799				
	DET I1						
	DET I2				.554		
	DET I3				.760		.565
	DET I4		.594	-.546	.651		
GM 8	CL 2			.545			
	DET I1						
	DET I2		—				
	DET I3						
	DET I4	.624	.629				
DODGE 6	CL 2	.60!	.515	.583			
	DET I1			.508			
	DET I2	.525					
	DET I3					.615	
	DET I4	.525	.658	.527	.583		

TABLE 17

PHYSICAL AND INFRARED TEST DATA - FORD CREW CAB, PROPANE GAS ENGINE

SAMPLE	FE PPM	VIS	TAN	SOLIDS %	GC %	CRACKLE	COBRA	CL2	DET I1	DET I2	DET I3	DET I4	FD1	FD2	FDI3	ZN1	MILES
PB01J	130	109	2.53	0.4	--	N	40.5	1.66	3543.24	398.85	597.12	2720.92	1.60	0	--	--	667
PB02J	74	84	2.94	0.4	--	P	15.0	1.83	4988.40	1513.92	1227.81	5376.25	25.66	26.52	--	--	450
PB03J	152	84	3.52	2.8	--	P	20.0	2.14	2136.71	1570.94	1321.84	6??9.19	24.06	28.12	--	--	729
PB04J	283	85	4.72	2.0	--	N	19.0	3.53	538.21	1226.39	1336.14	7404.43	20.91	0	--	--	846
PB05J	445	97	4.03	3.2	--	P	16.5	4.18	1868.55	993.89	1181.21	6118.41	10.39	0	--	--	1982
PB06J	447	109	4.92	2.3	--	N	16.5	3.21	3435.54	864.25	1310.40	6146.21	7.66	0	--	--	2733
PB07J	555	109	4.94	2.0	--	N	17.5	3.12	2697.16	881.13	1326.95	6343.27	7.17	0	--	--	2847
PB08J	41	101	3.62	0.4	--	N	18.0	0.50	---------- REFERENCE FOR REMAINING SAMPLES ----------								19
PB09J	94	97	3.55	2.8	--	P	17.5	0.50	7119.25	80.05	772.14	1795.18	6.60	0	--	--	341
PB10J	140	97	4.51	2.0	--	N	20.0	0.35	2247.78	106.64	783.14	2814.64	1.32	0	--	--	778

117

The infrared spectra, Figure 47, reflects light moisture, almost negligible oxidation, light nitration and light sulfation. There is no evidence of glycol/antifreeze contamination. Carbon loading (CL2, 1980 cm^{-1}) and solids were negligible for all samples analyzed. The differential infrared spectra, Figure 48, shows light to moderate hydroxyl (Det I1, 3600-3150 cm^{-1}), light oxidation (Det I2, 1810-1714 cm^{-1}), and light to moderate sulfation (Det I4, 1300-1000 cm^{-1}). Propane gas does not contain aromatics; therefore, aromatic fuel peaks are not present.

4. Regression Analysis.

Stepwise regression was used to design predictive models for viscosity, total acid number, and total solids. Percent fuel was not modeled because these engines are fueled with propane gas and leave no aromatic constituents in the oil. Only the Ford 6 cylinder engines were used in this analysis because of the limited sample size of the other engines. The best model for viscosity is at Table I-3. It has an R^2 of .76 and the following 11 independent variables:

Det I4	(Det I4)^2	CL2 x Det I4
FD1	CL2 x Det I1	Det I1 x Det I2
(Det I1)^2	CL2 x Det I2	Det I1 x Det I4
(Det I3)^2	CL2 x Det I3	

The best model for total acid number is at Table I-4. It has an R^2 of .90, and the following 11 independent variables:

Det I3	(Det I3)^2	Det I1 x Det I4
Det I4	CL2 x Det I1	Det I2 x Det I3
FD2	CL2 x Det I3	Det I2 x Det I4
(Det I2)^2	Det I1 x Det I3	

The best model for total solids is at Table I-5. It has an R^2 of .69, and the following 11 independent variables:

Det I3	(Det I1)^2	CL2 x Det I4
Det I4	(Det I3)^2	Det I1 x Det I2
FD1	CL2 x Det I2	Det I1 x Det I3
(CL2)^2	CL2 x Det I3	

The models for viscosity and, especially, total acid number are quite good. As noted earlier, our success with total acid number was due to the existance of considerable variation in the total acid number values.

118

FIGURE 47

IR SPECTRA - 4 SAMPLES
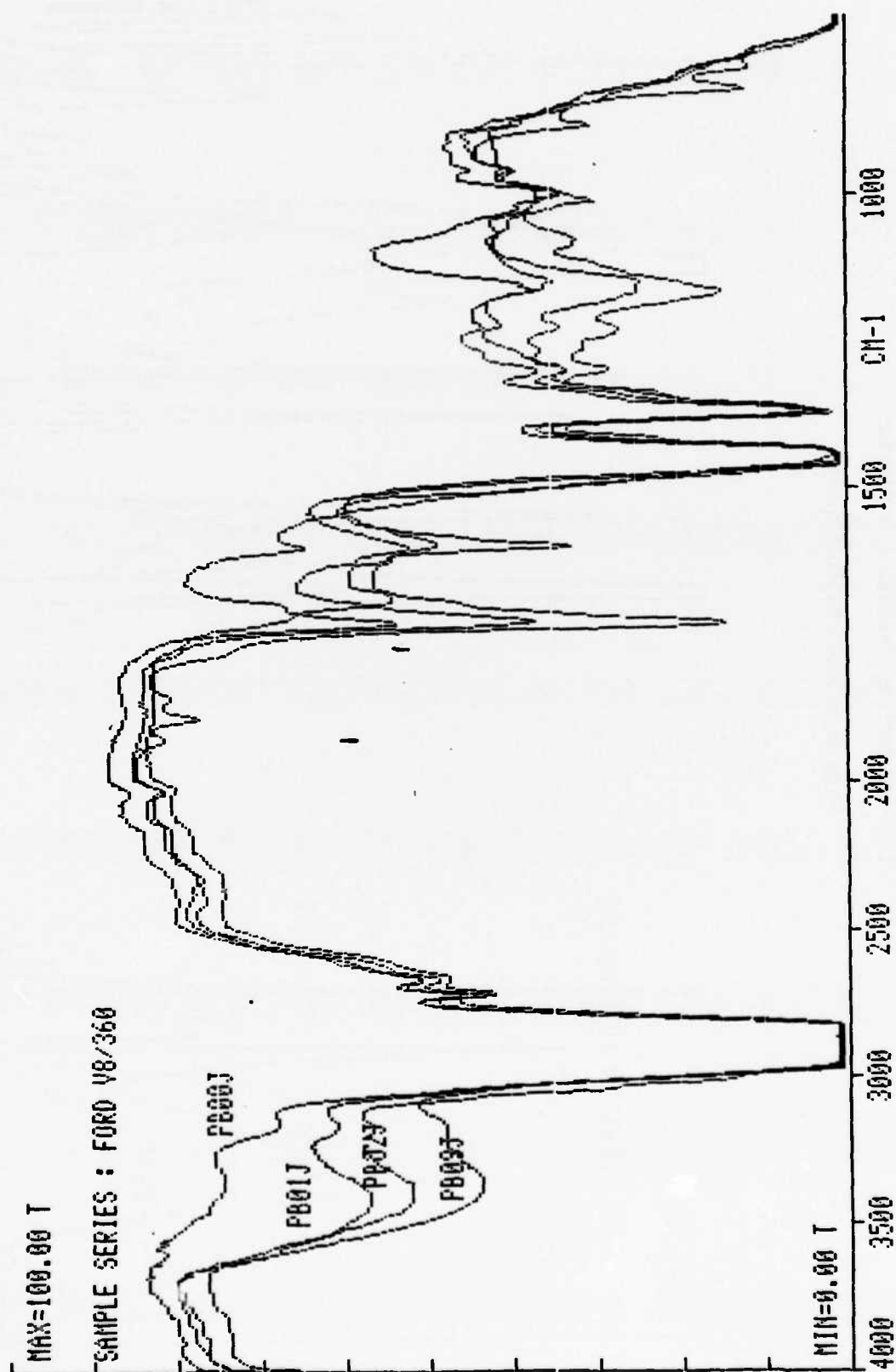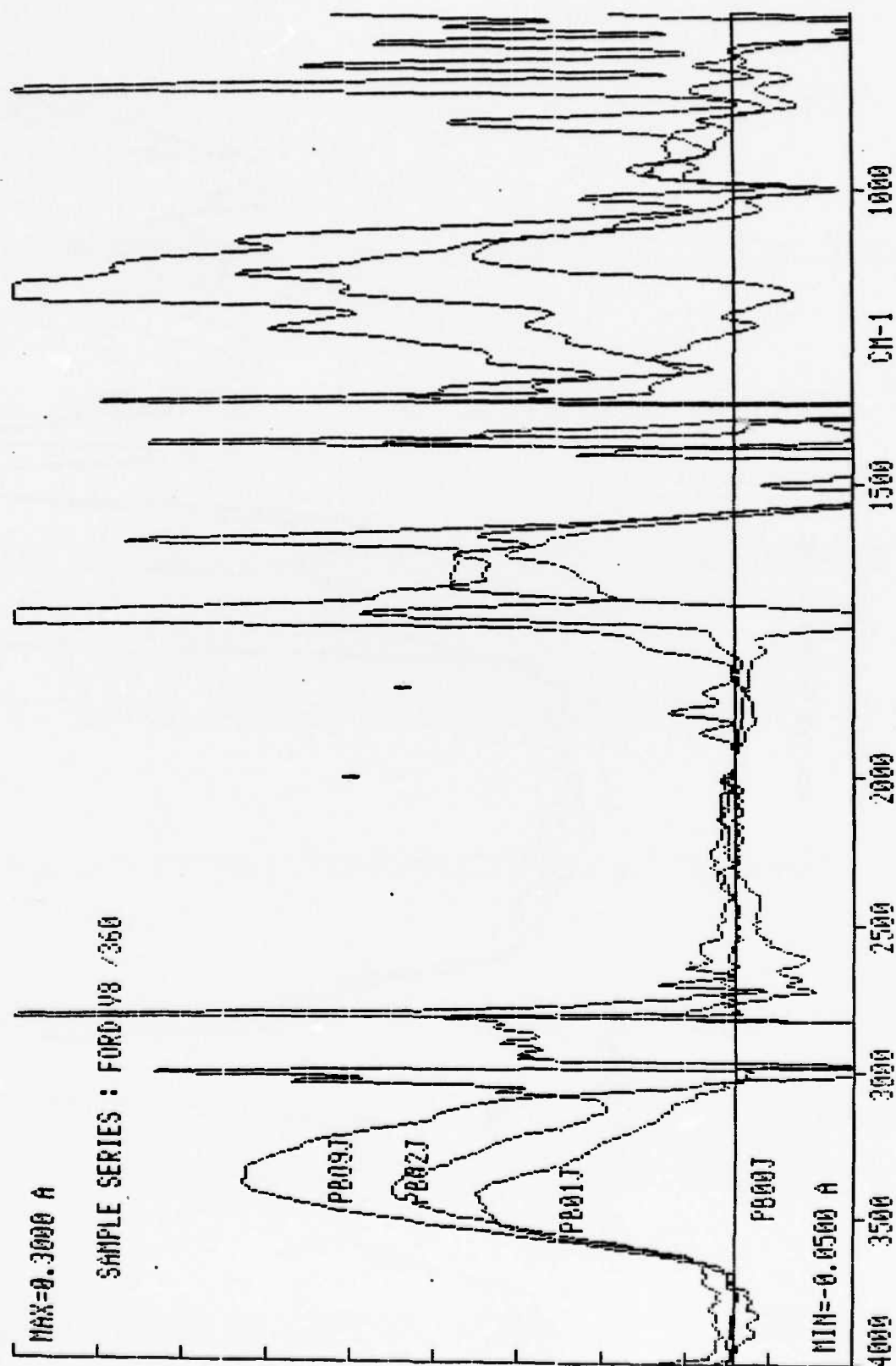
FORD CREW CAB V8-360 ENGINE

FIGURE 48

IR DIFFERENTIAL SPECTRA - 4 SAMPLES

FORD CREW CAB V8-360 ENGINE

MAX=0.3000 A

SAMPLE SERIES : FORD V8 /360

PB09J

PB82J

PB01J

PB00J

MIN=-0.0500 A

CM-1

1000
1500
2000
2500
3000
3500
4000

120

5. Selection of Threshold Levels.

Univariate statistics were performed on each variable in the data set for the four different engines; however, only the Ford 6 cylinder engines are discussed below because the engine population in the other data sets was too small. These data are also in Appendix I.

a. Ford 6-cylinder.

(1) Table I-6 contains a frequency table and plots for CL2 (1980 cm^{-1}), a measure of carbon loading in the oil for this engine. The distribution is skewed slightly toward the lower tail and is very flat. The abnormal threshold for CL2 in this engine is estimated at the 99th percentile or 3.27 absorbance units/cm.

(2) Table I-7 contains a frequency table and plots for Det I1 (3600-3150 cm^{-1}), a measure of hydroxyl (principally water contamination), for this engine. The distribution is strongly skewed toward the lower tail and slightly less peaked than a standard normal distribution. The abnormal threshold is estimated at the 95th percentile or 6489 integrated absorbance units/cm.

(3) Table I-8 contains a frequency table and plots for Det I2 (1810-1714 cm^{-1}), a measure of oil oxidation, for this engine. This distribution is skewed toward the upper tail and is less peaked than a standard normal distribution. There are a number of negative values in this distribution with an apparent secondary mode at about -3150 integrated absorbance values. These extreme negative values probably result from an abberation in the carbon loading correlation algorithm and were discarded. Only the upper tail is significant, and we estimate the abnormal threshold at the 94.7th percentile or 265 integrated absorbance units/cm. The 94.7th percentile was selected because there is a twofold increase in the value of the observation at the 95th percentile and we selected the observation immediately before the 95th percentile for the abnormal threshold.

(4) Table I-9 contains a frequency table and plots for Det I3 (1650-1538 cm^{-1}), a measure of oil nitration , for this engine. This distribution is skewed toward the lower tail and is more peaked than a standard normal distribution. The abnormal threshold is estimated at the 95th percentile or 1262 integrated absorbance units/cm.

(5) Table I-10 contains a frequency table and plots for Det I4 (1300-1000 cm^{-1}), a measure of oil oxidation, sulfation, and

121

glycol in the oil for this engine. The distribution is slightly skewed toward the upper tail and is much flatter than a standard normal distribution. The abnormal threshold is estimated at the 95th percentile or 5779 integrated absorbance units/cm.

(6) Table I-14 contains the frequency table and plots for iron wear metal contamination in parts per million (PPM) for this engine. The distribution is skewed toward the lower tail and is flatter than a standard normal distribution. Above the 89th percentile there are probable outliers and this value, 265 PPM, is taken as the abnormal threshold for iron wear metal.

(7) Table I-15 contains a frequency table and plots for oil viscosity in centipoise grams/cm^3 for this engine. The distribution is slightly skewed toward the lower tail and is very flat. The 5th and 95th percentile are assumed to be the lower and upper limits. These values are 86 and 145 centipoise grams/cm^3 respectively.

(8) Table I-16 contains a frequency table and plots for total solid contamination in percent solids in the lubricating oil. The distribution is strongly skewed toward the lower tail and sharply peaked. The upper tail is long and contains one probable outlier. The abnormal threshold is estimated at the 98.3rd percentile or 10% contamination.

(9) Table I-17 contains a frequency table and plots for COBRA for this engine. This distribution is slightly skewed toward the lower tail and is much flatter than a standard normal distribution. The lower abnormal threshold is estimated at the first percentile or 5 COBRA units. There are no apparent outliers in the upper tail, and the 99th percentile or 38 COBRA units may be assumed as an upper threshold.

b. Other Propane Engines. The data set for the Ford 8 cylinder engine contained only three engines; the GM V-8 engine set and the Dodge 6 cylinder engine set contained only two engines each. These engine populations are judged too small to make valid estimates of evaluation criteria for these engines. Nevertheless, the 95th percentile of the data for each variable for these engines is included in Table 18 to compare these values with the Ford 6 cylinder engine. Tables I-20, I-23, and I-26 in Appendix I contain univariate statistics computed from the data that were available for these engine.

Table 18

SUMMARY OF INFRARED EVALUATION CRITERIA FOR PROPANE ENGINES

ENGINE	FORD 6 CYLINDER	FORD 8 CYLINDER	GM V8 350 CID	DODGE 6 CYLINDER
CL2	3.27	3.89	4.45	2.4
Det I1	6489	6160	3592	4343
Det I2	265	1551	960	1186
Det I3	1262	1782	941	532
Det I4	5779	8012	4143	3451

G. ASTM Sequence III-D Test, 1977 GM Olds 350 CID V8 Engine.

   1. Background.

      This test uses a 1977, 350 CID (5.7 liter) Oldsmobile V8 engine.
It is operated at high speed (3000 rpm) and high oil temperature, 300 F
(149 C), for 64 hours. Oil additions are permitted. Samples were taken
at 0, 0.167, 4, 8, 16, 24, 32, 40, 48, 56, and 64 hours of operation.
The test is run with leaded gasoline and measures oil characteristics
for: (a) high temperature oxidation, (b) sludge and varnish deposits,
and (c) engine wear (cam and lifter). Six different oil formulations
were obtained from laboratories participating in the American Society
for Testing of Materials Test Monitoring Center (ASTM-TMC) system for
this test. Data were collected for each formulation. Three of the oils
were classified as pass oils and three were classified as fail oils.
The regression analysis on this data was done early in this study when
we used a very detailed methodology for extracting measurements from the
infrared spectra. Table J-1 in Appendix J shows the peaks and regions
used for these sets of engines. The data from these tests are in
Appendix J, Tables J-2, J-22, and J-24.

   2. Significant Correlations.

      Coefficients of correlation were computed between all variable
pairs for the three ASTM Sequence III-D pass oils, for the three ASTM
Sequence III-D fail oils, and for the combined pass and fail oils.
These data are in Tables J-3, J-23, and J-25. Correlation coefficients
between the infrared variables and the physical properties variables
that are greater than 0.5 for the pass oils, fail oils, and combined
set of oils are in Table 19. As can be seen from Table 19, especially
strong correlations exist between the infrared data, except ZN1 and the
physical properties.

   3. Representative Engine.

      Two test engines, one serviced with a pass oil and one with a
fail oil, were selected to highlight the changes in infrared data during
the tests. Data from the engine serviced with the pass oil are shown in
Table 20. Iron (Fe) wear metal increase is attributed to the high speed
and high temperature to which the oil was subjected. Study of Table 20
shows a continuous increase in viscosity, TAN, total solids, oxidation
(Det I2, 1810-1714 cm^{-1}), nitration (Det I3, 1650-1538 cm^{-1}), and
oxidation/sulfation/glycol (Det I4, 1300-1000 cm^{-1}). The increase in

124

TABLE 19

SIGNIFICANT CORRELATIONS - ASTM III-D TEST ENGINES

IR Variable	Oils	PHYSICAL PROPERTY VARIABLES					
		HRS	FE	VIS	TAN	SOLIDS	COBRA
CL2		---	.671	.780	.900	.770	---
Det I1		---	---	.646	.799	.650	---
Det I2		---	.538	.815	.971	.853	---
Det I3		---	.608	.790	.980	.884	---
Det I4	Pass	---	.580	.755	.983	.874	---
FD1	Oils	---	.516	.805	.934	.818	---
FD2		---	---	---	.897	.604	---
FDI3		---	---	.844	.927	.828	---
ZN1		---	---	---	---	---	---
CL2		---	.688	.866	.828	.820	---
Det I1		---	.504	.542	.793	.717	---
Det I2		---	.647	.853	.962	.740	---
Det I3		---	.623	.825	.978	.788	---
Det I4	Fail	---	.642	.829	.984	.726	---
FD1	Oils	---	.600	.782	.890	.728	---
FD2		---	.829	.835	.938	.965	---
FDI3		---	.587	.811	.910	.745	---
ZN1		---	---	---	---	---	---
CL2		---	.692	.766	.828	.803	---
Det I1		---	---	.596	.786	.668	---
Det I2		---	.606	.817	.965	.767	---
Det I3		---	.623	.777	.978	.806	---
Det I4	Pass/Fail	---	.609	.768	.984	.857	---
FD1	Oils	---	.558	.772	.897	.742	---
FD2		---	.588	.677	.916	.506	---
FDI3		---	.503	.822	.916	.764	---
ZN1		---	---	---	---	---	---

TABLE 20

PHYSICAL AND INFRARED TEST DATA - GM SEQUENCE III-D TEST ENGINE, PASS OIL

SAMPLE	FE PPM	VIS	TAN	SOLIDS %	GC %	CRACKLE	COBRA	CL2	DET I1	DET I2	DET I3	DET I4	FD1	FD2	FD13	ZN1	HRS
SW01C	4	95	3.16	0	0	N	26.0	------	------	------	REFERENCE OIL	------	------	------	------	------	
SW02C	19	92	3.23	0.4	--	N	25.0	0.55	- 19.66	- 32.68	5.39	- 109.56	0.30	0	39.57	-0.28	.167
SW03C	82	94	3.12	0.4	--	N	18.0	0.49	241.83	21.68	79.50	179.93	0.11	1.30	36.21	-3.95	4
SW04C	170	102	3.72	7.2	--	N	14.5	0.24	-1264.91	181.33	310.12	1307.81	-0.67	4.24	-116.27	-8.66	8
SW05C	195	110	4.40	2	--	N	14.0	0.21	-1415.06	265.50	405.00	2021.03	-0.53	5.23	-174.65	-9.15	16
SW06C	200	120	4.89	3.2	--	N	15.0	0.25	-1021.23	380.12	514.81	2830.62	-0.13	5.96	-174.59	-9.46	24
SW07C	224	130	5.23	4.0	--	N	15.0	0.25	-1485.96	473.37	611.56	3479.10	-0.14	7.22	-227.36	-9.91	32
SW08C	240	140	6.60	4.0	--	N	16.0	0.25	- 788.78	539.83	736.83	3911.15	0.76	8.24	-183.29	-9.59	40
SW09C	226	160	6.96	4.8	--	N	18.0	0.40	498.31	630.04	927.79	4545.34	1.50	0	- 79.44	-8.72	48
SW10C	243	163	7.58	4.8	--	N	18.0	0.37	- 751.27	786.85	1056.98	5331.00	0.93	0	-135.43	-9.71	56
SW11C	207	294	13.96	6.0	--	N	35.0	1.60	3252.69	2462.26	2437.79	11128.70	5.33	0	563.80	-7.27	64

solids to 7.2% for sample SW04C cannot be explained; however, it may be due to sample contamination. The COBRA readings characteristically decrease as the oil degrades and test hours increase; however, the last sample, SW11C, at 64 hours shows a dramatic increase in COBRA reading. The phenomenon is typical of severe water contamination; however, in this case we believe it to be caused by a sudden saturation of the additive package and build-up of an organic acid. The increases in hydroxyl (Det I1, 3600-3150 cm^{-1}), oxidation (Det I2, 1810-1714 cm^{-1}), nitration (Det I3, 1650-1538 cm^{-1}) and sulfation/glycol (Det I4 1300-1000 cm^{-1}) for these samples also are attributed to organic and/or mineral acid build-up due to oxidation of the oil at the high speed and high temperatures encountered in ASTM Sequence III-D tests. Note the corresponding TAN for this sample increases to 13.96. The infrared spectra, Figure 49, shows continuous degradation for each sample. The changes in sample SW11C are quite obvious in the spectra. The infrared differential spectra, Figure 50, shows only moderate change until the last sample (SW11C). There were no discernable aromatic peaks (3040, 1595 cm^{-1}) or glycol/antifreeze peaks (1079.8, 1032.8 cm^{-1}). FD1 and FDI3 do show sudden increases for sample SW11C: however, these increases are believed to be peripheral effects of the excessive oxidation of this sample. A quick depletion of the ZDDP additive peak (670 cm^{-1}) is observed also.

Data from the engine serviced with the fail oil, Table 21, clearly show more deterioration than the pass oil. The infrared spectra of the fail oil, Figure 51, shows a continuous increase in levels of hydroxyl, oxidation, nitration and sulfation. The infrared differential, Figure 52, shows moderate to heavy deterioration, especially for the last four samples (SW08B, SW09B, SW10B and SW11B). There are no discernable aromatic or glycol/antifreeze peaks; however, there are oxidation interference effects on these peaks and regions which cause the increasing values shown in Table 21. Again depletion of the ZDDP additive peak is observed.

4. Regression Analysis.

Stepwise regression was used to design predictive models for viscosity, total acid number, and total solids. Percent fuel was not modeled because these samples gave no indication of fuel dilution problems. Both the pass and fail data were combined for this analysis.

FIGURE 49

IR SPECTRA - 11 SAMPLES

ASTM SEQUENCE III-D TEST ENGINE, PASS OIL

MAX=100.00 T
SAMPLE SERIES : ASTM SEQ IIID REFERENCE OIL

SAMPLES : SW01C THROUGH SW11C

SW01C IS REFERENCE OIL
SW11C IS LAST OIL SAMPLE IN TEST

MIN=0.00 T
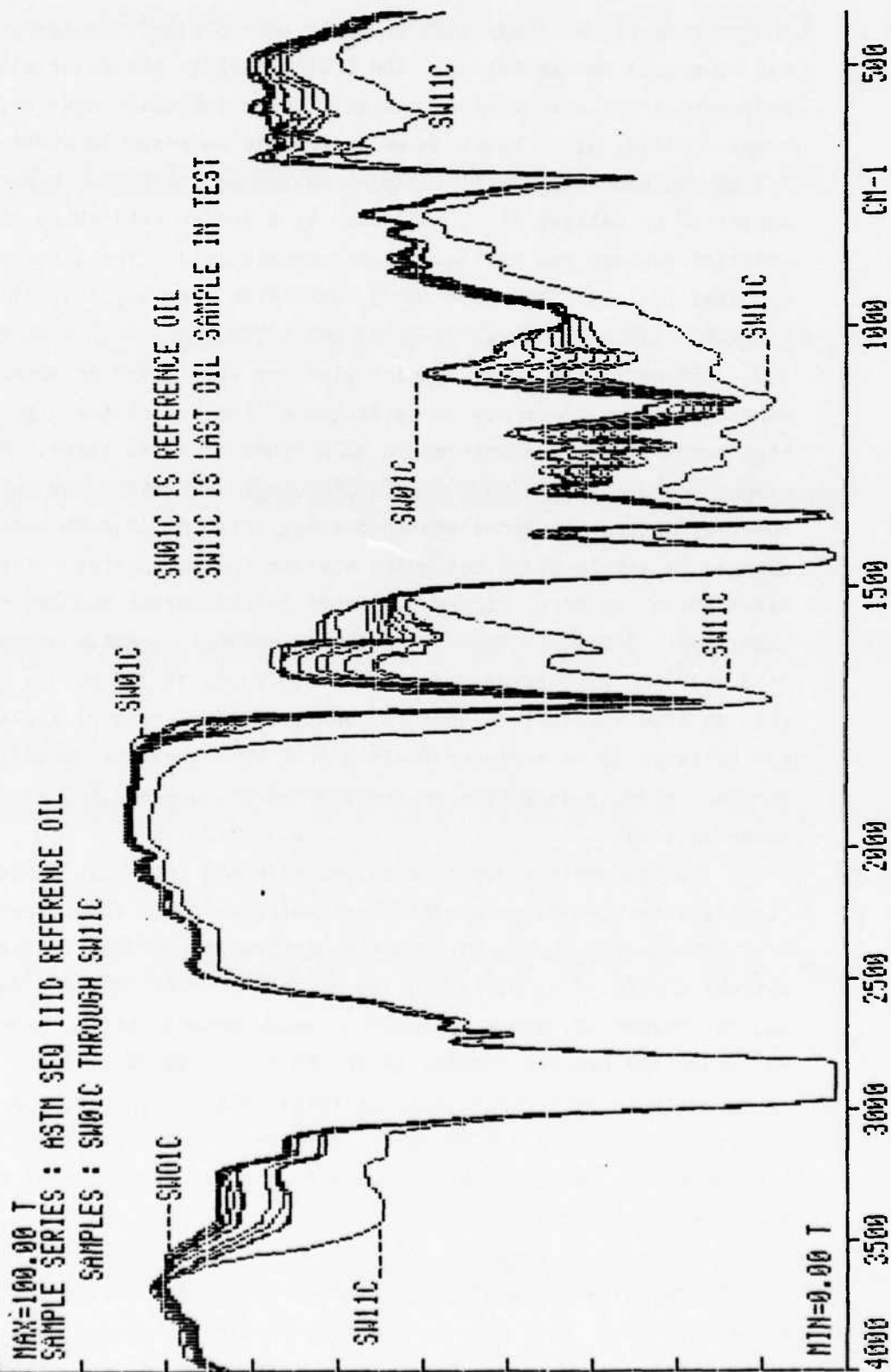
FIGURE 50

IR DIFFERENTIAL SPECTRA - 10 SAMPLES

ASTM SEQUENCE III-D TEST ENGINE, PASS OIL.

MAX=0.3000 A

SAMPLE SERIES : ASTM SEQ IIID REFERENCE OIL

SAMPLES : SW01C THROUGH SW11C
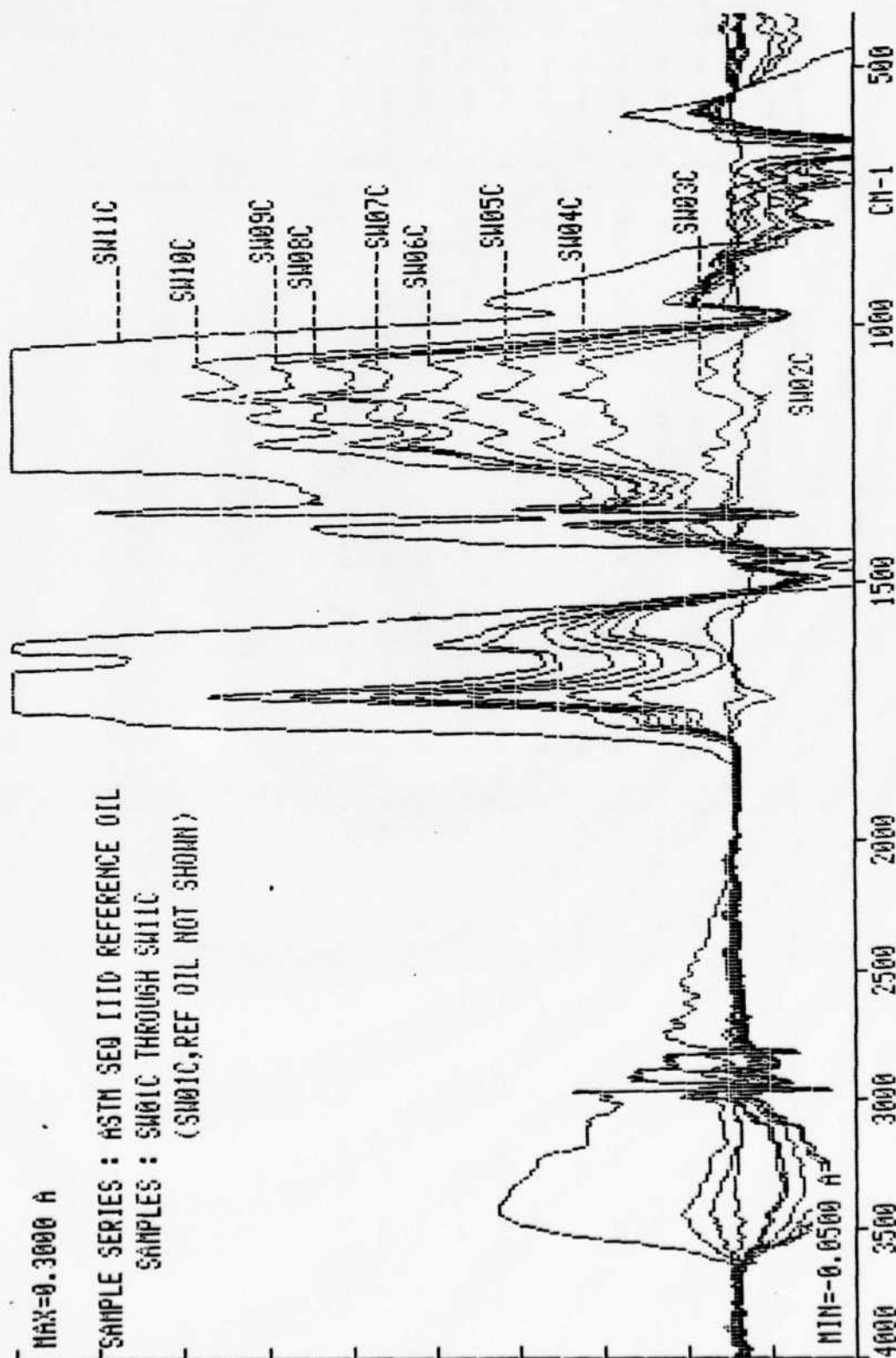(SW01C, REF OIL NOT SHOWN)

MIN=-0.0500 A

129

TABLE 21

PHYSICAL AND INFRARED TEST DATA - GM SEQUENCE III-D TEST ENGINE, FAIL OIL

SAMPLE	FE PPM	VIS	TAN	SOLIDS %	GC %	CRACKLE	COBRA	CL2	DET 11	DET 12	DET 13	DET 14	FD1	FD2	FD13	ZN1	HRS
SW01B	3	85	2.65	0	--	N	11.0	------	------	REFERENCE	OIL	------	------				
SW02B	23	80	3.10	0.4	--	N	10.0	0.33	16.03	-47.02	-18.92	-113.86	-0.42	0	- 4.61	-0.91	.167
SW03B	91	85	3.24	0.8	--	N	10.5	0.67	192.96	12.11	86.72	128.71	-0.52	1.29	- 22.18	-5.58	4
SW04B	212	100	3.99	1.2	--	N	8.0	0.24	-728.09	179.25	390.66	1234.23	-1.48	0	- 182.00	-9.38	8
SW05B	248	112	4.53	2.0	--	N	9.0	0.46	-662.70	287.07	560.66	2007.47	-1.45	5.77	- 242.38	-9.65	16
SW06B	270	125	4.92	4.8	--	N	11.0	0.45	-697.37	451.21	778.58	2837.81	-1.45	0	- 235.77	-9.96	24
SW07B	295	145	7.09	6.0	--	N	16.0	0.70	-36.95	793.99	1146.77	4424.41	-0.46	0	- 131.44	-9.65	32
SW08B	352	295	11.81	8.0	--	N	23.0	1.44	1919.80	2788.21	2397.42	10498.09	4.04	0	584.10	-7.21	40
SW09B	444	660	15.44	12.0	--	N	21.0	2.14	2256.46	4042.76	3158.63	13032.11	6.06	0	930.67	-7.01	48
SW10B	478	1100	16.07	16.0	--	N	16.0	2.93	2916.02	5015.26	3960.03	15162.20	7.59	0	1318.15	-6.44	56
SW11B	386	1700	16.68	22.0	--	N	13.0	3.39	3436.56	5490.10	4363.28	16220.13	8.56	0	1446.40	-5.85	64

130

FIGURE 51

IR SPECTRA - 11 SAMPLES
ASTM SEQUENCE III-D TEST ENGINE, FAIL OIL

MAX=100.00 T
SAMPLE SERIES : ASTM SEQ IIID REFERENCE OIL

SAMPLES : SW01B THROUGH SW11B

SW01B IS REFERENCE OIL
SW11B IS LAST OIL SAMPLE IN TEST

MIN=0.00 T

131
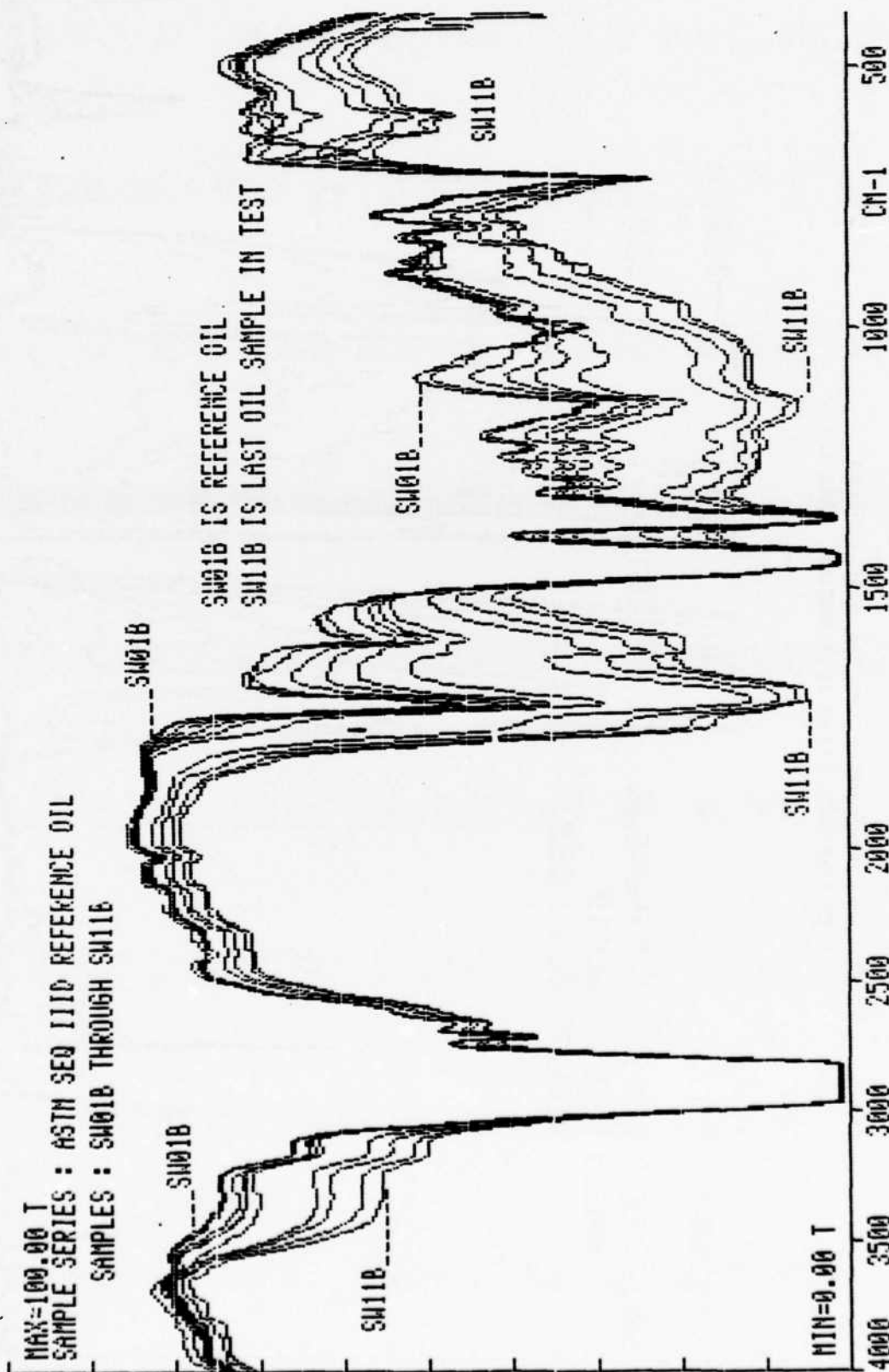
FIGURE 52

IR DIFFERENTIAL SPECTRA - 10 SAMPLES
ASTM SEQUENCE III-D TEST ENGINE, FAIL OIL.

MAX=0.3000 A

SAMPLE SERIES : ASTM SEQ IIID REFERENCE OIL

SAMPLES : SW01B THROUGH SW11B
(SW01B,REF OIL NOT SHOWN)

MIN=-0.0500 A
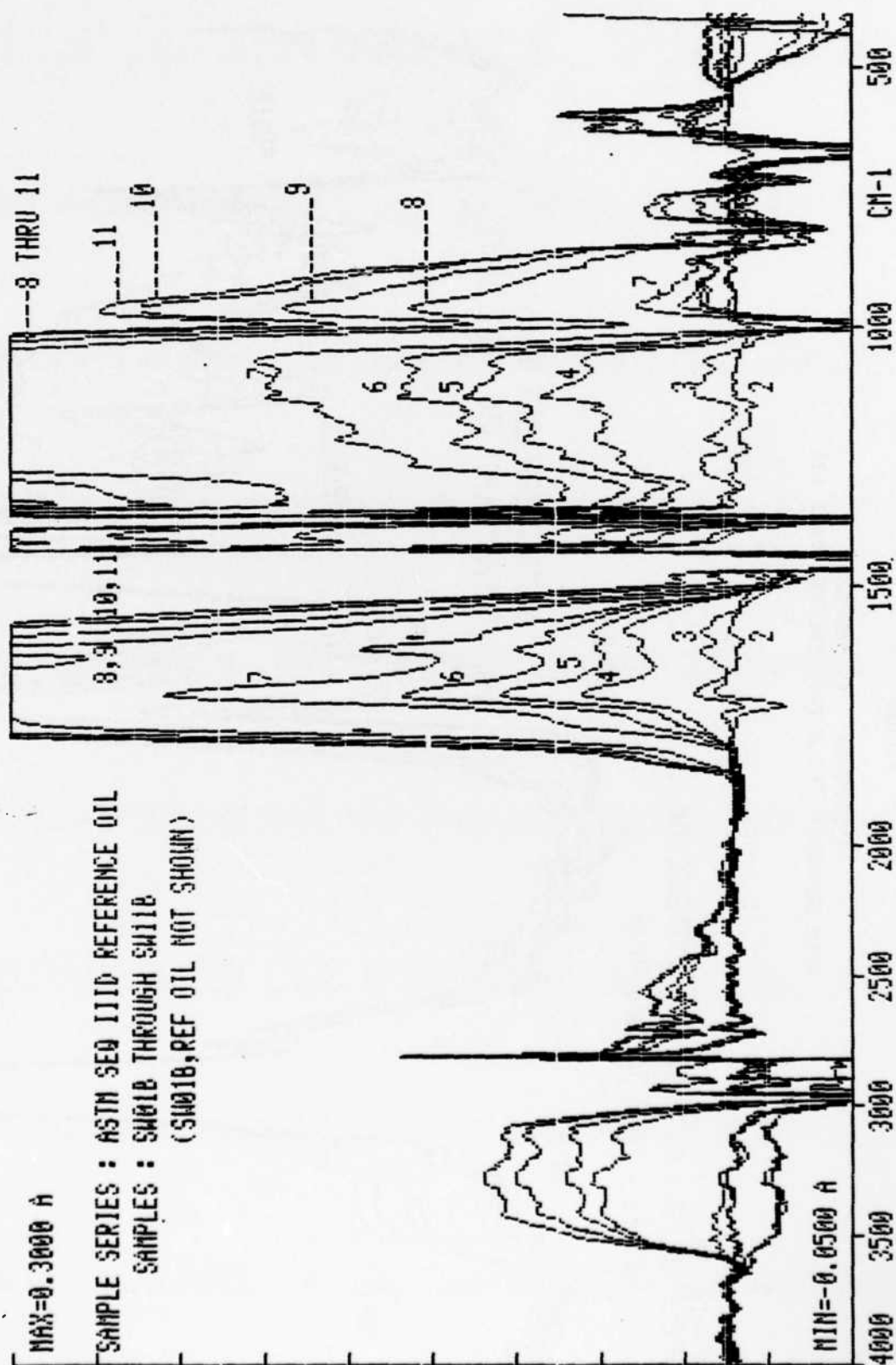
Very good models were possible for all three dependent variables, and they are discussed in detail in reference A-2. The models are shown in Appendix J. The best model for viscosity is at Table J-4. It has an R^2 of .95 and the following 8 independent variables:

Det 4   Det I5 x Det 4

Det I5   (Det I4)^2

(Det 2)^2 Det 2 x Det I4

Det I4 x Det 2   Det I4 x Det I4

The best model for total acid number is at Table J-5. It has an R^2 of .98 and 2 independent variables, Det I5 and (Det 2)^2. The best model for total solids is at Table J-6. It has an R^2 of .94 and the following 6 independent variables:

Det I4   Det I4 x Det 4

Det 4   Det 9 x Det I3

Det 4 x CL1   Det I2

The above models were the best predictive models we were able to design during this study. The reason is twofold. First, the data from these engines were collected under controlled laboratory conditions, and there was no mixing of base oils. Secondly, the nature of the test, and test oils, caused considerable degradation of the oil and subsequent, signi- ficant variation in the variables used to measure degradation. Conse- quently, we were able to develop efficient models to mathematically describe this change.

   5. <u>Selection of Threshold Levels.</u>

       Univariate statistics were performed on each variable in the combined data sets of both pass and fail oils. These data are also in Appendix J. By examining the frequency distribution of these variables and considering that approximately one half of the samples analyzed for these data set were classified as fail oil, an indication of typical behavior for normal and abnormal engines may be inferred as follows:

       a. Table J-7 contains a frequency table and plots for CL2 (1980 cm^{-1}), a measure of carbon loading in the oil for these engines. Generally carbon loading is not a problem for these engines and values for both pass and fail oils were relatively small. The distribution of these occurrences is skewed toward the lower tail and slightly less peaked than a standard normal distribution. There appear to be no out- liers in the upper tail; accordingly, we estimate an abnormal threshold at the 97th percentile or 7.7 absorbance units/cm.

133

b. Table J-8 contains a frequency table and plots for Det I1 $(3600-3150 \text{ cm}^{-1})$, a measure of hydroxyl (principally water contamination) in the oil. There is an apparent bimodal nature to the frequency distribution of these data. There is a primary mode at approximately -2000 integrated absorbance units/cm. A secondary mode exists at approximately 5000 integrated absorbance units. Considering these to be two separate distributions, they would appear to overlap at approximately 2300 integrated absorbance units/cm. Accordingly we estimate an abnormal threshold for Det I1 for these engines at 2300 integrated absorbance units/cm.

c. Table J-9 contains a frequency table and plots for Det I2 $(1810-1714 \text{ cm}^{-1})$, a measure of oil oxidation. These data also appear to be a combination of abnormal and normal occurrences. There is a primary mode between 100 and 400 integrated absorbance units/cm and a secondary mode at approximately 6500 integrated absorbance units/cm. It is difficult to identify an obvious overlap point or abnormal threshold in the distribution of these data; however, we selected 3200 integrated absorbance units/cm as the best judgement of this value.

d. Table J-10 contains a frequency table and plots for Det I3 $(1650-1538 \text{ cm}^{-1})$, a measure of oil nitration and carboxylate. This frequency distribution is skewed slightly toward the lower tail and is much less peaked than a standard normal distribution. The upper tail is large and may represent a separate distribution of abnormal data. Examination of the stem leaf plot suggests an apparent overlap in these two distribution at approximately 1700 integrated absorbance units/cm, and we estimate this value as the abnormal threshold for Det I3.

e. Table J-11 contains a frequency table and plots for Det I4 $(1300-1000 \text{ cm}^{-1})$, a measure of oil oxidation, sulfation, and/or glycol. As with the other variables from this test engine, these data appear to be divided into two distinct groups or distributions. The primary distribution has a mode at approximately 1700 integrated absorbance units/cm and the secondary distribution has a mode at approximately 15,300 integrated absorbance units/cm. The two distributions overlap at approximately 6000 integrated absorbance units/cm and we estimate this value to be the abnormal threshold for Det I4.

f. Table J-12 contains a frequency table and plots for FD1 (3040 cm^{-1}), a measure of aromatics in the oil at a single peak. Again,

these data appear to be a combination of two separate distributions. The primary distribution has a mode of approximately zero. The secondary distribution is near uniform in appearance and has a mode at approximately eight absorbance units/cm. These apparent distributions appear to overlap at approximately two absorbance units/cm, and we estimate this value as an abnormal threshold.

g. Table J-13 contains a frequency table and plots for FD2 (1595 cm^{-1}), a measure of aromatics at a single peak. Sixty-seven percent of these occurrences are zero. Any occurrence above zero should be cause to consider fuel dilution. We estimate the abnormal threshold at the 75th percentile of the data or 143 absorbance units/cm.

h. Table J-14 contains a frequency table and plots for FDI3 (905-685 cm^{-1}), a measure of aromatics in the oil. As before with these data, there are two apparent distributions in the data. We estimate that these distributions overlap at approximately 400 integrated absorbance units/cm and this value is estimated as the abnormal threshold for FDI3.

i. Table J-15 contains a frequency table and plots for ZN1 (670 cm^{-1}), a measure of the additive ZDDP in the oil. This distribution is nearly uniform, and there are no obvious indicators of normal and abnormal occurrences. There is a small cluster of occurrences between -9 and -10. Since this additive depletes as oil deteriorates, we assume the abnormal threshold to be in the lower tail of the data. We know that approximately half of these samples were from fail oils; therefore, we estimate the abnormal threshold at the 25th percentile or -7.3 absorbance units/cm.

j. Table J-17 contains a frequency table and plots for iron wear metal, contamination in parts per million (PPM). As with the other variables for this test and engine, these data appear to be from two separate distributions. The lower, or assumed normal distribution, has a mode at approximately 200 PPM. The upper or abnormal distribution, has a mode at approximately 900 PPM. The two distributions appear to overlap at 500 PPM, and we estimate the abnormal threshold at this value.

k. Table J-18 contains the frequency table and plots for viscosity measured on the Nametre viscometer in centipoise grams/cm^3. In every case viscosity increases for these test engines; in some cases

to very high values. We estimate the abnormal threshold at the 75th percentile at 353 centipoise grams/cm^3.

1.   Table J-19 contains the frequency table and plots for total acid number (TAN) of the oil in milligrams of KOH to neutralize. These data, as with others for this test engine, appear to be divided into two distributions. The distributions appear to overlap at approximately 10 milligrams, and we estimate this value to be the abnormal threshold of TAN.

m.   Table J-20 contains the frequency tables and plots for total solids measured in percent solid contaminates. This distribution is severely skewed toward the lower tail and much more peaked than a standard normal distribution. The upper tail is long and contains probable outliers above the 90th percentile. We estimate the abnormal threshold at 16% solid contamination.

n.   Table J-21 contains frequency tables and plots for COBRA. The distribution of these data are unimodal, skewed toward the lower tail, and slightly less peaked than a standard normal distribution. The lower tail is of interest because COBRA tends to decrease as mineral oils degrade. However, water contamination or high hydroxyl (Det I1) will cause high COBRA values. Accordingly, abnormal thresholds are estimated at the 5th percentile or 3 COBRA units and at the 95th percentile or 36.5 COBRA units.

SECTION V
CONCLUSIONS

A. General.

This study has addressed the major factors that influence the performance of a lubricant and lubricant condition. Further we have demonstrated that most of these factors may be monitored with infrared spectroscopy. When the engines monitored had seriously degraded the lubricating oil, infrared spectroscopy was shown to be an efficient and effective monitoring tool. When the engines monitored have not seriously degraded the lubricating oil, infrared spectroscopy, though operative, was not shown to be as effective. Typically the methodology developed in this study was more precise when the engines monitored experienced severely degraded lubricating oil. Further we have discussed the importance of maintaining an accurate reference sample in a differential, infrared experiment; however, we have acknowledged difficulty in this regard when undocumented oil changes and oil top off occurred. We have included techniques in the methodology for dealing with inherent problems maintaining a current reference sample during a routine monitoring program; however, strict controls are necessary if such a monitoring program were initiated. Specific regions and peaks within the infrared spectra to be monitored have been identified as part of our methodology. We have proposed abnormal thresholds for these variables for monitoring specific engines. These abnormal thresholds were developed intuitively by examining frequency tables and stem leaf plots of each variable, and are suggested as initial guidelines that would require refinement during actual use. They are summarized in Table 22. Finally, we note that though the procedure monitors many of the factors that influence oil viscosity such as oxidative stressing of the oil and fuel and water dilution, our best models for predicting viscosity from the infrared data generally have not been good. Since viscosity is now efficiently and effectively measured in the Joint Oil Analysis Program, we do not conclude that this methodology should replace separate viscosity testing of the oil.

B. Continental LD/LDS/LDT 465 Engine.

These engines monitored during this study exhibited significant oil degradation. Generally they produced high blow-by materials and

TABLE 22

SUMMARY OF ABNORMAL THRESHOLDS

VARIABLE	INFRARED AREA/PEAK	FIELD ENGINE					
		LDS-465	6V53T	NTC400	8V71T	AVDS 1790	Ford 6 cyl propane
CL 2	1980 cm^{-1}	130	67	16	53	48	3.27
DET I1	3600-3150 cm^{-1}	4000	2417	2878	2116	4800	6489
DET I2	1810-1714 cm^{-1},(1810-1660cm^{-1})*	1299	220	456	348	527	265
DET I3	1650-1538 cm^{-1},(1650-1535 cm^{-1})*	2090	780	860	855	1280	1262
DET I4	1300-1000 cm^{-1}	5222	2228	3000	2470	3424	5779
DET I5	(1725-1670 cm^{-1})*	770	---	---	---	---	---
FD 1	3040 cm^{-1}	5.8	3.62	7.1	9.1	9.3	---
FD 2	1595 cm^{-1},(1610.cm^{-1})*	2.4	2.8	2.2	3.84	3.9	---
FD I3	905-685 cm^{-1}	2346	657	882	903	1008	---
FD 4	(473 cm^{-1})*	1.16	---	---	---	---	---
ZN 1	670 cm^{-1}	-4.0	-3.44	---	-2.0	-2.09	---
SO 4	(604 cm^{-1})*	2.81	---	---	---	---	---

* Areas/Peaks in parentheses pertain to guidelines/limits for LDS/LDT Engines.

138

stressed the additive package oxidatively. Further many samples were contaminated with fuel. The methodology developed in this study worked most effectively for this engine. Progressive oil degradation was tracked easily in the differential spectra. Carbon loading effects in the lubricating oil were especially severe. The strong correlation between CL2 and total solids (.803) and the total solids regression model with R^2 of .86 confirm the effectiveness of the infrared technique. Simple correlations between the aromatic peaks and percent fuel by gas chromatograph were not strong; however, the regression analysis produced an optimal model with R^2 of .77. Predictions from this model clearly demonstrate that the methodology can monitor fuel dilution in this engine. A monitoring program for this engine based on infrared spectroscopy would appear highly feasible, and we have considerable confidence in the abnormal thresholds proposed.

C. Detroit Diesel Allison 6V-53T Engine.

Generally, this engine does not stress its lubricating oil as much as the LD-465 family of engines; however, oil degradation, principally carbon contamination, does occur in this engine during field use. The ability of this methodology to monitor this effect is confirmed by a .68 correlation between CL2 and total solids and an R^2 of .85 for the total solids regression model. While the field engines did not stress the lubricant oxidatively, the 240 hour endurance test did; and the methodology performed well again. For the test engines the correlation between Det I2 and total acid number was .521, and the five variable regression model for total acid number had an R^2 of .80. Fuel dilution ws not a problem with this engine, and there were not enough fuel contaminated samples to judge the effectiveness of the methodology for monitoring fuel. A monitoring program for this engine based on infrared spectroscopy would appear feasible, and we have confidence in the abnormal thresholds proposed.

D. Cummins NTC-400 Engine.

Generally, the lubricating oil in this engine does not become contaminated with carbon, moisture, or fuel. Neither does the oil deteriorate from high temperature nor from overstressing. As would be expected, the correlation and regression procedures we used during this study did not show strong relationships among the infrared variables and the physical properties for this engine. The univariate

139

procedure for this engine appeared to be effective, and the stem leaf plots show near normal distributions for most of the infrared variables. The few samples of oil that produced infrared measurements in the extreme tails of these distributions are easily identified as outliers and aid in the selection of abnormal thresholds. Although we cannot confirm that this methodology correlates with traditional measures of oil degradation, we do have confidence that the methodology will identify abberant responses to infrared spectroscopy and that this will suffice for a monitoring program.

E. Detroit Diesel Allison 8V-71T Engine.

This engine produces light carbon contamination, but it does not seriously degrade or contaminate the oil. The engine also exhibits moderate levels of fuel contamination. As with the LDS-465 and 6V-53T, CL2 and total solids were significantly correlated (.776). The regression model for total solids was not as good as for the other engines; however, its R^2 of .74 confirms the clear relationship. Other correlations and regression models are weak. We were able to develop a model (R^2 =.75), for the fuel dilution that existed in these samples. The univariate procedure appeared to work well for this engine, and the stem leaf plots produced generally well defined distributions closely approximating a normal distribution. However, the apparent outliers seen with the NTC-400 engine were not in these data, and we have somewhat less confidence in the abnormal thresholds proposed. Still, we feel the methodology and thresholds are useable for this engine though with caution.

F. Continental Diesel Engine AVDS-1790.

This engine experiences severe water contamination in its lubricating oil and produces light to moderate carbon loading. The correlation and regression procedures did not work well for this engine except that a surprisingly strong model for total solids with an R^2 of .94 was developed. This model is complex with many second order and interaction terms; nevertheless, it accounts for nearly all the variability in the data. Unfortunately we did not conduct a quantitative test for water for these samples and cannot demonstrate the correlation between Det I1 and percent water contamination. Still the data clearly show the severe water contamination. Det I1 values cause frequent high water caution flags. The univariate statistics produced

140

good stem leaf plots that showed near normal distributions in the infrared variables. We have confidence in the abnormal thresholds produced by this procedure and believe this engine could be effectively monitored using this infrared methodology.

G. Propane Fueled Engines.

Of the several propane fueled engines included in the study, we obtained sufficient data for only the Ford 6 cylinder truck to make judgements about the methodology. This engine tends to degrade its oil due to the stop and go, low RPM operating conditions for flight line vehicles. Mositure contamination is apparent. Det I3 is correlated with total solids and the regression models for viscosity and especially total acid number are good ($R^2=.76$ and .9 respectively). The methodology appears feasible for establishing a monitoring program for this engine, and we have confidence in the proposed abnormal thresholds.

H. ASTM Sequence III-D Test, 1977 GM Olds 350 CID V8 Engine.

These test data were included in this study as control data for the methodology. The test itself severely stresses the oil oxidatively plus three of the six oil formulations used were classified as failing quality oils. As expected, the samples included severely degraded oil, and the methodology worked well to identify these samples. Strong correlations existed between nearly every infrared variable monitored and the physical properties. Changes in the differential spectra for the sequential samples are obvious and abnormal occurrences are apparent. Regression models for viscosity, total acid number, and total solids have R^2 values of .95, .98, and .94 respectively. These results are extremely good and demonstrate the strength of the infrared technique when sampling is controlled and reference oils are accurate. Performance of the methodology on these samples confirms our basic hypothesis concerning the relationships between oil condition and the infrared spectra.

SECTION VI

RECOMMENDATIONS

A. That the Program Manager, Army Oil Analysis Program, conduct a
field test of the methodology developed in this study by placing the
LDS-465, 6V-53T, NTC-400, 8V-71T, and AVDS 1790 engines at a single
installation under an oil condition monitoring program based on this
methodology in lieu of physical property testing now included in the
Army Oil Analysis Program.

B. That current Army oil analysis procedures for monitoring wear metals
and viscosity of used oil samples be continued during the above field
test.

C. That infrared spectra be recorded for mineral oil samples received
by the field test laboratory for engines not included in the field test,
and magnetic disc copies of these spectra be forwarded to the TSC under
approval of the JOAP-CG for possible inclusion of these engines in this
infrared methodology.

D. That other members of the Joint Oil Analysis Program Coordinating
Group investigate possible application of this technique for mineral oil
serviced equipment in their respective services.

SECTION VII

APPENDICES

A. List of References

A-1. Coates, J.P. and Setti, L.C., Condition Monitoring of Crankcase
Oils Using Computer Aided Infrared Spectroscopy - Part I, pp
436-454, JOAP International Symposium Proceedings, Pensacola,
FL 17-18 May 1983.

A-2. McCaa, B.B., et al, Condition Monitoring of Crankcase Oils
Using Computer Aided Infrared Spectroscopy - Part II, pp
455-468, JOAP International Symposium Proceedings, Pensacola,
FL, 17-18 May 1983.

A-3. Brunner, F., Applications of Infrared Spectroscopy in Mineral
Oil Chemistry, Bodenseewerk Perkin-Elmer & Co., Gmbh Uberlinger/
See, 1963.

A-4. Butler, W.E., Jr., Owens, E.C., and Frame, E.A., Pilot Field
Test of Multiviscosity/Synthetic Engine Oil in Army Combat/
Tactical Vehicles at Ft. Bliss, TX, Interim Report AFLRL
No.160, AD-A134703, U.S. Army Fuels and Lubricants Research
Laboratory, Southwest Research Institute, San Antonio, TX,
and Bowen, T.C., U.S. Army Belvoir Research and Development
Center Materials, Fuels and Lubricants Laboratory, Ft. Belvoir,
VA, Jul 1982.

A-5. Centers, P.W., Private Communications, Lubrications Branch,
Aero Propulsion Laboratory, Wright-Patterson AFB OH.

A-6. Clark, G.L., The Encyclopedia of Spectroscopy, Reinhold
Publishing Corp., New York, 1960.

A-7. Cuellar, J.P., Jr., et al, The Feasibility of Oil Analysis for
AF Diesel Engines, AD-A079808, Southwest Research Institute,
San Antonio, TX, for Directorate of Material Management,
San Antonio Air Logistics Center, SAALC-006181, Kelly AFB,
TX. June 1979.

A-8. D'Orazio, A. and Georges, A., Private Communication, Naval
Air Propulsion Center, Trenton, NJ.

A-9. Hannah, R.W., & Swinehart, J.S., Experiments in Techniques
of Infrared Spectroscopy, Perkin-Elmer., Sep 1974.

A-10. Jamison, R.G., Water Absorption of Fluids/Oils, US Army
Mobility Equipment Research and Development Command, Ft.
Belvoir, VA, June 1978.

A-11. Joint Oil Analysis Program Laboratory Manual for Nonaeronautical
Equipment, (Army) TM-38-301-1 Dec 80.

A-12 Kincaid, R.L., Mechanical Systems Integrity Analysis, Spectron
  Caribe, Inc., Puerto Rico, March 79.

A-13. Magazine LUBRICATION, Instrumental Analysis of Petroleum,
  Texaco Inc., Vol.44, No.1, Jan 1958.

A-14. Magazine LUBRICATION, Analytical Advances, Texaco Inc.,
  Vol.52, No.1.

A-15. Magazine LUBRICATION, W.A. Snook, Used Engine Oil Analysis,
  Texaco, Inc., Vol.54, No.9, 1968.

A-16. Magazine LUBRICATION, E.D. Archer, Infrared Analysis - I - and
  II, Texaco Inc., Vol.55, No's.2 and 3, 1969.

A-17. Magazine LUBRICATION, K.L. Krenz, Gasoline Engine Chemistry,
  Texaco Inc., Vol.55, No.6, 1969.

A-18. Magazine LUBRICATION, R.F. Cashin, Marine Turbine and Diesel
  Engine Oil Analysis, Texaco Inc., Vol.56, No.3, 1970.

A-19. Magazine LUBRICATION, K.L. Kruez, Diesel Engine Chemistry,
  Texaco Inc., Vol.56, No.6, 1970.

A-20. Magazine LUBRICATION, W.M. Cummings, Fuel and Lubricant
  Additives - I and II, Texaco Inc., Vol.63, No's.1 and 2,
  1977.

A-21. Miller, R.G.J. & Stace, B.J., Laboratory Methods in Infrared
  Spectroscopy, 2nd Ed., Heyden & Son Ltd., New York 1972.

A-22. Moon, R.B. and Montemayor, A.F., Laboratory Evaluation of
  Multiviscosity Grade Engine Oils in US Army Diesel Engines,
  Interim Report AFLRL No.112, US Army Fuels and Lubricants
  Research Laboratory, Southwest Research Institute, San Antonio,
  TX, May 1981.

A-23 Myrick, Frank D., Lube Oil Analysis by the Infrared Technique,
  Continental Oil Co., Paper Presented at the Engineer's Meeting,
  Dallas, TX.

A-24. Ray, Alice A., Editor, Statistical Analysis System (SAS)
  User's Guide, Basics, SAS Institute Inc., 1982.

A-25. Roberts, John D. & Caserio, Marjorie C., Basic Principles
  of Organic Chemistry, W.A. Benjamin, Inc., New York 1965.

A-26. Sadtler Handbook of Infrared Spectroscopy, Sadtler Research
  Laboratories, Inc., Philadelphia, PA, 1978.

A-27. Smith, A.L., Applied Infrared Spectroscopy, John Wiley &
  Sons, 1979.

A-28.   Smith, H.A., Lubricant Monitoring Using the Complete Oil
        Breakdown Rate Analyzer (COBRA), AFWAL, Aeropropulsion
        Laboratory, Wright-Patterson AFB, OH, Mar 1983.

A-29.   Snowden, J.E., Jr., Conway, Jack, Sr., and Westerheid, J.P.,
        Journal of The American Society of Lubrication Engineers,
        Aug 1976.

A-30.   Stavinoha, L.L. & Wright, B.W., Spectrometric Analysis of
        Used Oils, Southwest Research Institute, San Antonio TX
        SAE Paper 690776.

A-31.   Stavinoha, L.L., et al, (USAFLRL), Analytical Approach to
        the Characterization of Military Lubricants, US Army Fuels
        and Lubricants Research Laboratory, Southwest Research
        Institute, San Antonio, TX, March 1976.

A-32.   Wilkes, Quantative Infrared Analysis, American Laboratory,
        June 1979.

A-33.   Wright, R.W., Determination of Lubricant Additives by Thin
        Layer Chromatography and Fluoresence, AFAPL-TR-75-50, Air Force
        Aero-Propulsion Laboratory/SFL, Wright-Patterson AFB OH, Oct 1975.

A-34.   Wright, R.W., Differential Oil Analysis by Infrared Absorption
        Spectroscopy, AFAPL-TR-75-74, Air Force Aero-Propulsion
        Laboratory/SFL, Wright-Patterson AFB OH, Sep 75.

END

FILMED

5-85

DTIC